Università Politecnica delle Marche

PhD Course in Life and Environmental Sciences

curriculum "Biomolecular Sciences" (XVI cycle)

HUMAN CHORIONIC VILLUS, AMNIOTIC FLUID AND AMNIOTIC MEMBRANE: THREE DIFFERENT GESTATIONAL TISSUES AS SOURCE OF VALUABLE MESENCHYMAL STEM CELLS FOR REGENERATIVE MEDICINE APPLICATIONS

PhD Student:
Dr.ssa Rossella, Soccorsa Pistillo

Tutor:
Prof. Davide Bizzaro

Co-tutor:
Dr.ssa Bruna Corradetti

2014-2017

CONTENTS

1. INTRODUCTION

Regenerative medicine is a newly emerging and multidisciplinary field which draws on biology, medicine and genetic manipulation for the development of strategies aimed at maintaining, enhancing or restoring the function of tissues or organs which have been compromised through disease or injury [1-3]. Stem cell-based regenerative medical therapies constitute promising opportunities to repair or replace disease or damaged tissues not presently treatable by conventional pharmaceutical remedies.

Stem cells are viewed as promising candidates for use in cell-based therapies, owing to their capacity for self-renewal and differentiation into diverse mature progeny. However, the source of stem cells, in order to maximize the safety and efficacy of regenerative therapies, is clearly of great importance. Both adult and embryonic stem cells are commonly used to develop therapies for various preclinical models of disease and injury.

Recently, induced pluripotent stem (iPS) cells, which are obtained by genetically reprogramming adult somatic cells to a pluripotent state, have also been proposed as an alternative cell source for use in regenerative medicine [4, 5]. However, a number of limitations hamper the clinical applicability of stem cells derived from either adults or developing embryos. While embryonic stem cells (ES cells) are highly proliferative and capable of differentiating into cells of all adult tissues, they pose a significant risk of tumour formation [6]. Furthermore, since ES cells are obtained by the destruction of embryos, they face serious ethical objections that have yet to be resolved. In contrast, although adult stem cells carry a reduced risk of tumorigenicity and fewer ethical restrictions, they are limited in number, have diminished differentiation capacity, and reduced proliferative potential [7, 8] which make the production of a sufficient number of cells for use in cell-based therapy difficult. In fact, mesenchymal stromal cells from bone marrow carry with them a risk of viral infection [9] and the differentiation capacity of these cells has been seen to decrease with donor age [10, 11].

Finally, despite major advances in iPS technology in recent years, reprogrammed cells often have an imperfectly cleared epigenetic memory of the source cells [12]. In addition, iPS cells are vulnerable to genomic instability [13, 14]. Due to the drawbacks associated with ES cells, adult

stem cells and iPS cells, much effort has been directed at finding an alternative source of stem cells that is safe, easily accessible, provides a high cell yield and for which cell procurement does not provoke ethical debate.

In human medicine, fetal placenta-derived MSCs have been reported as an alternative and novel class of stem cells with intermediate characteristics between embryonic and adult stem cells [15]. Firstly, placental tissues are generally discarded after birth and their supply is abundant so that a large number of cells can be collected. Secondly, the origin of these tissues during the first stages of embryological development supports the possibility that they may contain cells which have retained the plasticity of the early embryonic cells from which they derive. Lastly, although all MSCs are understood to have immunomodulatory capacities, placental involvement in maintenance of feto-maternal immune tolerance during pregnancy may distinguish placental derived MSCs from those sourced from adult tissue in this capacity. These three key aspects make cells from placental tissue good candidates for possible use in cell therapy approaches, with the possibility of providing cells that are capable of differentiating into multiple different cell types, and which also display immunological properties that would allow their use in an allo-transplantation setting, the recovery of cells from this tissue does not involve any invasive procedures for the donor, and their use does not pose any ethical problems.

This PhD work has sought to isolate homogeneous MSC populations from human amniotic membrane trough a newly established isolation protocol; to collect MSCs from human fetal (extra-embryonic) tissues during three different gestation periods (first- second- third- trimester) in order to understand, for the first time, whether the gestational stage of isolation affects stemness properties; and ultimately to observe the differences in phenotype, proliferative capacity, differentiation ability as well as in the immuno-suppressive/immuno-modulatory properties among them in order to assess whether they can be used for regenerative medicine applications.

1.1 DEFINITION AND SOURCES OF STEM CELLS

Stem cell have been defined as immature and undifferentiated clonogenic cells able to produce identical daughter cells. Stem cells have the remarkable potential to develop into many different cell types in the body during early life and growth, besides differing from other kinds of cells in the body [16].

Regardless of their source, all stem cells have three general properties:

i) they are capable of dividing and renewing themselves for long periods;

ii) they are unspecialized;

iii) they can give rise to specialized cell types, including cells belonging to the mesoderm, ectoderm and endoderm lineages (Figure 1).

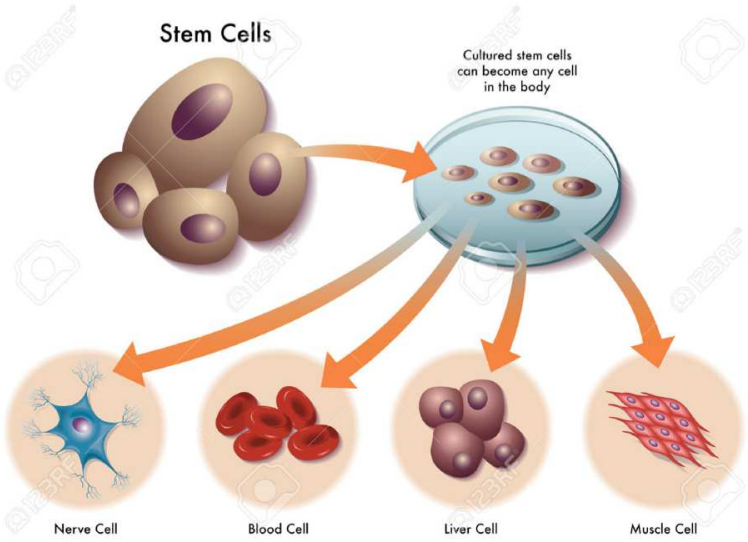

Figure 1. ***Stem cells: Cells that are able to self-renew (can create more stem cells indefinitely) and differentiate into specialized, mature cell types. (http://www.allthingsstemcell.com/glossary/)***

The properties described above for stem cells derive from their capability to undergo asymmetric divisions. Two types of cell divisions exist in different organisms: the symmetric and the asymmetric one. These divisions are controlled by a combination of intrinsic and extrinsic mechanisms. The major purpose of the symmetric divisions is proliferation, as one cell produces two identical daughter cells that acquire the same developmental fate. On the contrary, the asymmetric cell division is a characteristic property of stem cells that give rise to two daughter cells with different developmental fates. One cell differentiates along a specific lineage, whereas the other cell has the potential to renew stem cell identity and

continue to divide in an asymmetric manner. The ability of cells to divide asymmetrically to produce two different cell types provides the cellular diversity found in every multicellular organism [17].

Stem cells have been isolated from all stages of life, from preimplantation embryos through to adulthood. Three categories of stem cells have been described based on their tissue of origin [18, 19].

- Embryonic stem cells, derived from in the inner cell mass (ICM) of the early preimplantation embryo [20];
- Fetal stem cells, isolated from fetal and extra-embryonic tissues (such as amniotic membranes [21] and umbilical cord [22-24];
- Adult stem cells isolated from mature tissues [8] such as, for example, bone marrow [25], adipose tissue [26], periosteum [27], brain [28], muscle.

Stem cells can be classified according to their differentiative potential mainly into four categories: totipotent, puripotent, multipotent and unipotent.

The bestknown **totipotent** cell is the zygote, which has the ability to give rise to an entire living organism. Strictly speaking, zygote cannot be considered stem cell: in fact, as it grows the daughter cells that follow division differ from the parent cell.

Once the blastocyst stage is reached, ESCs isolated from the inner cell mass loose the totipotency of the zygote but are still able to differentiate into the three germ layers (**pluripotent**). Based on their self-renewal and differentiation abilities, ESCs are hierarchically higher than other cell types that have more restricted properties, but it is important to take into account potential problems in clinical applications aroused by their high tumorigenic rate after transplantation [29] and ethical issues.

Adult stem cells, commonly termed mesenchymal stem cells represent a population of stem cells with more restricted differentiation potential respect to ESCs. These cells are considered to be **multipotent**. MSC is the archetype of post-natal/adult cells endowed with multiple developmental potentials [25, 30]. Multipotent mesenchymal progenitors exist in a variety of tissues, including fetal and adult organs [31, 32].

Among stem cells, there are mature cells committed only for a single cell line and for this reason are defined **unipotent** [33].

1.2 MESENCHYMAL STEM CELLS

Mesenchymal stem cells (MSCs) are multipotent progenitors present in both adult and fetal tissue [34] and that have been extracted from multiple mouse and human organs, such as compact bone [35], muscle [36], bone marrow, skin [37], pancreas [38], fat [39], dental pulp [40], placenta and umbilical cord [41].

MSCs were first isolated by Haynesworth et al. [42] and characterized by Friedenstein and colleagues more than 30 years ago, and were described as fibroblastic-like cells with the properties of adhering to plastic when cultured onto dishes and capable of forming fibroblastic colony forming units (CFU-F) [43]. In 2006, the International Society for the Cell Therapy listed the minimal criteria for defining a multipotent mesenchymal stromal cell [44]:

(i) the adherence to plastic under standard culture conditions;

(ii) being positive for the expression of *CD105, CD73* and *CD90* and negative for expression of the hematopoietic cell surface markers (*CD34, CD45, CD11a, CD19* or *CD79a, CD14* or *CD11b*, and histocompatibility locus antigen (*HLA)-DR*);

(iii) under specific stimuli, they can differentiate into mesodermic-specific tissues, generating osteoblasts, adipocytes, and chondroblasts in vitro [25].

Recently, researchers focused on the understanding of the native identity, tissue distribution, and frequency of these multipotent progenitor cells [30]. It has been found that what we normally define as MSC originates from the Stromal Vascular Fraction-cells that associate with the vasculature and capillaries in vivo [31, 32, 45]. In particular, since every mature organ contains blood vessels, it has been reported that perivascular cells constitute a stock of multilineage progenitor cells [46] and that once isolated and expanded in vitro they turn into the cells described above.

The best characterized source of MSCs is bone marrow (BM) [43]. However, BM-MSCs have been shown to have limited proliferative and /or functional potential depending on the age of the donor and the passages in

culture [47, 48]. Moreover, it has been reported that only 0.001-0.1% of cells in adult bone marrow comprises of MSCs. Tissues that contain unique and primitive cells whose potential is as yet undefined, but which represent attractive candidates as a resource for stem cell biotechnology and biomedicine, are gestational tissues [49-54].

1.3 FETAL ADNEXA

In fetal and extra-embryonic tissues, abundant multipotent cells can be obtained from the starting material for differentiation protocols or for cell transplantation and regenerative medicine applications. Fetal tissues (such as the amniotic fluid, the chorionic villus and the amniotic membrane) are routinely discarded at parturition, so there is little ethical controversy attending the harvest of the resident stem cell populations. Hematopoietic and MSCs from these tissues have been clinically used in human medicine and have already successfully treated a number of diseases.

The fetal adnexa are composed of the *placenta*, *fetal membran*es, and *umbilical cord*.

1.3.1 Placenta

The *placenta* is the mother-fetal connection organ, necessary for nutrition, respiration, hormones production, immune protection of fetus and the maintenance of the pregnancy. Human placenta is discoid in shape with a diameter of 15–20 cm and a thickness of 2–3 cm and it is composed by two sides: the fetal side that is bordered by chorionic plate and the maternal side that is delimited by decidual plate (Figure 2). The fetal part of the placenta is formed by the placental disc and amniotic and chorionic membranes [55].

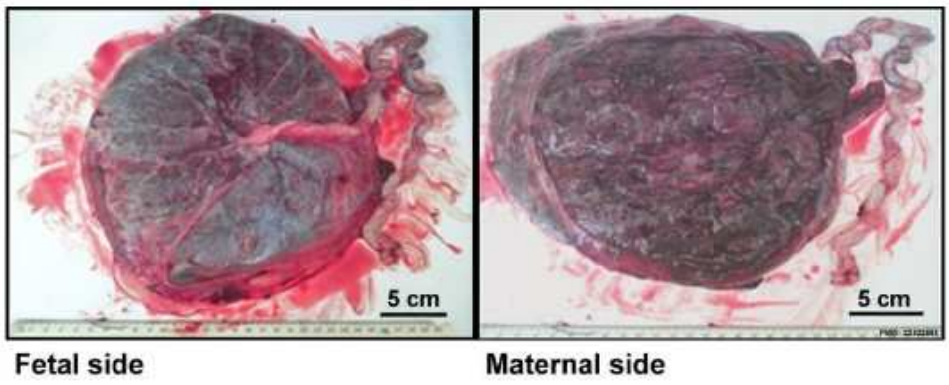

Figure 2. ***Term Placenta (https://embryology.med.unsw.edu.au/embryology/index.php/Placenta_Development)***

The placenta is defined structurally in the fourth week of gestation. The process of its formation is called placentation and provides:

· implantation of the blastocyst (cells mass that derived from the zygote) to the uterine wall;

· the creation of vascular connections for the removal of fetal catabolites through maternal blood and to exchange gas and nutrients. The outer layer of the blastocyst becomes the trophoblast (which forms the outer layer of the placenta) that is divided into two further layers: the underlying cytotrophoblast layer and the overlying syncytiotrophoblast layer that contributes to the barrier function of the placenta. The morpho-functional placenta unit is the villus; this unit allow the transfer of nutrients from maternal to fetal blood. Placenta has also represent a reserve of progenitor/stem cells.

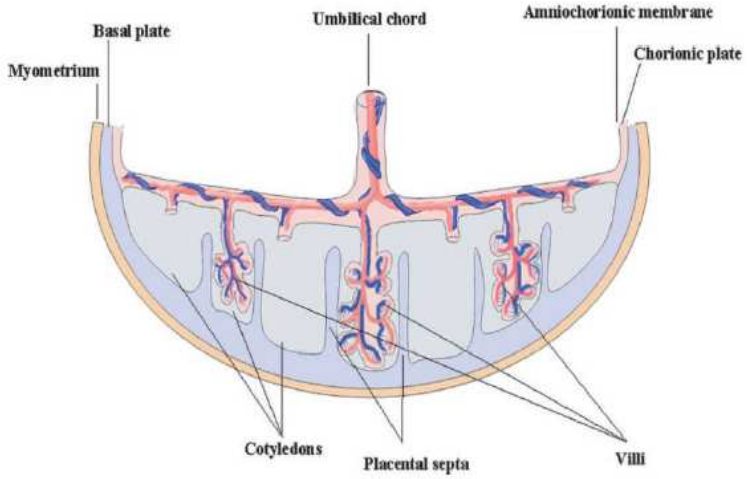

Figure 3. ***Schematic section of the human term placenta [41]***

1.3.2 Fetal membranes

From the margins of the chorionic disc extend the fetal membranes, amnion and chorion, which enclose the fetus in the amniotic cavity and the endometrial decidua.

The fetal membranes are necessary for protection and nutrition and they provide the indispensable aquatic developmental environment.

Amnion consists of a bag that contains a serous liquid, the amniotic fluid, in which it is immersed in the embryo. It is located inside the chorion membrane: it is thin, transparent and free of vases. It covers the umbilical

cord and reaches the navel of the fetus. The amnion and the amniotic fluid, contained therein, represent a sort of phylogenetic inheritance of the fact that life would originate in the aquatic environment.

Chorion is composed by a membrane that envelops the embryo and delimits the extraembryonic cavity; it has an important nutritional function by linking the embryo with the mother through presence of chorionic villi, which are formed on the surface of the chorion.

Yolk sack is a small bladder that provides the necessary nourishment to the embryo. In human the yolk sack is smaller and looks like a sack disposed around a cavity that contains liquid. In the thickness of the walls of the bag there are veins belonging to the yolk circle through which the nutrients and oxygen arrive at the embryo.

Allantoid is an attached fetal that has respiratory, nutritional and excretory function for the embryo. It develops on the central part of the intestine of the embryo and during its development it becomes elongated, protruding from the embryo itself.

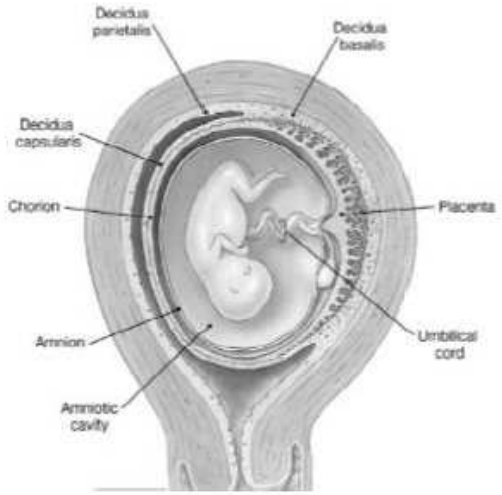

Figure 4. ***Fetal membranes (http://www.luciopesce.net/zoologia/svilup.html)***

1.3.3 Umbilical cord

In placental Mammals, the umbilical cord is a rapidly developing tissue connecting the fetus with the placenta. It provides the fetus with the nutrients, oxygenated blood and carries away deoxygenated, nutrient depleted blood. MSCs have been successfully isolated from the umbilical

cord blood (UCB) and different compartments of the UCM [48, 56-58]. Umbilical cord matrix is a mucoid connective tissue surrounding umbilical vessels. In humans it is comprised of specialized fibroblast-like cells and occasional mast cells embedded in an amorphous ground substance rich in proteoglycans, mainly hyaluronic acid. Human umbilical cord shows tissue compartmentalization in which cell characteristics and extracellular matrix elements differ from one another. Based on structural and functional studies, at least six distinctive zones are now recognized in the umbilical cord:

(i) surface epithelium (amniotic epithelium),
(ii) subamniotic stroma,
(iii) clefts,
(iv) intervascular stroma named classically as Wharton's jelly),
(v) perivascular stroma and
(vi) vessels [23]

During development, primordial germ cells (which express alkaline phosphatase) are formed in the yolk sac and migrate through the developing umbilical cord en route to their final destination in the gonadal ridge, thus, it is possible that some of these migrating germ cells or their descendants remain in the umbilical cord matrix [56, 59, 60]. In the last 10 years, hematopoietic UCB-MSCs have been shown to have the highest proliferation capacity, the longest telomere length, broadest differentiation potential [48] and the capacity for extended expansion in culture prior to becoming senescent compared to AT- or BM- derived MSCs. Moreover, they have been reported to be therapeutically useful for rescuing patients with BM related deficits and inborn errors of metabolism [61] offering advantages over bone marrow since cord blood does not require perfect Human Leucocyte Antigens (HLA) tissue matching, has less incidence of graft vs host disease, and may be used allogeneically [62].

1.4 Amniotic membranes

Amniotic membranes (AM) have also attracted attention as a potential cell source for regenerative therapy. Amnion is a thin, avascular membrane composed of an epithelial layer and an outer layer of connective tissue. To obtain cells from term delivered amnion, this membrane is separated from

allantois by peeling them apart. The elastin lamina present in the loose connective tissue of the amnion and adjacent to the allantois facilitates the separation of the membranes. Typically, human amnion stromal cells are obtained after complete removal of the epithelial layer using trypsin followed by digestion in collagenase [63]. Because human amniotic epithelium differentiates from the epiblast at a time when it retains pluripotency, it is reasonable to speculate that amniotic epithelial cells (AEC) may have escaped the specification that accompanies gastrulation and that these cells may preserve some or all of the characteristics of the epiblast such as pluripotency [64]. Immunohistochemical and quantitative real-time RT-PCR analysis demonstrated that there is an abundance of stem cell marker-positive cells (*TRA 1-60, TRA 1-81*) and stem cell marker gene expression (*Nanog* and *SOX-2*) that together indicate that some stem cell marker-positive cells are conserved over the course of pregnancy.

This evidence suggests that stem cell marker-positive amniotic epithelial cells in the amnion at term are retained from epiblast-derived fetal amniotic epithelial cells [65]. These cells possess multipotent differentiation ability [18, 21] low immunogenicity [66], and anti-inflamatory functions [67]. Several clinical trials demonstrated prolonged survival of human AM or human AECs after xenogenic transplantation into immunocompetent animals, including rabbits [68] , rats [69], guinea pigs [70] and bonnet monkeys [71], suggesting active migration and integration into specific organs, and indicating active tolerance of the xenogenic cells [54]. Recent studies demonstrated that AM-MSCs have immunomodulatory properties and can strongly inhibit T lymphocyte proliferation [72]. Evidence to support the hypothesis that fetal membranes are non-immunogenic comes from clinical studies in which AM has been used for treatment of skin wounds, burn injuries, chronic leg ulcers and prevention of tissue adhesion in surgical procedures [54]. More recently, AM has been used in ocular surface reconstruction for substrate transplantation to promote the development of normal corneal or conjunctival epithelium without acute rejection in absence of immunosuppressive treatment [73]. AM transplantation is an effective clinical therapy for reconstruction of the ocular surface also in veterinary patients such as horses [74-76] and dogs

[77] because it is avascular and strong, promotes re-epithelialization, decreases inflammation and fibrosis [78] and modulates angiogenesis [79]. Several growth factors produced from AM are involved in these processes, such as transforming growth factor, keratinocyte growth factor, and hepatocyte growth factors [80].

1.5 Amniotic fluid

Human amniotic fluid (hAF) is a dynamic environment, which undergoes multiple developmental changes in order to sustain fetal growth and well being. The amniotic cavity first appears at 7-8 days after fertilization and in early gestation the amniotic fluid originates mostly from maternal plasma that crosses the fetal membranes [81]. Fetal urine first enters the amniotic space at 8–11 weeks gestation [81, 82], and in the second half of pregnancy, fetal urine becomes the major contributor to amniotic fluid [82].

Amniotic fluid contains electrolytes, growth factors, carbohydrates, lipids, proteins, amino acids, lactate, pyruvate, enzymes, and hormones [83]. In addition, fluid secretions from the fetus into the AF carry a variety of fetal cells, resulting in a heterogeneous population of cells derived from fetal skin, gastrointestinal, respiratory and urinary tracts, and the amniotic membrane. As the fetus develops the volume and composition of the amniotic fluid change drastically, and the complement of cells detected in amniotic fluid samples taken at different gestational ages varies considerably [84, 85]. Despite this heterogeneity, cultures of amniotic fluid cells obtained by amniocentesis have been used for decades for diagnostic purposes, including standard karyotyping as well as other genetic and molecular tests. AF samples are routinely used in the evaluation of fetal lung maturity, metabolic diseases, fetal infections, and intrauterine infections. These tests have recently been complemented by applying chromosomal microarray (CMA) as a more efficient prenatal genetic screening tool to detect fetal abnormalities [86].

The multitude of cell types existing within the amniotic fluid lead to the hypothesis that stem cells might also be present. In fact, stem cells within the amniotic fluid were first isolated and described in 1993 by Torricelli et al. at 7–12 weeks of gestation [87]. In 2007, cells from the amniotic fluid

have been reported as a population of intermediate MSCs according to their behavior and gene expression. They were expanded extensively without requiring any feeder and were able to differentiate into cell types representing each embryonic germ layer, including cells of adipogenic, osteogenic, myogenic, endothelial, neuronal and hepatic lineages [88]. Moreover, human AF-MSCs showed no karyotypic abnormalities or transformation potential in vitro and no tumorigenic effect in vivo representing a relatively homogeneous population of immature mesenchymal stromal cells with long telomeres, immunosuppressive properties and extensive proliferative potential [88, 89].

1.6 Chorionic villus tissue

In the human placenta, villous development starts between 12 and 18 days post-conception, when the trophoblastic trabeculae of the placental anlage proliferate and form throphoblastic protusions into the maternal blood surrounding the trabeculae [90]. Mesenchymal villi are the first structures to provide the morphologic prerequisites for materno-fetal exchange of gases, nutrients [91] and they are continuously newly formed out of the trophoblastic sprouts throughout pregnancy. Because of this they exist in all stages of pregnancy and have to be considered the basis for growth and differentiation of the villous trees.

The basic structural features of these villous types are summarized in Figure 5. First attempts to analyze their developmental interactions [92] led to the following conclusions: until about the 7th week p.m. the villous trees are composed of mesenchymal villi. Beginning at approximately the 8th week of gestation, the mesenchymal villi are gradually transformed into immature intermediate villi which are the prevailing villous type until the end of the second trimester. Already in the course of the first trimester, bundles of collagen fibres become visible in the proximal immature intermediate villi, resulting in the formation of the first stem villi. Near the end of the second trimester, the first mature intermediate villi as the fourth villous type appear. A few weeks later these villi start producing the terminal villi as small grape-like outgrowths along their surface. Our previous studies have focused on small randomlyoriented samples of

normal immature and mature placentas [92-95] as well as placentas showing villous maldevelopment [92, 94, 95]. Numerous questions remained open, such as the heterogeneous distribution of the various villous types within the villous tree, and the significance and future fate of the trophoblastic sprouts which according to Boyd and Hamilton (1970) should be considered to be the initial step in villous development. Also, the mechanisms of formation of mature intermediate villi are still obscure. We assume that in the villous tree the most proximal parts positioned near the chorionic plate are the oldest ones, whereas the most peripheral branches are the recently developed ones.

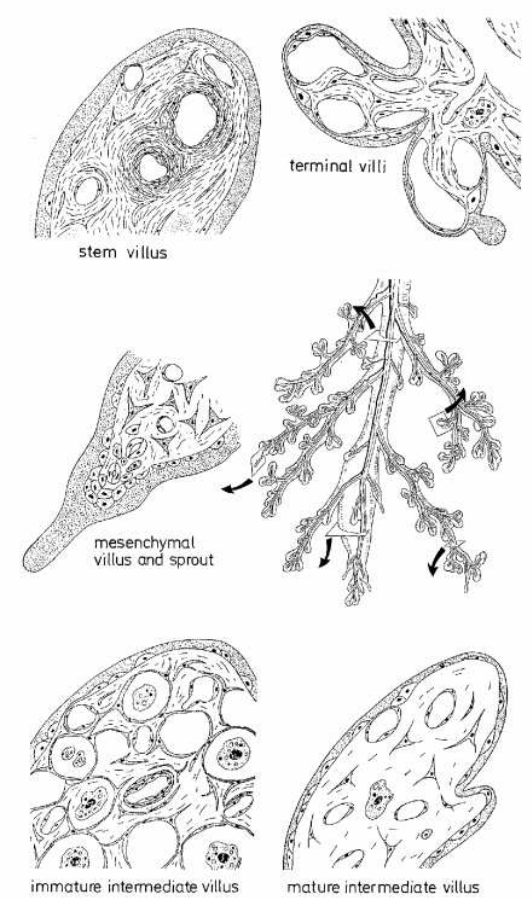

Figure 5. ***Schematic rapresentation of the villus types [90].***

1.7 MSCs FROM HUMAN EXTRA-EMBRYONIC TISSUES

1.7.1 MSCs from chorionic villi

The chorionic villi from human term placenta are a rich source of MSCs. MSCs are present in human chorionic villi (hCV) from the first trimester of gestation and they can be collected either prenatally, by means of chorionic villus sampling for routine prenatal testing at 10-12 weeks of gestation [96], or at birth [97]. The potential utility of hCV-MSCs in therapeutic and regenerative medicine drives current research into their *in vitro* properties. The differentiation potential of hCV-MSCs *in vitro* is now well known but there is scant knowledge of the natural distribution and biology of hCV-MSCs in the chorionic villi of the placenta. hCV-MSCs are readily using a variety of methods. The most popular, routinely used method involves mechanical mincing of the chorionic placental tissue, followed by enzymatic digestion and seeding in stem cell-specific medium [98]. hCV-MSCs selectively attach to the plastic cultureware, proliferate rapidly and are usually prepared without additional enrichment strategies. hCV-MSCs can be differentiated *in vitro* under specific stimulatory environments into derivatives of the mesenchymal cell lineage such as osteocytes, adipocytes, myocytes and chondrocytes [18, 98-101]. In addition, there is evidence of differentiation *in vitro* into cell types characteristic of other lineages such as hepatocyte-like cells and neural-like cells [18, 99, 100], but *in vivo* evidence for such differentiation is very limited. hCV-MSCs show functional characteristics comparable with those of adult hBM-derived MSC and a higher proliferative potential. Previous studies on fetal MSC described genome stability after in vitro expansion and absence of tumors after in vivo transplantation [89, 102]. Fetal MSCs have been used in both autologous and allogeneic settings in clinical trials since 2005. For this reason, concerns regarding the possibility of *in vitro* transformation have been raised and extensively discussed [103]. Previous studies claiming potential transformation of adult hMSCs in senescent [104] or long-term *in vitro* culture were later denied by demonstration that these phenomena were caused by cross-contamination of hMSC cultures with tumor cell lines [105]. To date, a direct evidence regarding the occurrence of tumorigenicity

in *in vitro* expanded adult hMSC does not exist [103], and no tumors were induced after their long-term *in vivo* transfer [104, 106]. Furthermore, more than 200 trials that were based on application of adult MSC are currently registered (ClinicalTrial. gov), and no significant adverse events have been reported.

1.7.2 MSCs from amniotic fluid

The amniotic fluid contains various cell populations, stem cells and differentiated cells that originate from the developing fetus. Since 2003 it was demonstrated that amniotic fluid contains positive stem cells for marker pluripotency *Oct-4* and for mesenchymal markers, such as *CD29, CD44*, *CD73, CD90, CD105* [107]. To prove that amniotic fluid contains pluripotent stem cells it was crucial to demonstrate the differentiation in different cell types such as adipogenic and osteogenic. These stem cells were called amniotic fluid-derived mesenchymal stem cells (AF-MSCs). Many features of this cell type make them different and unique to other stem cells: a very high proliferation ability, that allows them to replicate many times and overcome the problem of cellular quantity; a good differentiation capacity, which allows them to give origin to many cell lines, such as those of bone tissue, muscular, adipose, nervous, cartilage and blood. hAF-MSCs extracted, can be easily expanded in culture, they maintain genetic stability and can be induced to differentiation. Thus these cells represent a new source of cells that may have tissue engineering applications or can be used in cellular therapy. Some studies have shown that these cells could be useful for handling simple injuries such as reconstruction of the knee cartilage, creation of a trachea or a heart valve (Figures 6-7) [108, 109].

Figure 6 ***Cardiac valve obtained from hAFMSC***

Figure 7 ***Trachea obtained from hAFMSCs***

1.7.3 MSCs from amniotic membrane

MSCs isolated from human placenta have gained increased importance in the recent years for their demonstrated differentiation potential, together with their immunomodulatory properties, features that enable them as an attractive source in regenerative/reparative medicine. As already mentioned above, cells with characteristics of MSCs have been isolated from different placental regions [110]. Considering the complexity of the structure of the placenta, we have focused our attention only on cells isolated from the amniotic membrane (AM). Cells isolated from placental tissue should be verified to be of fetal origin to detect maternal contamination of 1% cells or less. hAM-MSCs derived from extraembryonic mesoderm have been extensively characterized, at a phenotypical and functional level. To isolate hAM-MSCs the term amnion has to be dissected from the deflected part of the fetal membranes to minimize the presence of the above maternal cells and to obtain homogenous hAM-MSCs populations.

hAM-MSCs are defined as a population of cells that proliferate in vitro as plastic-adherent, spindle-shaped cells capable of producing fibroblast colony-forming units and displaying a specific pattern of cell surface antigens comparable to that of bone marrow mesenchymal stem cells (BM-MSCs) and other adult sources.

The surface marker profile of cultured hAM-MSCs and mesenchymal stromal cells from adult bone marrow are similar. They are both negative for the hematopoietic *CD34* molecule (*CD34*) and protein tyrosine phosphatase, receptor type C (*CD45*), and are positive for 5'-nucleotidase, ecto (*CD73*), Thy-1 cell surface antigen (*CD90*), endoglin (*CD105*), *CD44* molecule (*CD44*). In addition to the conventional markers reported by the International Society for Stem Cell Therapy (2006) hAM-MSCs express several pluripotent cell surface and intracellular markers, such as octamer-binding protein (*Oct-4*) and Nanog homeobox (*Nanog*).

After isolation the cell yield obtained from term amnion is of about 1x 10^6 adherents and proliferative hAM-MSC that can be kept until passages 5–10 [41]. These cells are also capable of differentiating toward one or more lineages, including osteogenic, adipogenic, chondrogenic, and vascular/endothelial [111].

The minimal criteria for defining hAM-MSCs are the same of MSCs as already mentioned above, despite their fetal origin. Beside this, the cell properties can also vary due to the passage number *in vitro* [41].

Many anatomical and histological studies have tried to explore the diversity of vertebrates by studying the fetal membranes of different animal species. At present the identification of new sources of stem cells with regenerative potential has been under investigation. In this regard due to the cellular diversity and different biological characterization of amniotic cells, it is considered a promising source of stem cells. As stated by Parolini et al (2008), because of the characteristic of amniotic cells, along with their high regenerative and proliferative abilities, the amniotic membrane is undoubtedly a source of MSC. In fact many studies have reported the successful isolation of mesenchymal stem cells derived from both amniotic membrane in human [112], rat [113], horse [114], bovine [115], swine [116], sheep [117], dog [118], cat [119] and chicken [120].

1.8 MSCs IMMUNOMODULATORY-IMMUNOSUPPRESSIVE PROPERTIES

MSCs appear to be important in therapeutics to regulate the immune response invoked in settings such as tissue injury, transplantation, and autoimmunity. One of the salient characteristics of MSCs is their ability to migrate to sites of damaged tissue, a property that is key to their potential use in regenerative medicine [121, 122]. The secretion of a broad range of bioactive molecules is now believed to be the main mechanism by which MSCs achieve their therapeutic effect. This mechanism can be divided into six main actions: immunomodulation, antiapoptosis, angiogenesis, support of the growth and differentiation of local stem and progenitor cells, antiscarring, and chemoattraction. In particular, the immunomodulatory effects of MSCs consist of inhibition of the proliferation of $CD8^+$ and $CD4^+$ T lymphocytes and natural killer (NK) cells, suppression of immunoglobulin production by plasma cells, inhibition of maturation of dendritic cells (DCs), and stimulation of the proliferation of regulatory T cells. The secretion of prostaglandin E2 (*PGE2*), human leukocyte antigen G5 (*HLA-G5*), hepatocyte growth factor (*HGF*), inducible nitric oxide

synthase (*iNOS*), indoleamine-2,3-dioxygenase (*IDO*), transforming growth factor β (*TGF-β*), leukemia-inhibitory factor (*LIF*), and interleukin (*IL)-10* contributes to this effect (Figure 8).

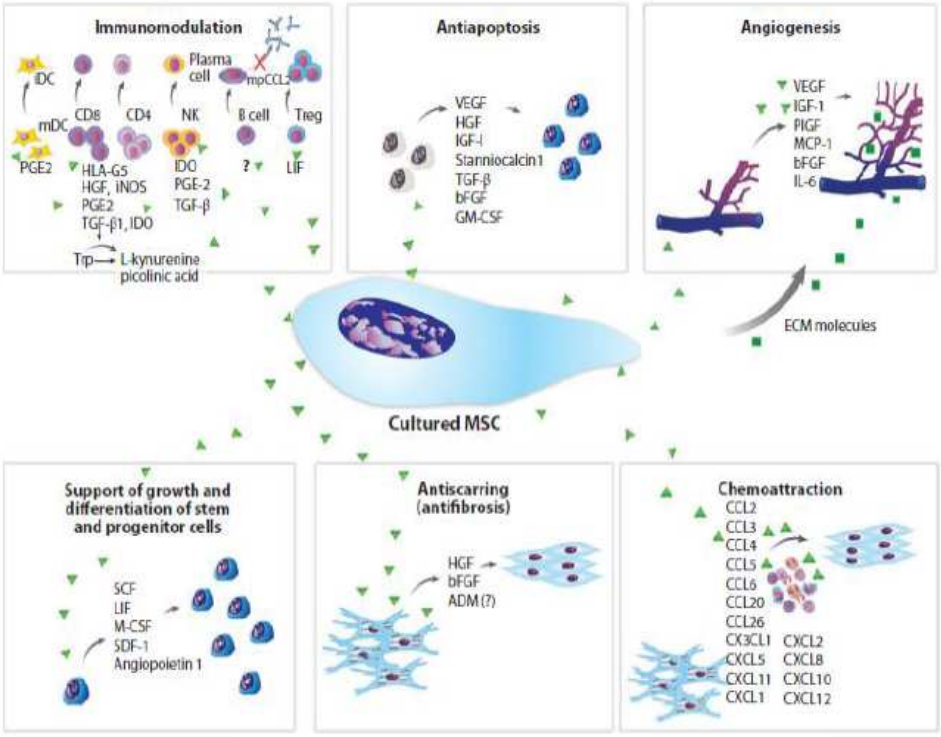

Figure 8 Paracrine effects of cultured MSCs

Furthermore MSCs have been shown to be highly immunosuppressive, unlike ESCs. In some studies, MSCs were found to suppress T cell proliferation and cytokine production [123]. It is known that the MSCs proliferative potential, differentiative potential, purity, and yield significantly differ among tissues of origin. These source-specific features of MSCs directly contribute to the trophic and immunosuppressive activity they exert [124, 125].

In vivo, the use of hMSCs for therapeutic indications does not require priming of MSCs. However, *in vitro*, MSCs must be activated by activating stimuli such as interleukin-1β (*IL-1β*), tumor necrosis factor α (*TNF-α*) and interferon ɣ (*IFN-ɣ*) in order for them to suppress T cell proliferation. *IL-1β* may not require combinations of cytokines and may alone be sufficient to prime hMSCs, whereas the effect of *IFN-γ* may be amplified in the presence of other proinflammatory cytokines, such as *IL-1β* and *TNF-α* [126].

MSCs effects on T cell proliferation *in vitro* appear to have both contact-dependent and contact-independent components [127].

MSC-mediated immunosuppression has been variously demonstrated to involve *IL-10*, *TGF-β* [127] nitric oxide [128] (Sato et al., 2007), indoleamine 2,3-dioxygenase (*IDO*) [129] (Meisel et al., 2004), and prostaglandin (*PG*) E2 [107] (Aggarwal and Pittenger, 2005), cytochrome c oxidase subunit II (*COX2*) [130] (Corradetti et al., 2014); however the exact mechanism is uncertain. One prominent candidate in the mechanism of MSC-mediated immunosuppression is nitric oxide (NO) [128, 131] (Sato et al., 2007), a rapidly diffusing gaseous and bioactive molecule [130].

NO and NO-derived reactive nitrogen species can interact with many enzymes, ion channels, and receptors . NO production is catalyzed by the nitric oxide synthases (*NOS*), for which there are three genes in humans and mice: *iNOS*, inducible primarily in macrophages; *nNOS*, in neurons; and *eNOS*, in endothelial cells. *iNOS* expression is inducible and plays a major role in immune regulation. NO has a well-established role in macrophage function, and recently has been shown to affect TCR signaling, cytokine receptor expression, and the phenotype of T cells. At high concentrations, NO inhibits TCR-induced T cell proliferation and cytokine production [132]. The mechanism regulating *iNOS* expression in MSCs, however, is unknown (Figure 9).

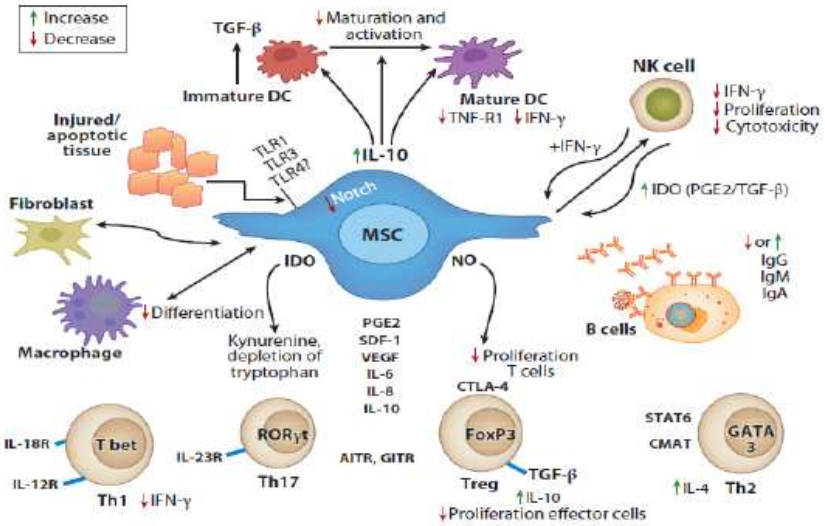

Figure 9. ***A summary of the range of soluble and cell-surface proteins that may both mediate the effects of hMSCs and provide information to hAMSCs about the local environment***

1.9 OVERVIEW OF THE IMMUNE SYSTEM

The immune system is a set of cells, tissues and organs that perform the function of defense against infectious agents such as bacteria, viruses, parasites, and fungi or non-infectious foreign substances. The immune system is capable to distinguish between the body's own cells known as self-cells and foreign cells called, in contrast, non-self-cells. Generally the immune system launches an attack against non-self markers to eliminate them from the body through a defense mechanism defined "immune response". Every molecule capable of triggering an immune response is called "antigen" that is any substance that induces immune system to produce antibodies against it. Not always this happens, in fact, in particular conditions an immune response is wrongly triggered against self-molecules therefore is defined "autoimmune response" [133].

1.9.1 The Structure of the Immune System

The lymphoid organs are organized tissues containing large numbers of lymphocytes. Lymphoid organs can be divided into central or primary lymphoid organs, bone marrow and thymus, where lymphocytes are generated, and peripheral or secondary lymphoid organs, lymph nodes and spleen, where adaptive immune responses are initiated and where lymphocytes are maintained.

1.9.2 Immune cells

The cells of the immune system derive from the multipotent hematopoietic stem cells in the bone marrow. These multipotent cells divide to produce two specialized types of stem cells, a common lymphoid progenitor that gives rise to the T and B lymphocytes responsible for adaptive immunity and a common myeloid progenitor that gives rise to different types of leukocytes, erythrocytes and the megakaryocytes that produce platelets [134].

Lymphocytes mature in the primary lymphoid organs, precisely B cells mature in the bone marrow and T cells mature in the thymus. B cells leave the bone marrow when they are still immature, therefore they complete their maturation in secondary lymphoid organs unlike T cells leaving the thymus

only when they are ripe. B lymphocytes, or B cells, when activated differentiate into plasma cells that secrete antibodies. T lymphocytes, or T cells, are divided in two main classes: one class differentiates on activation into cytotoxic T cells, which kill cells infected with viruses, whereas the second class of T cells differentiates into cells that activate other cells such as B cells and macrophages. A third lineage of lymphoid cells, called natural killer cells are able to recognize and kill some abnormal cells, for example some tumor cells and virus-infected cells.

The leukocytes that derive from the myeloid stem cell are the monocytes, the dendritic cells, the basophils, eosinophils and neutrophils. The latter three are collectively termed either granulocytes, because of the cytoplasmic granules whose characteristic staining gives them a distinctive appearance in blood smears, or polymorphonuclear leukocytes, because of their irregularly shaped nuclei [134]. They circulate in the blood and enter the tissues only when recruited to sites of infection or inflammation. Neutrophils are recruited to phagocytose bacteria. Eosinophils and basophils are recruited to sites of allergic inflammation. Immature dendritic cells travel via the blood to enter peripheral tissues, where they ingest antigens. When they encounter a pathogen, they mature and migrate to lymphoid tissues, where they activate antigen-specific T lymphocytes. Monocytes, or mononuclear phagocyte, enter tissues, where they differentiate into macrophages that are the main tissue-resident phagocytic cells of the innate immune system. Mast cells arise from precursors in bone marrow but complete their maturation in tissues, they are important in allergic responses.

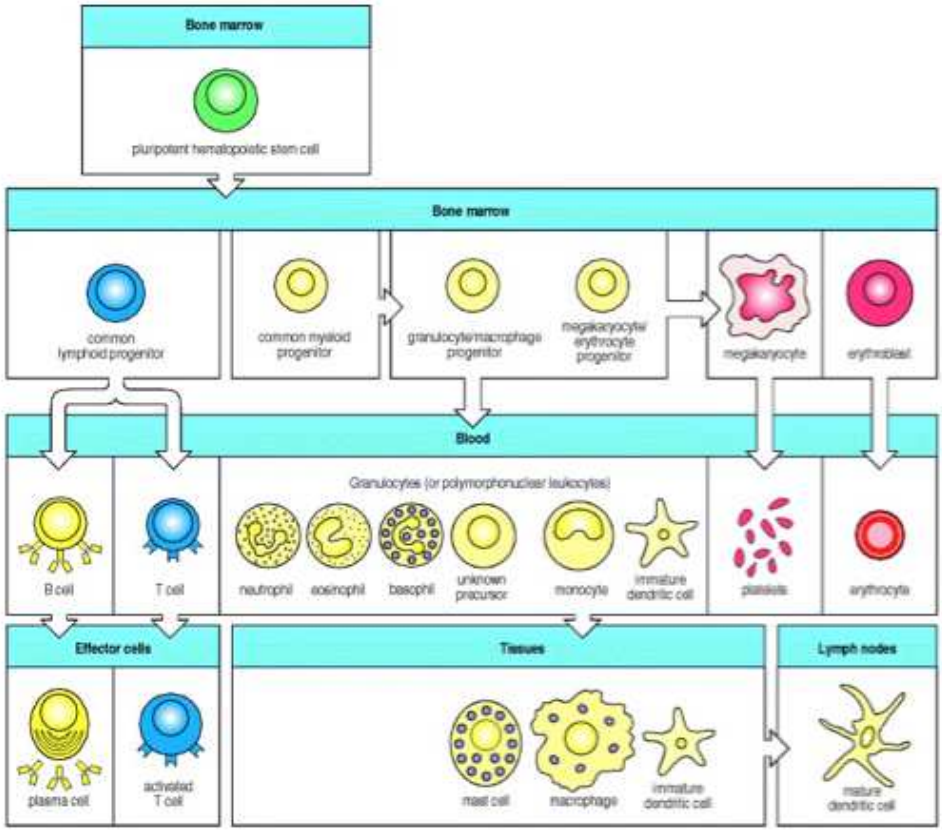

Figure 10. ***All the cellular elements of blood, including the lymphocytes of the adaptive immune system, arise from hematopoietic stem cells in the bone marrow.***
These pluripotent cells divide to produce two more specialized types of stem cells, a common lymphoid progenitor that gives rise to the T and B lymphocytes responsible for adaptive immunity, and a common myeloid progenitor that gives rise to different types of leukocytes (white blood cells), erythrocytes (red blood cells that carry oxygen), and the megakaryocytes that produce platelets that are important in blood clotting. The existence of a common lymphoid progenitor for T and B lymphocytes is strongly supported by current data. T and B lymphocytes are distinguished by their sites of differentiation—T cells in the thymus and B cells in the bone marrow—and by their antigen receptors. Mature T and B lymphocytes circulate between the blood and peripheral lymphoid tissues. After encounter with antigen, B cells differentiate into antibody-secreting plasma cells, whereas T cells differentiate into effector T cells with a variety of functions. A third lineage of lymphoid-like cells, the natural killer cells, derive from the same progenitor cell but lack the antigen-specificity that is the hallmark of the adaptive immune response (not shown). The leukocytes that derive from the myeloid stem cell are the monocytes, the dendritic cells, and the basophils, eosinophils, and neutrophils. The latter three are collectively termed either granulocytes, because of the cytoplasmic granules whose characteristic staining gives them a distinctive appearance in blood smears, or polymorphonuclear leukocytes, because of their irregularly shaped nuclei. They circulate in the blood and enter the tissues only when recruited to sites of infection or inflammation where neutrophils are recruited to phagocytose bacteria. Eosinophils and basophils are recruited to sites of allergic inflammation, and appear to be involved in defending against parasites. Immature dendritic cells travel via the blood to enter peripheral tissues, where they ingest antigens. When they encounter a pathogen, they mature and migrate to lymphoid tissues, where they activate antigen-specific T lymphocytes. Monocytes enter tissues, where they differentiate into macrophages; these are the main tissue-resident phagocytic cells of the innate immune system. Mast cells arise from precursors in bone marrow but complete their maturation in tissues; they are important in allergic responses [134] .

1.9.3 Cytokines and Chemokines

Components of the immune system communicate with one another by exchanging chemical messengers called cytokines. Cytokines are a class of secreted proteins, which regulate and coordinate many activities of the cells of innate and adaptive immunity. Cytokines include a diverse assortment of interleukins, interferons, and growth factors. Chemokines are a group of cytokines that regulate cellular migration from the blood to several tissues. They are released by cells at a site of injury or infection and call other immune cells to the region to help repair the damage or fight off the invader [135].

1.9.4 Innate and Adaptive Immunity

Defense against microbes is mediated by the early reactions of innate immunity and the later responses of adaptive immunity. Innate immunity or natural/ native immunity is characterized by defended mechanism already existing against infection such as physical and chemical barriers, phagocytic cells (neutrophils, macrophages), dendritic cells, natural killer (NK) cells and blood proteins, including members of the complement system. The adaptive immunity or specific immunity or acquired immunity develops in response to infection itself [134].

1.9.5 Mononuclear Phagocytes: Macrophages

The majority of tissues in the body contain tissue-resident macrophage populations that have a long life and arise from yolk sac and fetal liver precursors during fetal development. These cells differentiate in specific tissue phenotype such as Kuppffer cells in the liver, microglia in the brain, alveolar macrophages and macrophages in the spleen.

In adulthood, macrophage cell line derives from hematopoietic populations in bone marrow and it is stimulated by a cytokine called M-CSF (Monocyte Colony-Stimulating Factor). In fact myeloid progenitors originate monocytes that enter the peripheral blood stream and move to the tissues, especially during the inflammatory reactions, where they differentiate into macrophages.

Activated macrophages secrete many different cytokines for the recruitment of more monocytes and leukocytes from the blood into sites of infections. The activation of several macrophage-associated functions is performed after recognition of microbial structures and host molecules produced in response to infections and injury. These various activating molecules bind to specific signaling receptors located on the surface of or inside macrophages. Examples of these receptors are the Toll-like receptors (TLR). Depending on the types of activating stimuli they are exposed to macrophages can acquire distinct functional capabilities.

Three different subsets of human macrophages exist: classical and non-classical macrophages, which are identifiable on the basis of different expression levels of *CD14* on their surface and specific functions.

- Classical macrophages are rapidly recruited to sites of infection or tissue injury and have the role of effector cells in Th1 cellular immune response. In the classical activation cytokines activate macrophages to become efficient at killing microbes and they can prime them to secrete pro-inflammatory cytokines and to produced increased amount of superoxide anion and oxygen and nitrogen radicals that enhanced their microbicidal and tumoricidal capacity.
- Non-classical macrophages are involved in repairing damaged tissue and are known as patrolling due to their crawling movement on the endothelial cell surface. The major function of macrophages is to ingest and kill microbes throughout enzymatic generation of reactive oxygen species (ROS). Activated macrophages secrete several cytokines that act on endothelial cells lining blood vessels to enhance the recruitment of more monocytes/macrophages and other leukocytes from the blood into sites of infection. Activating molecules, that are both molecular structures produced by microbial pathogens and endogenous molecules produced by or released from damaged and dying cells, bind to specific signaling receptors located on the surface of or inside the macrophage. Examples of these receptors are the Toll-like receptors. Macrophages can acquire distinct functions depending on the types of stimuli [134-135].

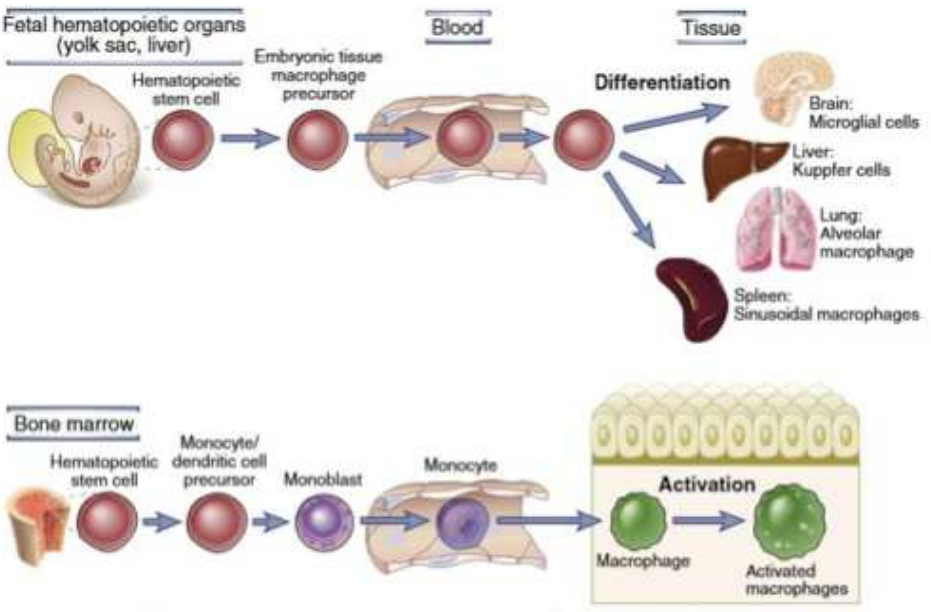

Figure 11. ***Maturation of mononuclear phagocytes. Tissue resident macrophages, which differentiate into specialized forms in particular organs, are derived from precursors in the yolk sac and fetal liver during fetal life. Monocytes arise from a precursor cell of the myeloid lineage in the bone marrow, circulate in the blood, and are recruited into tissues in inflammatory reactions, where they further mature into macrophages. Subsets of blood monocytes exist, which have distinct inflammatory or reparative functions (not shown) .***

1.9.6 Macrophage Polarization

Classically activated macrophages (M1) exhibit inflammatory functions, whereas alternatively activated macrophages (M2) exhibit anti-inflammatory functions.

Macrophages derived from monocyte precursors undergo specific differentiation depending on the local tissue environment. They respond to environmental cues within tissues such as damaged cells, activated lymphocytes, or microbial products, to differentiate into distinct functional phenotypes.

The M1 macrophage phenotype is characterized by the production of high levels of pro-inflammatory cytokines, an ability to mediate resistance to pathogens, strong microbicidal properties, high production of reactive nitrogen and oxygen intermediates, and promotion of Th1 responses.

In contrast, M2 macrophages are characterized by their involvement in parasite control, tissue remodeling, immune regulation, tumor promotion

and efficient phagocytic activity. Lipopolysaccharide (LPS), interferon gamma (*IFN-γ*) and granulocyte-macrophage colony-stimulating factor (GM-CSF) polarize macrophages towards the M1 phenotype, which induces secretion of large amounts of cytokines such as interleukin-1-beta (*IL-1β*), tumor necrosis factor-alpha (*TNF*)-alpha, interleukin-12 (*IL-12*), interleukin-18 (*IL-18*) and interleukin-23 (*IL-23*). Phenotypically, M1 macrophages express high levels of major histocompatibility complex class II (*MHC-II*), the *CD68* marker, and co-stimulatory molecules *CD80*. M1 macrophages have also been shown to up-regulate the expression of the intracellular protein suppressor of cytokine signaling 3 (*SOCS3*), as well as activate inducible nitric oxide synthase (*NOS2* or *iNOS*) to produce nitric oxide from L-arginine. In disease contexts, M1 macrophages are implicated in initiating and sustaining inflammation, and can therefore be detrimental to health. In contrast, M2 macrophage activation is induced by fungal cells, immune complexes, helminthic infections, complement components, apoptotic cells, macrophage colony stimulating factor (*M-CSF*), interleukin-4 (*IL-4*), interleukin-13 (*IL-13*), interleukin-10 (*IL-10*) and transforming growth factor-beta (*TGF-beta*) [134]. This activation leads to the secretion of high amounts of *IL-10* and low levels of *IL-12*. Phenotypically M2 macrophages have been characterized as *IL-12* low, *IL-10* high, *IL-1decoyR* high, *IL-1RA* high. They are also defined as *IL-2low*, *IL-23low*, *IL-1betalow* and *caspase-1low* [136] . In addition, they express high levels of scavenger mannose and galactose E-type and C-type receptors, and repurpose arginine metabolism to express ornithine and polyamine, which promotes growth [135, 137, 138]

M2 macrophages can be further divided into subsets (Table 1), specifically M2a, M2b, M2c and M2d based on their distinct gene expression profiles [1].

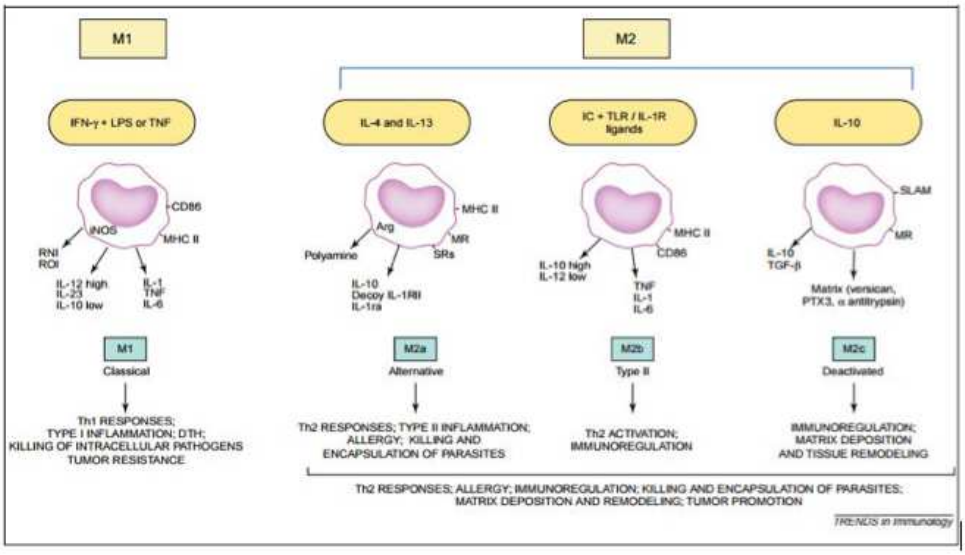

Figure 12. ***Inducers and selected functional properties of different polarized macrophage populations. Macrophages polarize and acquire different functional properties in response to environment-derived signals. Macrophage exposure to IFN-g and LPS drives M1 polarization, with potentiated cytotoxicand antitumoral properties, whereas M2 macrophages are in general more prone to immunoregulatory and protumoral activities. In particular, M2a (induced by exposure to IL-4 and IL-13) and M2b (induced by combined exposure to immune complexes and TLR or IL-1R agonists) exert immunoregulatory functions and drive type II responses, whereas M2c macrophages (induced by IL-10) are more related to suppression of immune responses and tissue remodeling. Abbreviations: DTH, delayed-type hypersensitivity; IC, immune complexes; IFN-g, interferon-g; iNOS, inducible nitric oxide synthase; LPS, lipopolysaccharide; MR, mannose receptor; PTX3, the long pentraxin PTX3; RNI, reactive nitrogen intermediates; ROI, reactive oxygen intermediates; SLAM, signaling lymphocytic activation molecule; SRs, scavenger receptors; TLR, Toll-like receptor.***

The M2a subtype is elicited by *IL-4, IL-13* or fungal and helminthic infections. The M2b subtype is elicited by *IL-1* receptor ligands, immune complexes and LPS whereas the subtype M2c is elicited by *IL-10*, TGF-beta and glucocorticoids. The fourth type, M2d, is elicited by interleukin 6 (*IL-6*) and adenosine [137].

M1 and M2 macrophages have distinct chemokine and chemokine receptor profiles, with M1 secreting the Th1 cell attracting chemokines *CXCL9* and *CXCL10* and M2 secreting *CCL17, CCL22 and CCL24* [1]. It has recently been demonstrated that in vitro, macrophages are capable of complete repolarization from M2 to M1 and vice versa depending on the chemokine environment [138].

Table 1. ***Classically activated (M1) and alternatively activated (M2) subset phenotypes [1]***

	M1	M2a	M2b	M2c
Stimulation/activation	IFN-Y LPS GM-CSF	IL4 IL-13 Fungal and Helminth infection	ICs IL-1R	IL-10 TGF-beta GCs
Marker expression	*CD68 CD86 CD80* MHC II IL-1R TLR2 TLR4 iNOS SOCS3	*CD163* MHC II SR MMR/CD206 *CD200R* TGM2 DecoyR IL-1R II	*CD86* MHC II	*CD163* TLR1 TLR8
Cytokine secretion	TNF IL-1beta IL-6 IL-12 IL-23	IL-10 TGF-beta IL-1ra	IL-1 IL-6 IL-10 TNF-alpha	IL-10 TGF-beta
Chemokine secretion	CCL10 CCL11 CCL5 CCL8 CCL9 CCL2 CCL3 CCL4	CCL17 CCL22 CCL24	CCL1	CCR2

2. IMMUNOMODULATORY PROPERTIES OF HUMAN AMNIOTIC STEM CELLS OBTAINED THROUGH A NEWLY ESTABLISHED ISOLATION PROTOCOL

INTRODUCTION

With the field of mesenchymal stem cell research taking off in the late 1980's and the early 1990's, scientists made significant observations that highlighted the importance of adult mesenchymal stem cells (MSCs) for regenerative medicine, including their presence in most adult tissues [139-141]. Various projects arising from these initial observations refined isolation methods and characterization of these cells and ultimately led to their translation into clinical therapies. Among MSCs, amnion-derived stem cells are considered as a novel and convenient source in cell-based applications due to their great plasticity and demonstrated differentiative capacity, together with their immuno-suppressive and -modulatory properties. Furthermore, human term placenta is easy to procure as it is routinely discarded post partum, and it allows for the collection of a large number of cells, without posing ethical debate [41]. Despite the possible clinical importance of these cells for the repair/regeneration of damage or diseased tissues or organs, there is no a well-defined protocol for the isolation and expansion of MSCs from human term placenta. Several protocols of MSCs isolation have been reported such as explants and enzymatic procedure whose results are still controversial. The first aim of the present study was to optimize protocols for the isolation, expansion and in vitro characterization of a homogenous MSC population from the human amniotic membrane (hAM-MSCs). One of the most intriguing features of hAM-MSCs is that they escape immune recognition and can inhibit immune responses. Knowledge about their capability to interact with immune cells and modulate them is still incomplete. The second aim of this study was to investigate in vitro the immunomodulatory and immunosuppressive properties and to assess whether they can be exploited in human regenerative medicine.

2.2 MATERIALS & METODS

Amnion collection

Placentas (n=21) were isolated from healthy women, that gave informed consent, after vaginal delivery and caesarean section and gently provided by Children's Hospital Salesi. All samples were obtained from uncomplicated pregnancies and were therefore considered normal. Portions of amnion were kept at 4°C in phosphate-buffered saline (PBS; Sigma) with 2% Antibiotic/Antimycotic (A/A) (100 U/ml penicillin–100 µg/ml streptomycin- 250 µg/ml amphotericin, Euroclone) and processed within 12h-24h.

Isolation of human amniotic mesenchymal stem cells

Isolation of amnion-derived cells (hAM-MSCs) was performed by adapting Marongiu et al. protocol [63]. The amnion was manually separated from the chorion as demonstrated in Figure 13A and was washed two to three times with PBS 1X supplemented with 2% Antibiotic/Antimycotic 100X. Each wash was performed moving the amnion to a clean beaker with sterile forceps (Figure 13B). This washing step is crucial for the trypsin to work properly, because the blood clots reduce the efficiency of the trypsin (Figure 13C).

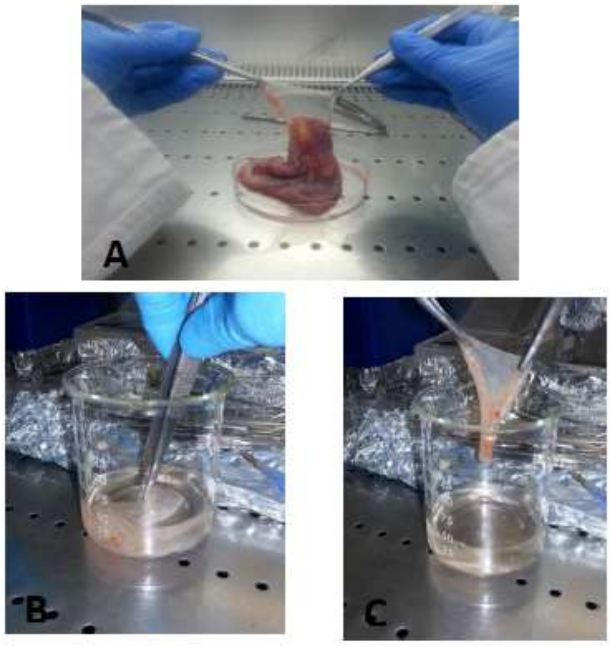

Figure 13. ***Isolation of hAMSCs (A) Peeling and (B-C) washing the amniotic membrane in HBSS***

Once cleared all clots on the membrane (Figure 14 A, B), amnion was placed onto a clear surface (Figure 14 B), expanded (Figure 14 C, D) and cut in large fragments (about 10 cm^2).

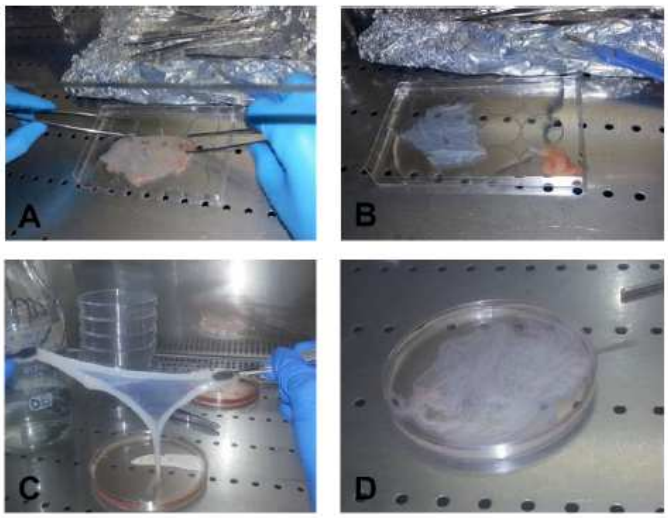

Figure 14 ***Isolation of hAM-MSCs. (A-B) Peeling the amniotic membrane from the underlying chorionic membrane. (C-D) the amniotic membrane***

The amniotic fragments were then incubated with 0.05% trypsin/EDTA solution (trypsin/EDTA 0.25% (Corning), HG-DMEM, and 2% A/A prewarmed at 37°C in a water bath. Incubation lasted for 1 h at 37°C. Fragments were vigorously shaked every 15 minutes to allow for the proper release of amniotic epithelial cells (AEC). The amniotic membranes were then transferred into a 50 ml beaker with cold Hanks' Balance Salt Solution (HBSS, Lonza) discarding the trypsin solution, and washed two to three times with ~20 ml cold HBSS, each time by moving the amnion to a clean beaker. Membranes were then smashed into smaller fragments (5-10 mm^2). Fragments were transferred into two (or more) 15 ml centrifuge tubes, allowing the excess of HBSS to drip from the membrane. The fragments were digested with the digestion solution, consisting of Minimum Essential Medium Eagle (EMEM, with 25mM HEPES buffer without L-glutamine, with Earle's BSS; Lonza) supplemented with Collagenase type IV 1mg/ml (Life Technologies) and 25 μg/ml DNase I (Sigma). The digestion solution was added to completely fill the tubes. Incubation occurred in a rotator for 3h at 37°C, checked every half hour. After 3h incubation the tissue appeared completely dissolved. The remaining undigested amniotic fragments were

then removed and non-adherents cells were filtered through a 100µm cell strainer (Sigma) before being collected by centrifugation at 5 min at ~200 × g 4°C. The supernatant was gradually discarded and the pellet was resuspended with fresh HBSS to fill the tube and centrifuged again 5 min at ~200×g at 4°C. The pellet was finally resuspended in 1 ml of Standard Culture Medium consisting of DMEM High Glucose, Dulbecco's Modified Eagle's Medium, HG-DMEM Sigma, 10% heat-inactivated fetal bovine serum (FBS, v/v) (Euroclone), 100 mM non-essential amino acid (Invitrogen), 200 mM L-glutamine (Cellgro), 55 mM 2-mercaptoethanol (Life Technologies), 2% A/A solution, 10 ng/ml human recombinant epidermal growth factor (EGF; Life Technologies) to determine the cell number.

Cells were plated at the density of 1×10^5 cells per cm^2 in Standard Culture Medium. To remove slow-adherent amniotic epithelial cells, the medium was replaced for the first time 1 to 2h after plating. Cultures of presumptive human amniotic membrane-derived mesenchymal stem cell were let grow. Then the medium was changed two/three times a week or according to the experiment requirements.

The efficacy of the isolation protocol reported above was gradually improved by changing one condition at the time. Subsequent protocols included modifications of the enzymatic digestion procedure. They consisted of:

- Amnion fragmentation;
- Extension enzymatic treatment (3h);
- 100µm cell strainer filter.

Some modifications at the Marongiu et al. protocol [63] were performed in order to obtain uniformity of the cell population from the amniotic membrane, and to minimize the presence of maternal cells for large-scale in vitro expansion. These changes consisted of:

- Amnion fragmentation: this step was added to increase the cell harvesting efficiency;

- Prolonged digestion treatment (3h): the longer duration from 1h to 3h of the digestion treatment was performed to achieve a complete tissue dissolution;
- Filtration: a 100µm cell strainer was used to reduce the presence of the debris.

Cell expansion and culture maintenance

hAM-MSCs have the capacity to adhere to culture dish. When the adherent cells reached confluence, covering 80% of culture flask, the cells were washed once with HBSS and trypsinized with 0.25% Trypsin-EDTA for 5-6 minutes at 37°C. After detachment of the adherent cells, suspension centrifuged at 500xg for 5 minutes, the supernatant was discarded, and cell pellets were resuspended in Standard Culture Medium. The number of viable cells was counted by the trypan blue dye exclusion method, using a Burker chamber. Cells were transferred to new culture flask at different densities according to the experiment to be performed. Cultures were performed in Standard Medium Culture, which was replaced 2 to 3 times a week, after washing the cells with HBSS. For culture maintenance and to perform experiments, cells were kept at 37°C in a humidified atmosphere with 5% CO_2.

Amniotic mesenchymal stem cells characterization

The hAM-MSCs cultures, the phenotype, growth of primary and passaged cells were routinely visualized using an inverted research microscope (MEIJI TECHNO). To determine their stem cell potential presumptive the proliferative rate, MSC-associated markers expression, and their immunomodulatory and immunosuppressive potential were tested.

Proliferation assay

Growth curves were studied at passages 2 (P2) with 3 replicated biological (P1A, P1B, P1C). To this hAM-MSCs were plated at density $9.5x10^3$ cells/well into six-well tissue culture polystyrene dishes (EuroClone). Every 2 days, over 12 days-culture period, cells from one well of plate were

trypsinized and counted. The total number of live cells was obtained at each time point by staining cells with the trypan blue dye method.

Doubling time (DT) was assessed from passage (P)2 to P5. Cells (9.5×10^3 cells/well) were seeded into six-well tissue culture polystyrene dishes. Cells were trypsinized every 4 days, counted and replated at the same density.

The DT value was obtained for each passage according to the formula DT=CT/CD, where CT represents the culture time and CD = ln(Nf/No)/ln2 represents the number of cell generations (Nf represents the number of cells at confluence, No represents the number of seeded cells).

Colony-forming unit-fibroblastic (CFU-F) assay was performed at P1 plating cells at different densities (1×10^3, 3.5×10^3, 35×10^3 cells/cm^2). Cells were plated in six-well plates and cultured in 5% CO_2 and 90% humidity at 37°C for 2 weeks in Standard Medium Culture. Then, colonies were fixed with PFA 1% and stained with Giemsa at room temperature, and washed twice.

At the end of the 2 weeks culture period, the colonies were counted under an inverted research microscope (MEIJI TECHNO). Colonies were considered if formed by 15-20 nucleated cells.

Immunomodulatory potential assessment

U937 cell line was treated with RPMI (Roswell Park Memorial Institute) 1640 Medium with 10% heat-inactivated FBS containing 10 ng/ml phorbol 12-myristate 13-acetate (PMA) and was incubated for 48h. This is a critical step to make monocytes adhere to the bottom of the plate and differentiate them into macrophages. After that, U937 cells were cultured for 48h and 72h at 37°C with and without a combination of either tumor necrosis factor alpha (*TNF-α*) + interferon, gamma (*IFN-γ*) or interleukin 13 (*IL-13*) + interleukin 4 (*IL-4*) at the concentrations of 20 ng/ml each. Adding *TNF-α* and *IFN-γ* cells will polarize already differentiated macrophages towards a pro-inflammatory phenotype (M1), whereas adding *IL-13* and *IL-4* will polarize macrophages towards an anti-inflammatory M2-like phenotype.

U937 (1×10^6) were seeded alone and in some experiments together with hAM-MSCs (1×10^5) by a trans-well membrane (0.4 μm pore size, Corning)

at a 1:10 ratio and cultured for 48h and 72h at 37°. At each time point the supernatant was harvested from the cultures and stored at –20°C.

After 48h/72h U937 were removed from cultures and co-cultures and total RNA was then extracted using TRI REAGENT according to manufacturer's instruction.

Quantitative reverse transcription polymerase chain reaction (qPCR) analysis was used to evaluate the expression of immunomodulation-associated markers in monocytes such as *IL-10, IL-1β, IL-6, iNOS, TNF-α.*

Immunosuppressive potential assessment

hAM-MSCs-associated immunosuppressive potential

hAM-MSCs were seeded at the density of 3,5 x 10^3 in the 24-well plate and cultured for 48h at 37°C before stimulation started. Stimulation was performed using soluble recombinant rat *TNF-α* and *IFN-γ* (Prepotech) at the concentrations of 20 ng/mL each, for 48h/72h. At each time point the supernatant was harvested from the cultures and stored at –20°C. After 48h/72h hAM-MSCs were removed from cultures and total RNA was then extracted using TRI REAGENT according to manufacturer's instruction.

Quantitative reverse transcription polymerase chain reaction (qPCR) analysis was used to evaluate the expression of immunosuppressive-associated markers in hAM-MSCs such as *PGE-2, TGF-β, COX-2, iNOS*.

U937 monocytes proliferation test

U937 monocytes 1 x 10^6 were labeled with 5Mm carboxyflurescein diacetate succinimidyl ester (CFSE) for 45 minutes at room temperature. The labeling was than terminated by adding PBS 1X. After washing cells were cultured in 3 ml of Standard Culture Medium in 6-well plate with and without hAM-MSCs in cell-cell contact setting at a 1:10 ratio. U937 proliferation was assessed by flow cytometry after three days of culture.

Extraction total RNA

Total RNA was extracted from cells at different passages (P1, P5) to characterize the presumptive hAM-MSCs and at P1 to determine their

immunomodulatory/immunosupressive potential cells after exposing them to pro/anti-inflammatory cytokines (*IFN-γ / TNF-α* and *IL-4 / IL-13*). Total RNA was extracted from cells using TRI Reagent® (Sigma) according to the manufacturer's protocol. Cells were lysed in TRI REAGENT by repeated pipetting. The homogenate was centrifuged at 12000 x g for 15 minutes at 4°C to remove the insoluble material. The supernatant containing RNA, DNA and protein was transferred into to a fresh tube. To ensure complete dissociation of nucleoprotein complexes, samples were allowed to stand for 5 minutes at room temperature. Then chloroform was added, the samples were tightly shaked vigorously for 15 seconds, and allowed to stand for 2-15 minutes at room temperature. The resulting mixture was centrifuged at 12000 x g for 15 minutes at 2-8°C. This centrifugation separates the mixture into 3 phases:

- a red organic phase (containing protein)
- as interphase (containing DNA)
- a colorless upper aqueous phase (containing RNA)

The aqueous phase was transferred into a fresh tube and 2-propanol was added. The samples were allowed to stand for 10 minutes at room temperature and were then centrifuged at 12000 x g for 10 minutes at 4°C. The RNA precipitate formed a pellet on the side and bottom of the tube. The supernatant was removed, the RNA pellet washed by adding ethanol 75%, and the sample vortexed and then centrifuged at 7500 x g for 5 minutes at 4°C. The RNA pellet was finally let dry for 10 minutes by air-drying. To facilitate dissolution 30µl RNase free water were used, mixing by repeated pipetting for 10 minutes. Afterwards the samples were treated with 0.3 µl DNase for 10 minutes at room temperature, in order to avoid DNA contamination. RNA concentration and purity were measured by Nanodrop® Spectrophotometer (Nanodrop® ND1000).

Retrotranscription

The cDNA was synthesized from total RNA (500 ng) using a PrimeScriptTM RT-Reagent Kit Takara, under the following conditions: 37°C for 15 minutes, 85°C for 5 seconds and hold at 4°C.

Gene expression analysis

The gene expression evaluation was performed using human specific sequences. Oligonucleotide primers were designed using open source Primer-BLAST, across an exon–exon junction in order to avoid genomic DNA amplification and make manual corrections to make better amplification. Sequence conditions and the references used are shown in tables 1-2.

Table 1-2. The primer sequences, the melting temperature used and the size of the amplification product

GENE	Sequences (5'→3')	Tm (°C)	Product size (bp)
Mesenchymal markers			
CD44 molecule (CD44)	S: GGAGCAGCACTTCAGGAGGTTAC	63	129
	A: GGAATGTGTCTTGGTCTCTGGTAGC	63	
5'-nucleotidase, ecto (CD73)	S: GCTCTTCACCAAGGTTCAGC	59	203
	A: GTGGCTCGATCAGTCCTTCC	60	
Thy-1 cell surface antigen (CD 90)	S: CTTTGGCACTGTGGGGGTGC	64	211
	A: GATGCCCTCACACTTGACCAG	61	
Endoglin (CD105)	S: CCTGGAGTTCCCAACGGGCC	65	186
	A: GGCTCTTGGAAGGTGACCAGG	62	
Hematopoietic markers			
CD34 molecule (CD34)	S: GTGTCTACTGCTGGTCTTGG	57	200
	A: CAGTGATGCCCAAGACAGC	58	
protein tyrosine phosphatase, receptor type C (CD45)	S: GACAACAGTGGAGAAAGGACG	58	170
	A: GCTGTAGTCAATCCAGTGGGG	60	
Pluripotent markers			
POU class 5 homeobox 1 (Oct-4)	S: CGATCAAGCAGCGACTATGC	59	200
	A: AGAGTGGTGACGGAGACAGG	60	
Nanog homeobox (Nanog)	S: GCAAGAACTCTCCAACATCC	56	178
	A: GGTCTGGTTGCTCCACAT	56	
Housekeeping			
glyceraldehyde-3-phosphate dehydrogenase (GAPDH)	S: TCCACTGGCGTCTTCACC	68	78
	A: GGCAGAGATGATGACCCTTT	70	

GENE	Sequences (5'→ 3')	Tm (°C)	Product size (bp)
Pro-inf			
tumor necrosis factor (TNF-α)	S: TCTGGCCCAGGCAGTCAGATC	64	180
	A: TACAGGCCCTCTGATGGCACC	64	
interleukin 1 beta (IL-1β)	S: TGCTCTGGGATTCTCTTCAGC	59	164
	A: CTGGAAGGAGCACTTCATCTG	60	
inositol-3-phosphate synthase (Inos)	S: GAGCATCCCAAGTACGAGTG	58	141
	A: AATCTCGGTGCCCATGTACC	60	
Anti-inf			
prostaglandin E receptor (PGE-2)	S: GGAAGGAGAAAGCTCGCAAC	59	173
	A: TGAGCCAGTACTTATTGCCG	57	
interleukin 10 (IL-10)	S: GAGATGATCCAGTTTTACCTGG	56	142
	A: AGGGAAGAAATCGATGACAGC	58	
transforming growth factor beta (TGF-β)	S: TGGTCATGAGCTTCGTCAAC	58	171
	A: TCTCATTGTCGAAGCGTTCC	58	
cytochrome c oxidase subunit II (COX2)	S: TGAGTTATGTGTTGACATCCAG	62	190
	A: TCATTTGAATCAGGAAGCTGC	60	

S, sense; A, antisense; bp, base pairs.

The Polymerase Chain Reaction (PCR) was performed in a 20 µl final volume with JumpStartTM Taq DNA Polymerase (Sigma) under the following conditions: initial denaturation at 95°C for 2 minutes, 32 cycles at 95°C for 30 seconds (denaturation), 58°C for 30 seconds (annealing), 72°C for 30 seconds (elongation) and final elongation at 72°C for 10 minutes. For conventional PCR, primers were used at 10 µM final concentrations. After the amplification reaction, the resulting products were examined by electrophoresis in a 1.6% agarose gel impregnated with ethidium bromide and photographed with a UV trans-illuminator.

Quantitative PCRs were performed with SYBR® green method in a StepOne™ Real-Time PCR System, StepOne cycler software v2.3. Triplicate PCR reactions were carried out for each sample analyzed. The reactions were set on a strip in a final volume of 10 µl by mixing, for each sample, 1 µl of cDNA, 5 µl of PowerUp SYBR™ Green Master Mix containing SYBR Green as a fluorescent intercalating agent, 0.4 µl forward primer, 0.4 µl of reverse primer and 3,5 µl MQ water. The thermal profile for all reactions was 10 minutes at 95°C and then 40 cycles of 15 seconds at 95°C, 1 minute at 60°C. Fluorescence monitoring occurred at the end of each cycle. Human glyceraldehyde-3-phosphate dehydrogenase (*GAPDH*)

was employed as a reference gene in each sample in order to standardize the results by eliminating variation in cDNA quantity.

Evaluation of MSC-associated markers by Flow Cytometry

MSCs isolated from the amniotic membranes were analyzed at P4 for surface cell markers by flow cytometry. A total of 5×10^5 cells were trypsinized, fixed with ethanol 75% and incubated for 20 minutes with 0.5% bovine serum albumin (BSA) in PBS for blockage all non-specific sites. Sample was then divided into aliquots containing $1x10^5$ cells each, resuspended in PBS 1X, and centrifuged at 500xg for 5 minutes at 20°C. The surnatant was then discarded, and 5µl fluorescently labeled antibody was added to each eppendorf. Directly conjugated antibodies were as follows: phycoerythrin (PE)-conjugated ecto-5'-nucleotidase (PE-CD73; BioLegend), fluorescein isothiocyanate (FITC)-conjugated thymocyte differentiation antigen 1 (FITC-CD90; BioLegend) and the glycoprotein CD44 (FITC-BioLegend), Allophycocyanin (APC)-conjugated for integrin b1 (APC-CD29; BioLegend). Incubation was performed for 45 min at room temperature in the dark. Cells were then washed twice with filtered PBS to remove the excess of antibody and analyzed using Guava Easycite Millipore flow cytometer with GUAVASOFT 2.2.3.

Statistical analysis

Statistical analysis was performed using GraphPad Instat 3.00 for Windows (GraphPad Software). Three replicates for each experiment (doubling time, colony forming unit, quantitative PCR, cytometry analysis and PBMC proliferation test) were performed and the results are reported as mean ± standard deviation (SD). One-way analysis of variance for multiple comparisons by the Student-Newman-Keuls multiple comparison test were used to assess differences between gruops. Differences were considered statistically significant for p values < 0.05. For quantiative PCR data, non-parametric tests were used. For quantiative PCR data, non-parametric tests were used. Saphiro-Wilk normality test proved that the datasets were normaly distributed ($p > 0.05$).

2.3 RESULTS

Amnion collection and isolation of amniotic mesenchymal stem cells

The cellular yield from term amnion was up to $3x10^6$ hAM-MSCs per 10 cm^2 of starting material following the adapting protocol (Figure 3).

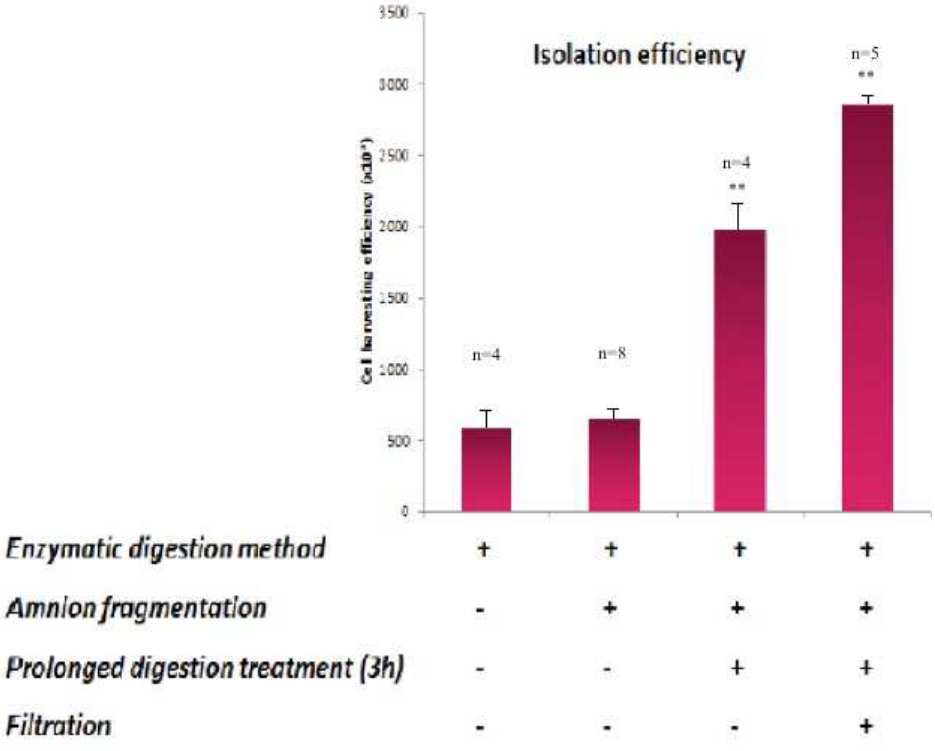

Figure 15. ***Isolation efficiency. Steps of the isolation efficiency devided into several phases: enzymatic digestion method, amnion fragmentation, prolonged digestion treatment (3h), and filtration. Values are mean ± SD. Asterisks depict highly significant (**p<0.01) differences with enzymatic digestion method.***

Cells were selected purely on their ability to adhere to plastic. The initial growth of hAM-MSCs at primary culture (P0) was highly heterogeneous and included different populations (it is possible that it could carry fetal/maternal contamination).

Cell adhesion occurred 9-10 days after the initiation of primary culture. At first the cells displayed an oval/round shape and as the process progressed they became elongated, finally acquiring fibroblastic-like morphology (Figures 4A, 4B and 4C). The fibroblast-like cells became predominant after the two-third passage of culture and these popolations were easily expanded *in vitro* for at least 6 passages (P6) without any visible modifications. Initially, the cells proliferated very rapidly with small sized spindle shaped

cells morphology. But the features gradually changed at later passages (P onwards), whereby they showed morphological changes; appeared unhealthy, larger in size and eventually died. After thawing at P1 the vitality was 60 % and conserved then shapes fibroblastic-like.

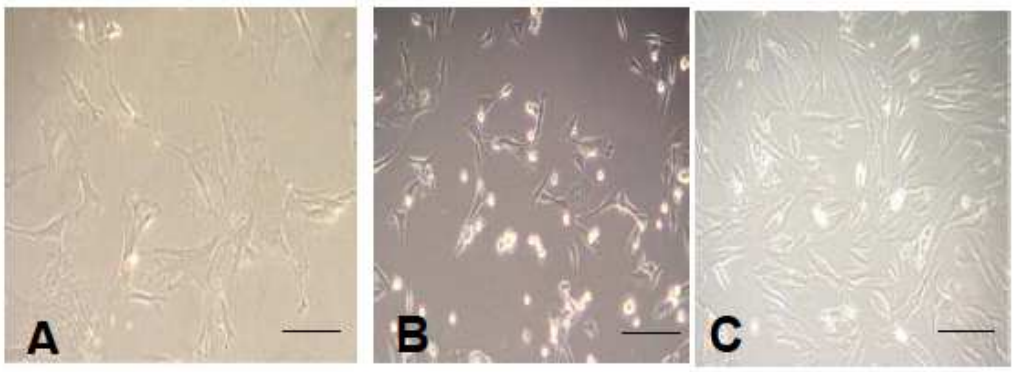

Figure 16. ***Mesenchymal stem cells of human amniotic membrane (A) on day 2 (passage 0) (B) at the passage 1 and (C) passage 4, 10X magnification. Scale bars 10µm***

Proliferation studies

Growth curve and DT

The growth curves were set up using three biological replicates. At P1 hAM-MSCs demonstrated a growth curve with an initial lag phase of 2 days that decreased after 7 days (Figure 5). The proliferative potential of hAM-MSCs was similar between P1A and P1C and differences were not statistically significant ($p<0.05$).

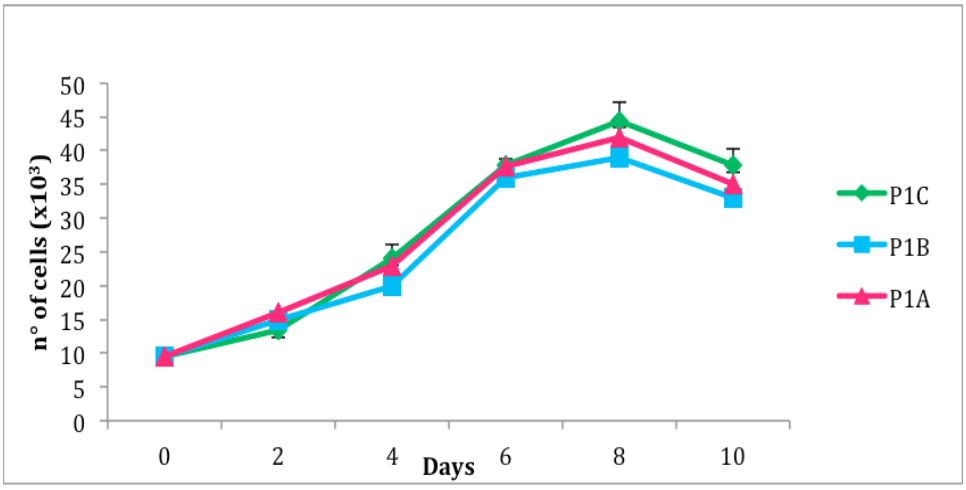

Figure 17. ***Proliferation studies. Growth curve at P1 for three hAM-MSCs biological replicates***

The DT values were similar at P1, P2, P3 (5.2 ±.0.6). They were found increased toward P4. The greater proliferative ability associated to hAM-MSCs was found at P2 (Figure 6).

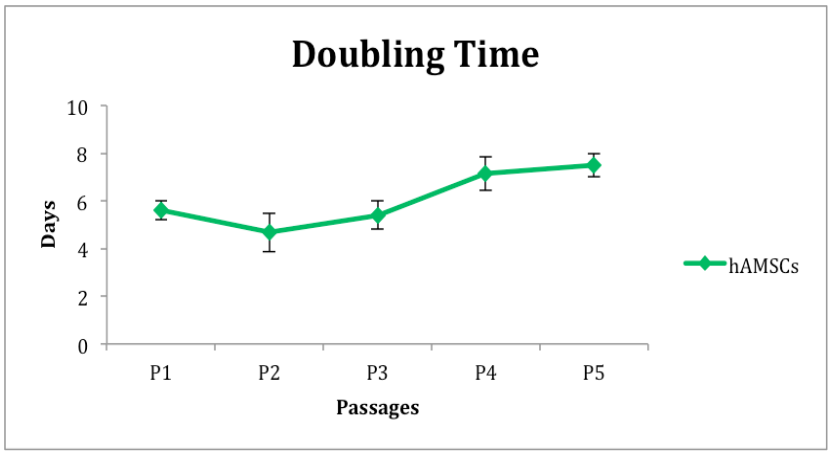

Figure 18. ***Proliferation studies. Doubling times from passage 1 to passege 5.***

CFU-F Assay

After 15 days, the number of cell colonies formed (Figure 7) was counted at P1 after seeding cells at different density/cm^2 (Table 3). The results demonstrated an increase in CFU-F frequency with increasing cell seeding density.

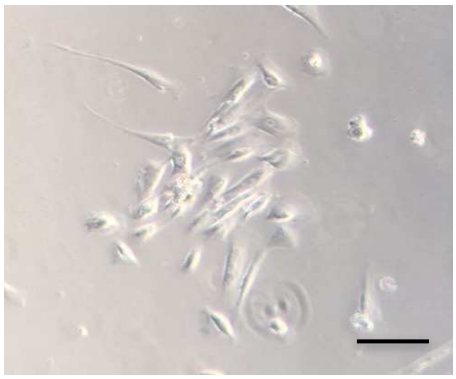

Figure 19. ***Representative colony forming unit. 10X magnification. Scale bar 10 µm***

Table 3. CFU-F assay

	density cells/cm^2	Total cells	CFU	1 CFU each
hAM-MSCs	350	3325	0	0
	1000	9500	2 ± 0.3	4750
	3500	33250	10 ± 0.6	3325

Molecular characterization

Molecular studies demonstrated that at P2 hAM-MSCs display a typical mesenchymal phenotype, that is, they are positive for *CD73, CD90, CD44*, and *CD105* and negative for the hematopoietic markers *CD34* and *CD45*. Besides very high expression of molecular markers associated with pluripotent stem cells such as *Nanog* and *Oct-4* (Figure 8).

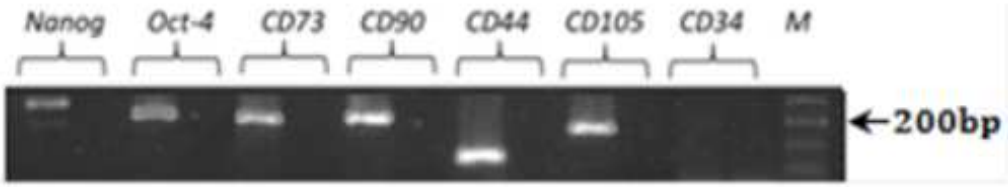

Figure 20. ***Molecular characterization of hAM-MSCs. Qualitative PCR analysis for the expression of pluripotent, mesenchymal and hematopoietic genes.***

Flow Cytometry Analysis

Immunophenotypic analysis was performed to examine the expression of the main mesenchymal and hematopoietic markers. The isolated cells were strongly positive for MSC-specific surface markers, such as *CD44, CD90,* and *CD73* (which are considered markers of adult mesenchymal stem cells). The expression profiles of these cells at passage 4 are shown in Figure 9.

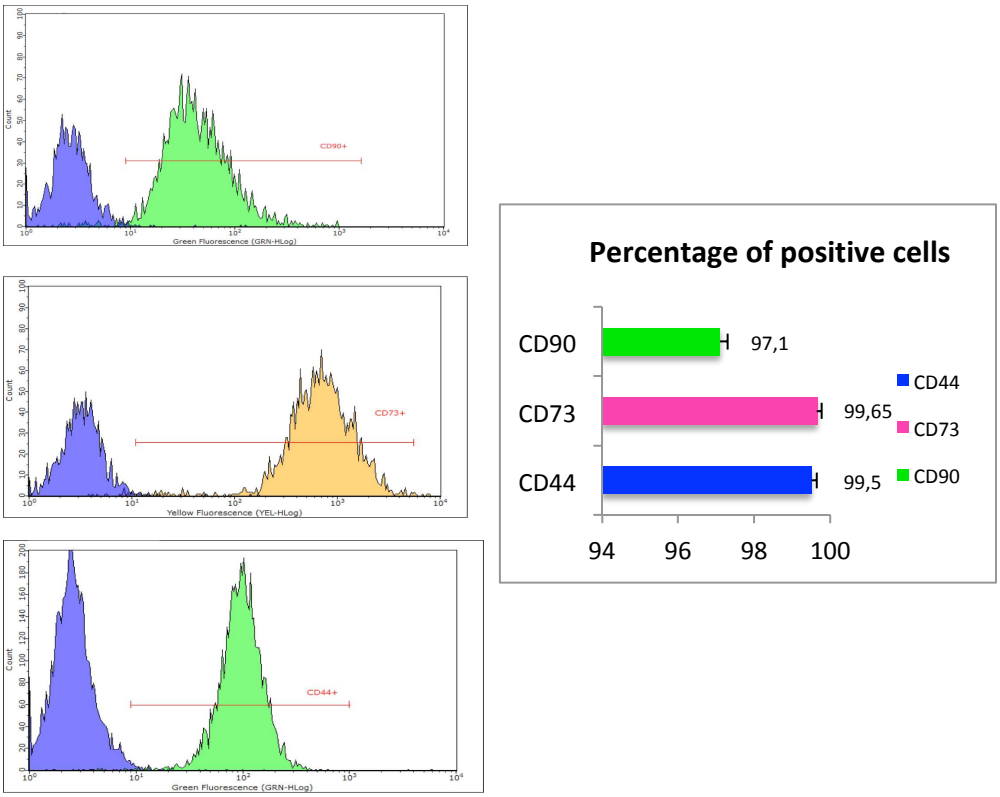

Figure 21. Flow cytometry analysis reveals CD44+, CD90+ and CD73+. The histograms on the right represent mean and SD values of three independent experiments.

Immunomodulatory potential assessment

The anti-inflammatory potential of hAM-MSCs was evaluated on the activity of the immune cells (U937 monocytes) stimulated or not with PMA. RT-PCR was performed to evaluate the expression of anti-inflammatory genes in U937. As shown in (Figure 10) U937 display a M2-like phenotype when treated with anti-inflammatory cytokines (*IL-4* and *IL-13*) displaying a significant 667.67 ± 202-fold increase in the expression of *IL-10* at 48h and a 80.28 ± 21-fold increase at 72h ($p<0.01$). The expression of *TGF-β* was found 31.49 ± 5.2-fold increased at 48h and only 2.20 ± 0.8-fold at 72h in the comparison of unstimulated monocytes (MØ). Moreover, data showed a significant upregulation in the expression of *IL-10* (3480.31 ± 1302-fold and 761.66 ± 154-fold at 48h and 72h, respectively ($p<0.01$). The expression of *TGF-β* was detected about 16.19 ± 4.2-fold increased at 48h ($p<0.05$) when monocytes were co-cultured with hAM-MSCs. The level of *TGF-β* was found lower (8.09 ± 1.4-fold) in comparison with that observed at 48h.

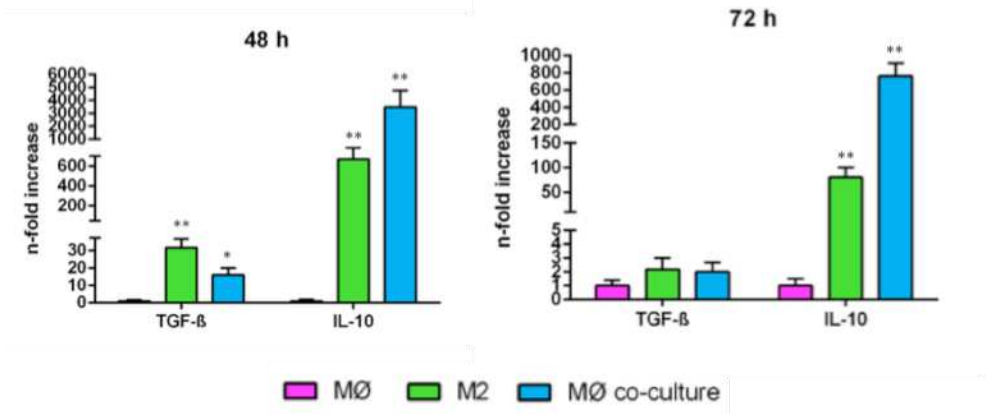

Figure 22. Quantitative PCR analysis for the expression of genes associated to anti-inflammatory potential TGF-β and IL-10. * = p<0.05, ** = p<0.01 in comparison with the negative control MØ.

On the other hand, U937 displayed a M1-like phenotype when induced with pro-inflammatory cytokines (*TNF-α* and *IFN-ɣ*). We wanted to test the potential of hAM-MSCs to reduce inflammation when co-cultured with inflamed monocytes (M1). Following exposure to pro-inflammatory cytokines for 48h M1 monocytes expressed increased levels of *IL-1β* (8.09 ± 0.6-fold), *IL-6* (1.8. ± 0.2-fold), *TNF-α* (1.47 ± 0.2-fold) in the comparison with unstimulated cells (MØ). Moreover, the expression of *IL-1β* (16.25 ± 1.2-fold), *IL-6* (16.6 ± 1.3-fold), and *TNF-α* (21.26 ± 1.8-fold) was further induced at 72h. Compared with the levels observed in M1, M1 co-cultured with hAM-MSCs produced lower levels of *IL-1β* (4.8 ± 0.32), *IL-6* (0.31 ± 0.18) and *TNF-α* (0.7 ± 0.13) at 48h. A further significant decrease ($p<0.05$) in *IL-1β* (10 ± 0.4), *IL-6* (11 ± 0.8) and *TNF-α* (14 ± 1,2) expression was detected at 72h of co-culture, thus confirming the ability of hAM-MSCs to reduce the inflammation.

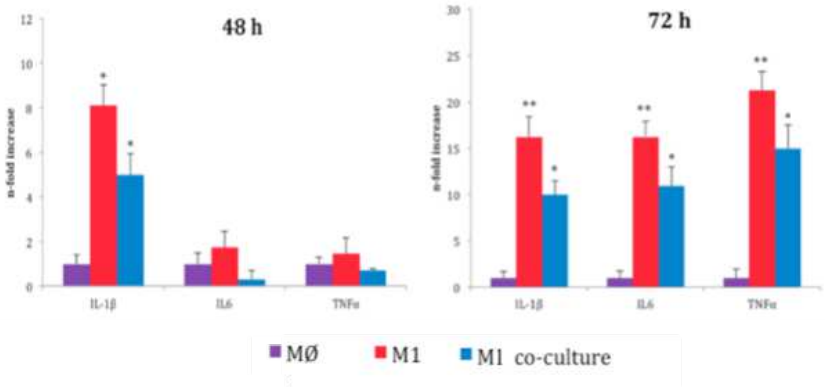

Figure 23 Quantitive PCR analysis for the expression of genes associated to immunomodulatory potential IL-1β, IL-6, TNF-α. Data represent the mean and the SD of at least three independent experiments. Asterisks depict significant (*p<0.05) and highly significant (**p<0.01) differences with negative control MØ.

Immunosuppressive potential assessment

To study the immunosuppressive features of hAM-MSCs we examined the production of anti/pro-inflammatory cytokines, as immunosuppression mediators. As shown in Figure 12 the expression of *TGF-β, PGE-2* and *COX-2*, increased of about 2.33 ± 0.7-fold, 7.99 ± 0.5-fold and 2.00 ± 0.8-fold, respectively, in hAM-MSCs stimulated with *TNF-α* and *IFN-γ* at 48h with the only exception of iNOS whose expression was decreased in comparison with the untreated cells and assessed around 0.32 ± 0.07-fold.

The expression of *PGE2* (4.54 ± 0.45-fold), *TGF-β* (67.90 ± 24-fold), and *COX-2* (427.61 ± 151-fold) significantly increased in hAM-MSCs stimulated with *TNF-α* at *IFN-γ* at 72h ($p<0.01$). Compared with untreated cells *iNOS* mRNA levels were found very low (0.1 ± 05-fold).

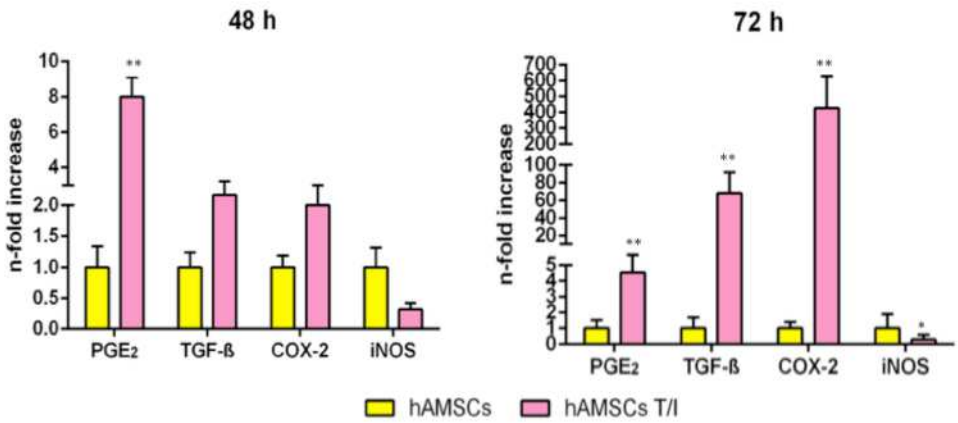

Figure 24 Quanitative PCR analysis for the expression of genes associated to immunosuppressive potential PGE-2, TGF-β, COX-2 and iNOS at 48h and 72h Data represent the mean and the SD of at least three independent experiments. *p <0.05, and **p <0.01 versus negative control MØ.

Consistent with the previous findings, when the immunosuppressive potential was functionally evaluated through U937 monocytes proliferation test, hAM-MSCs demonstrated the ability to inhibit their proliferation following 3 days of co-culture (Figures 13). The inhibitory effect was great, showing a significantly 89% decrease in monocytes proliferation ($p<0.01$).

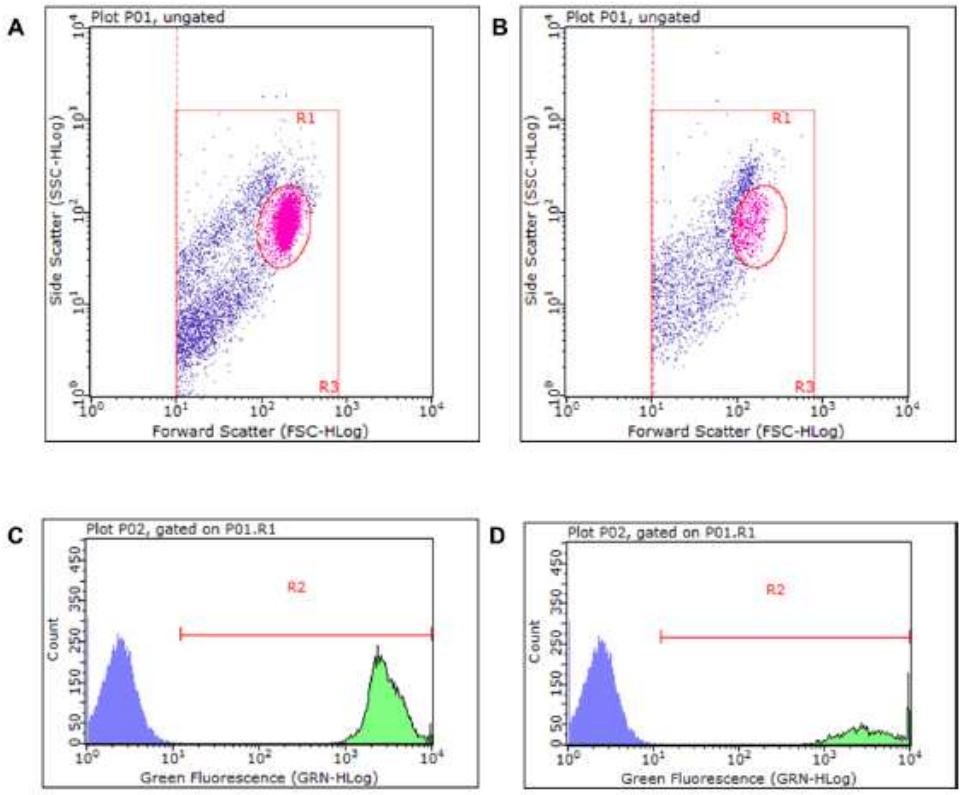

Figure 13. ***Flow cyrometric analysis showing morphological plots for U937 monocytes in absence (A) or presence (B) of hAM-MSCs. Fluorescence histograms showing U937 monocytes in absence (C) or presence (D) of hAM-MSCs positive for CFSE labeling (green).***

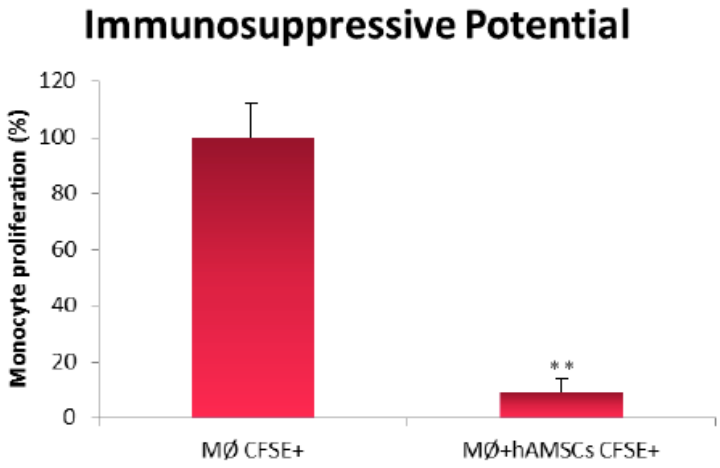

Figure 14. ***Effect of immunosuppressive potential on the proliferation of U937 monocytes in absence (MØ) or presence of hAM-MSCs (MØ+hAMSCs). Data represent the mean and the SD of at least three independent experiments. Asterisks depict highly significant (**p<0.01) differences with MØ CFSE+.***

2.4 DISCUSSION

In addressing the need to identify a source of multipotent cells that is plentiful, easy to procure and ethically acceptable, we and others have recently started to look at human term placenta. In this regard, due to the cellular diversity and different biological characteristics of its cells, human term placenta has emerged a promising tool for clinical applications and it has been primarily used in medicine in order to stimulate the healing of skin and corneal desease. More recently, it has been used in regenerative medicine because the amniotic-derived stem cells exhibit cellular plasticity, angiogenic, cytoprotective, immunosuppressive properties, antitumoural potential and the ability to generate induced plutipoten stem cells [15].

Several different protocols have been described to isolate mesenchymal stromal cells from these tissue, including cultures of unfractionated placenta or of cells recovered after rinsing of placental vessels, mechanical separation or enzymatic digestion [63, 99, 142].

Here we reported a refined isolation protocol for cells derived from mesenchymal regions of placental fetal membranes. hAM-MSCs constitute a population of cells which share common features with adult counterparts and retain them during long-term culturing.

The morphological features of fetal mesenchymal cells isolated with our methods were similar to those described for BM-MSCs, and included plastic adherence and fibroblast-like growth.

Immunophenotypic characterization of our isolated fetal mesenchymal cells showed immunopositivity to *CD90, CD44, CD73, CD105*, which represent the common and well-defined MSC markers and to pluripotent stem cells markers *Oct-4* and *Nanog*, while they were negative for hematopoietic markers such as *CD34* and *CD45* [41].

These findings suggest that our isolation procedures can effectively yield mesenchymal cells from amniotic membranes, thus expanding the possible sources of MSCs of human placental origin.

Human fetal adnexa have been recently suggested as appealing candidates for the derivation of MSCs to be used in cell-based therapies and they are believed to have higher proliferative capacity, plasticity than MSCs from bone marrow [130, 142, 143].

To test this hypothesis we investigated the proliferative activity and the doubling time. AM-derived cells were expanded rapidly with highly proliferation rate and the population doubling was decreased to 7.2 ± 0.42 prior to reaching the senescence at the 6th passage. In fact, our data demonstrated that the proliferative potential was highest at P2 and then tended to slow beyond passage 3 as already reported by Parolini at al [41].

In our study the biological properties of hAM-MSCs was also exanimated. There is a great deal of discussion on how stem/stromal cells isolated from the placenta, or other tissues, can contribuute to the regeneration of damaged tissues [144, 145]. One mechanism is by means of cell differentiation into tissue-specific cell types in order to replace damage tissue. A more recent but widely accepted mechanism is that these cells can act via paracrine signaling, thus releasing bioactive mediators that may stimulate resident target cells to proliferate, or may induce resident progenitor cells to differentiate. In the context of the deseases whereby an exacerbated inflammatory activation status persists, switching inflammation off is necessary for the resolution of injury. Since the bioactive mediators secreted by stem cells could modulate the immune response, a new proposed mechanism is that these cells could favour the repair and regeneration of damaged tissues by suppressing the immune response that is activated following the injury itself. Among the paracrine actions underlying the anti-inflammatory effect of placenta-derived cells are their interactions with immune cells of innate and adaptive immunity.

Many studies have reported the ability of placenta-derived cells to "educate" macrophages to adapt an anti-inflammatory, immune-suppressive phenotype [146-149] and to abolish the production of inflammatory cytokine by immune cells, likely through the action of soluble inhibitory factor [150].

Consistent with the previous results, when U937 cell line was treated with *IL-4* and *IL-13*, the production of anti-inflammatory cytokines (*IL-10* and *TGF-β*) by immune cells considerably increased displaying an M2-like phenotype. In addition, an increase of the expression of the anti-inflammatory cytokines *TGF-β* and *IL-10* at both time points, 48h and 72h, and a decrease of the expression of pro-inflammatory cytokines *IL-1β, Il-6* and *TNF-α* has occurred in comparison with the negative control (MØ)

when hAM-MSCs were cultured in a trans-well system with U937 monocytes (MØ co-culture), confirming the immunomodulation properties. Importantly, we demonstrated that hAM-MSCs induce macrophage differentiation in promonocytic U937 cell line favouring the generation of macrophages with M2-like features, consequently affecting their functions, such as higher phagocitosis. Moreover, this cytokine profile expression is associated with a lower stimulatory activity that rendered these cells poor inducers of T cell proliferation.

Our data also demonstrated that the immunomodulatory effect of the hAM-MSCs is non always related to the presence of external stimuli. hAM-MSCs are indeed able to release soluble factor with inhibitory effect when cultured also in non-stimulated conditions, proving that the effect is an intrinsic characteristic. Similar results were observed in work by Rossi et al. [124].

Interestingly, *IL-10* cytokine by immune cells showed a strong increase, indicating that the immune cells might be influenced by a paracrine effect [151]. Future studies are need to verify the effects of *IL-10* induce by hAM-MSCs on immune cells.

A similar behavior has occurred at 48h when the M1-like phenotype was induced, with the only exception that priming by inflammatory cytokine (*TNF-α + IFN-ɣ*) is essential for hAM-MSCs-mediated immunomodulation (M1-coculture). Several studies demonstrated that immunomodulatory function of MSCs is elicited by *IFN-ɣ* and the concomitant presence of any of three other pro-inflammatory cytokines, *TNF-α, IL-1α, IL-1β* [111, 123].

In common with previous reports we found that hAM-MSCs alone were insufficient to induce significant immunomodulation unless they were pre-activated by inflammatory cytokines [123].

Some studies have indicated that hAM-MSCs produce growth factors such as *TGF-β* and release large amount cytokines such as *PGE-2, COX-2, iNOS*, that are involved in hAM-MSCs-mediated immunosuppression [124, 130, 148, 150, 151]. In the present study we provided compelling evidence of the soluble factors-mediated immunosuppression and we demonstrated that the production of *PGE-2, COX-2*, (with only the exception of *TGF-β* at 48h) by hAM-MSCs, stimulated with pro-inflammatory cytokines, increased at 48h and this effect is enhanced at 72h. Interestingly, our data showed that

stimulated hAM-MSCs expressed very low levels of *iNOS*, at both time points, 48h and 72h, confirming the hypothesis that the mechanism of hAM-MSCs-mediated immunosuppression varies among different species. In the mouse model it has been reported that inflammatory cytokines induce significant production of NO, which then directly suppresses proliferation and cytokine production by immune cells [152]. We found that, unlike that for mouse MSCs, NO isn't involved in hAM-MSCs-mediated immunosuppression. Given that, this finding provide critical information about immunosuppression of hAM-MSCs that required further investigations.

To better understand the immunosuppressive potential of hAM-MSCs we further investigated their role in inhibiting U937 monocytes proliferation. The functional study confirmed the immunosuppressive properties of hAM-MSCs. For the first time, in this study we showed that secreted factors from hAM-MSCs impact the generation of both M1- and M2-macrophage-like cells from peripheral blood monocytes by switching the differentiation of classical activated/pro-inflammatory M1-macrophages into M2-like anti-inflammatory/regulatory macrophages, and inducing regulatory/wound healing M2-macrophages like cells wtih an enhanced anti-inflammatory profile.

This study reinforce our hypothesis that hAM-MSCs hold the ability to react to pro-inflammatory stimuli provided by microenvironment, to interact with immune cells modulating their function and to play a key role in inhibiting immune responses.

CONCLUSIONS

In 1800s, a baby born with a caul, a remnant of the amniotic sack or fetal membranes, was thought to be lucky, special or protected. Over time, fetal membranes lost their legendary power and were soon considered nothing more than biological waste after birth.

Since 1900s an increasing body of evidence has shown that this tissue have clinical benefits in a wide range of wound repair and surgical applications. Nowadays there is a concerted effort to understand the mechanisms underlying the beneficial effect of placental tissues and this study discuss

immunomodulatory/immunosuppressive properties thought to be responsible for the therapeutic effects observed after tissue and/or cell transplantation.

Although there are still many open questions regarding the mechanism by which hAM-MSCs modulate the immune response, it is evident that it involves the release of soluble factors and not only the cell to cell contact. Recent studies have shown that these paracrine effectors are instrumental in cell-to-cell communication.

In conclusions, the present work lays the foundation for further analyzing of the tools MSCs use to communicate with surrounding cells and could be relevant for the development and definition of the application of hAM-MSCs for the resolution of pathologies on altered macrophage activation, opening exciting possibilities for its future therapeutic use.

3. HUMAN CHORIONIC VILLUS, AMNIOTIC FLUID AND AMNIOTIC MEMBRANE: THREE DIFFERENT GESTATIONAL TISSUES AS SOURCE OF VALUABLE MESENCHYMAL STEM CELLS FOR REGENERATIVE MEDICINE APPLICATIONS

Regenerative medicine involves the use of living cells to repair, replace or restore normal function to injured tissues and organs [2, 3]. Although much progress has been made in characterizing different types of stem cells to date, several limitations exist in the potential clinical applicability of these cells. For example, although embryionic stem cells undoutbtedly dispaly a great deal of clinical potential owing to their high differentiation potential and ease of propagation, these cells are also associated with a high rate of tumor induction after transplantation [153, 154], while their use provokes ethical debate since the procurement of these cells requires destruction of the human embryo. Recently, the generation of induced pluripotent stem (iPS) cells from differentiated human somatic cells has been reported through retroviral transduction of key transcription factors [155, 156]. Although these findings are very promising for the field of regenerative medicine because they provide the possibility of generating patient- or desease-specific pluripotent stem cells without the need for human embryos, the presence of transgenes in these cells could limit their therapeutic use. Multipotent adult stem cells represent an attractive alternative stem cell source for regenerative medicine and are currently used for a variety of therapeutic purposes.

Among adult stem cells, mesenchymal stem cells (MSCs) derived from fetal tissues (bone marrow, blood and liver) and extra-embryonic compartments (amniotic fluid, umbilical cord blood, amniotic membrane, chorion and placenta) are promising in cell-based therapies because of their beneficial properties in wound healing. Moreover, these tissues are ideal sources for studying the features of stem cell characteristics due to the possibility of harvesting large amount of tissue, without posing ethical debate, following prenatal diagnosis (as in the case of chorion from chorionic villi sampling and amniotic fluid from amniocentesis) or at birth (as in the case of amniotic membrane). In addition, MSCs isolated from fetal sources non only fulfill

general characteristic of MSCs but exhibit features of embryonic stem cells including the expression of specific pluripotent markers. In fact, they possess higher proliferation rates, lower immunogenicity and wider differentiation capacity than their adult counterparts as well as immuno-suppressive/immuno-modulatory properties [157, 158]. Scarce information on the behavior of MSCs from different stages of human gestation are so far available [159]. The first aim of this study was the isolation of MSCs from fetal (extra-embryonic) tissues during first- second- and third- gestation period and their long-term culturing; secondly, the detection of the common features between chorionic villi (CV), amniotic fluid (AF) and amniotic membrane (AM)-derived MSCs; thirdly, the observation of differences in phenotype, proliferative capacity, differentiation ability as well as in the immuno-suppressive/immuno-modulatory properties among them.

3.1 MATERIALS & METODS

Human Sample Collection

All samples were from leftover samples of chorionic villus tissue and amniotic fluid and from placental tissue after vaginal delivery and caesarean section. All samples, gently provided by Cytogenetic Laboratory and Obstetrics and Ginecology Department of Children's Hospital Salesi according to the guidelines of the local Ethical Committee, were isolated from healthy women upon informed written consent for the use of tissue for research purposes and generally processed immediately as follows.

Isolation and culture of hCV-MSCs

Chorionic villi (CV) samples included in these experiments were obtained from 24 pregnant women. All samples included in the study showed a normal karyotype.

In chorionic villus sampling (CVS), a small sample of chorion (placental) tissue is excised from pregnant women undergoing prenatal diagnosis between the 10^{th} and the 13^{th} weeks of gestation. The biopsy is performed using a thin plastic catheter transabdominally or transcervically inserted into the interior of the pregnant uterus under real-time ultrasound guidance.

Chorionic villi are composed of an outer layer of trophoblastic cells and an inner mesenchymal cell core, both of fetal origin. Cytogenetic analysis of CV is accomplished following two procedures in parallel, the "basic" and "direct" tecniques. In the long-term culture (basic protocol), fragments of villus core, containing mesenchymal cells, are used to establish primary cultures. The mesenchymal cells hold a variety of cellular elements, fibroblast, endothelial cells and macrophages. Fibroblasts of the villus core are capable to adhere to the plastic dish and rapidly proliferate *in vitro*.

In the "direct" technique (short-term protocol), cells of the cytotrophoblast, which are actively dividing cells in first-trimester villi, are treated with Colcemid to induce mitotic arrest and hypotonic treatment is used to swell the cells prior the fixation. Mitotic cells are then released from intact villi by brief exposure to 60% acetic acid. Metaphase spreads are therefore obtained, the cells are fixed and processed for staining and analysis. Cytogenetic analysis of short-term protocol can be completed in as little as 24 hours after sampling. Generally, both approaches are used for clinical study but only cells taken from back-up cultures were used for our experiments.

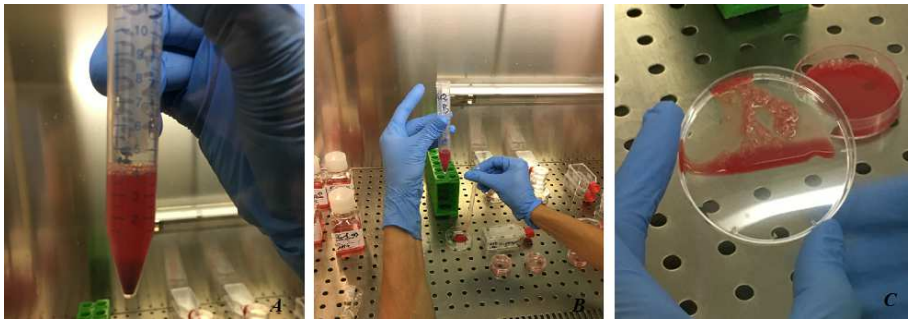

Figure 1. ***Chorionic villi samples in a tube (A-B) and in a Petri dish (C). Villi are visible to the eye.***

Chorionic villus tissue was carefully separated from maternal decidua using sterile fine forceps. Although villi are visible to the eye, dissection is done under observation with an inverted microscope to ensure a clean preparation. Tissues were then washed in fresh, sterile 1X phosphate-buffered saline (PBS) containing 100 UI/mL of penicillin and 100 µg/mL of streptomycin until blood residues are gone. Sample from a single patient was then divided into two parts – one part for culturing following long-term

protocol and the other part for direct preparation following the short-term protocol.

Tissue for long-term culture was disaggregated by mechanical treatment and subsequently minced into small pieces (roughly 3 mm^2 each), resuspended in complete Chang Medium® C (Irvine Scientific), transferred to two flasks and incubated overnight in two different CO_2 incubators to prevent any accidental loss of culture.

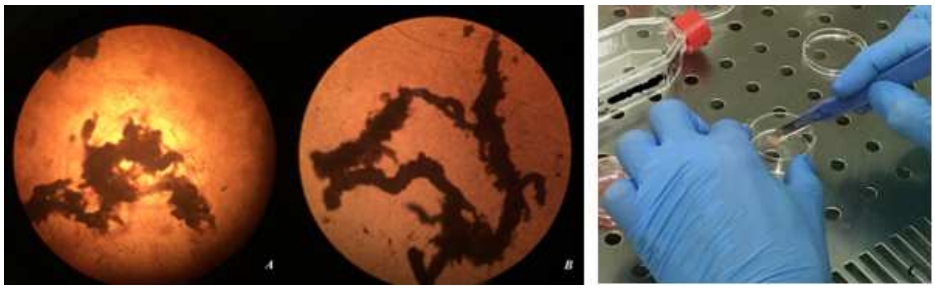

Figure 2. Low-power (2.5X) inverted microscope view of chorionic villi tissue (A-B).Tissue dissected in a Petri-dish (C).

Cells were allowed to migrate out from the tissue and adhere to the surface of the flask using an explant culture method. Primary cells proliferating in cluster were left to expand. Some drops of complete medium were added to the flasks and cells were left undisturbed for two days. After this incubation time, additional 3 ml of complete growth medium was added to each flask. These cells took eight days to adhere to the flask. Once the culture was established, the medium was changed twice a week. At 70% - 80% confluence, cells were harvested by trypsin (0.25%) and 1mM EDTA (0,02%) and subsequently plated onto new flask.

Isolation and culture of hAF-MSCs

Human Amniotic Fluid (hAF) is traditionally obtained during planned amniocentesis. It has been used for decades in routine prenatal diagnosis to identify a variety of genetic and developmental disorders of the fetus.

The amniocentesis is performed during the second trimester, after 15 week of gestation. It consists of the withdrawal of 20 to 30 ml of amniotic fluid, the most common source of fetal cells for biochemical assays, DNA testing and chromosome analysis. At this stage of pregnancy, the amniotic fluid is a

generous resource of a number of viable cells, which allows for consistently establishing cell cultures. The fluid is drawn from the amniotic sac surrounding the fetus using a disposable 20- or 22-gauge and a hypodermic syringe, with the aid of ultrasound.

AF specimens were obtained from 15 pregnant women and all samples included in the experiments showed a normal karyotype.

Equal amounts of fluid (~10 ml) were placed in two pre-labeled 15-ml centrifuge tubes and centrifuged at 1200 x g for 10 minutes at room temperature. While tubes were centrifuging, four amniodish (35 mm Petri-dish including slide, Euroclone) and two T-25 flasks were labeled.

Figure 3. ***Amniotic fluid samples. (A) Amniodish and flasks for in situ and the flask method respectively (B).***

The amniodish are used for the in situ method, a technique where cells are grown in adherence and are harvested for the preparation of metaphase spreads without being removed from the glass coverslips. The flasks, instead, are used for the flask method, an alternative protocol to expand cells starting from a backup monolayer culture. Since fewer cells can be processed following the in situ method compared to the flask method, results could be representative of an artifact. On the other hand, an advantage of the in situ culture is that is usually shorter. Flask cultures need sub-culturing procedures, thus resulting in a longer experimental period. The supernatant was removed leaving ~1 ml fluid above pellet, transferred to new tube and kept for biochemical testing. The pellet of the two initial tubes was gently resuspended with 5 ml of pre-warmed complete growth medium (Chang Medium® B, Irvine Scientific, a medium formulated for amniocytes). Cell suspension was equally distributed (2 ml per plate) into the two amniodish containing a glass coverslip and into the standard flask

where the cell monolayer will form. Additional 3 ml of growth medium was added to the flask.

Cultures from each initial tube were incubated in two different CO_2 incubators to prevent any accidental loss of culture and left undisturbed from 4 to 5 days. One ml of pre-warmed medium was added to the amniodish. A period of eight days is needed for cells to adhere. Media was then replaced in both, the amniodish and the flasks by adding 3 ml and 5 ml, respectively. Cultures were then examined daily under an inverted microscope for the number and the size of colonies. Cells were harvested when the number of colonies with active cell proliferation was adequate. To proceed with the study it was essential to have healthy, and actively proliferating colonies.

Isolation of hAM-MSCs

For the isolation of hAM-MSCs, the amniotic membranes were obtained from 21 healthy pregnant women over 37 gestational weeks after vaginal delivery and caesarean section, as previously described (Paper I). Briefly, the amniotic membrane was stripped from the underlying chorionic membrane followed by extensive washing in sterile 1X phosphate-buffered salt (PBS) solution and subsequent cutting of the membrane into small pieces (about 10 cm^2 each). The resulting pieces were submitted to two enzymatic digestion treatments (incubation with trypsin/EDTA and with Collagenase type IV/ Dnase I) with subsequent cell culture expansion of the initially adherent cell population.

Cell expansion and culture maintenance

hAF- hCV- and hAM-MSCs are able to adhere to plastic flask under standard culture conditions. When they reached confluence, covering 80% of culture flask, the cells were washed with HBSS and trypsinized with 0,25% Trypsin-EDTA for 5-6 minutes at 37°C. In this way the cells were detached from the surface and the suspension was centrifuged at 500 x g for 5 minutes; the supernatant was discarded and cell pellets were resuspended in Standard Culture Medium with a supplement. Cellular vitality was evaluated making the count through the trypan blue dye exclusion method,

using a Bunker Chamber. After the cells were counted, they were transferred to a new flask at the density of 20 x 10^3/ cm^2 if the cells were at low passages or 15 x 10^3/ cm^2 if the cells were at higher passages.

The Standard Culture Medium used is composed by: HG-DMEM with sodium pyruvate, 1% 200 Mm L-glutamine, FBS 10%, 1% 100 mM non-essential amino acids, 0.1% 5 mM 2-β-mercaptoethanol, 1% antibiotics (penicillin and streptomycin) and 1% antifungal (amphotericin B). In addition it was supplemented with 10 ng/ml epidermal growth factor (EGF). The culture medium from the flask was changed 2 to 3 times a week, after washing the cells with HBSS. For culture maintenance and to perform experiments, cells were kept at 37°C in a humidified atmosphere with 5% CO_2.

Preparation of conditioned medium

To obtain conditioned medium (CM) generated from MSCs freshly isolated from early (CV and AF) and late (AM) fetal tissues, MSCs from each cell line were cultured for 3 days in T25 flask at a density of 20 x 10^3 cells/cm^2 in Standard Culture Medium. At the end of the culture period, CM were collected, centrifuged at 500 x g, filtered through a 0.4 μm pore size (Corning) and kept at -80 °C until use.

Immunostaining

The imaging techniques allow to visualize the different cell compartments and the cytoskeleton and permit the evaluation of cell morphology and function. For the visualization of the MSCs from the three cell lines, through fluorescence microscopy (OLYMPUS BX51 with SPOT ADVANCED pc program), fluorescent probes such as ActinGreen (Life technologies) and Hoechst (Sigma-Aldrich) were used to highlight specifically the cytoskeleton and the nucleus. Cells were seeded at 14 x 10^3/well in chamber slide and let adhere. Cells were then washed in 200 μl/well 1% PBS twice and immediately afterwards they were fixed with 200 μl/well 4% PFA for 15 minutes. Subsequently, the amniotic cells were washed for another three times in 200 μl/well PBS. They were then permeabilized with 200 μl/well 0.1% Triton (in PBS) for 10-15 minutes and

then were washed for another three times in 200 µl/well PBS 1%. After the last washing, MSCs were blocked in 1% BSA in PBS for 30 minutes at room temperature. Subsequently the cells were incubated with 200 µl/well of ActinGreen for 20 minutes at room temperature in the dark and then washed in PBS. Cells were finally incubated with Hoechst for 5 minutes. Slides were kept in the dark until observation started.

Cells characterization

Stem cells isolated from these three different tissues at early and late stages of pregnancy were compared in their proliferative rate, MSC-associated markers expression and *in vitro* plasticity. To investigate their involvement as modulators of anti-inflammatory fenomena, the immuno-modulatory/suppressive potential was also tested.

Proliferation assays

Growth curves were set using hAM-MSCs, hAF-MSCs and hCV-MSCs at passage 2 (P2) with 3 biological replicates. To this, hCV, AF- and AM-MSCs were plated at density 10 x 10^3 cells/well into 12-well tissue culture polystyrene dishes (EuroClone). Every 2 days, over 14-15 days-culture period, cells were trypsinized and counted by using trypan blue exclusion dye method.

Doubling time was assessed from passage 2 (P2) to P5. Cells (15 x 10^3 cells/well) were seeded into 12-well tissue culture polystyrene dishes. Cells were trypsinized every 3 days, counted and replated at the same density. The DT value was obtained for each passage according to the formula DT=CT/CD, where CT represents the culture time and CD = ln(Nf/No)/ln2 represents the number of cell generations (Nf represents the number of cells at confluence, No represents the number of seeded cells).

Colony-forming unit-fibroblastic (CFU-F) assay was performed at P2 plating cells at different densities (1.5 x 10^3, 3 x 10^3, 4.5 x 10^3 cells/cm^2) in six-well plates and cultured in 5% CO_2 and 90% humidity at 37°C for 2 weeks in Standard Medium Culture. Then, colonies were fixed with 1% PFA and stained with Giemsa at room temperature, and washed twice. At

the end of the 2 weeks culture period, the colonies were counted under an inverted research microscope (MEIJI TECHNO). Colonies were considered if they were formed by 15-20 nucleated cells.

Evaluation of hAF-MSC-associated markers by Flow Cytometry

MSCs isolated from early and term fetal tissues were analyzed at P2 for the presence of surface MSC-associated markers by flow cytometry. A total of 5 x 10^5 were trypsinized, fixed with 75% ethanol and incubated for 20 minutes with 0.5% bovine serum albumin (BSA) in PBS for blockage all non-specific sites. Sample was then divided into aliquots containing 1 x 10^5 cells each, resuspended in PBS 1X and centrifuged at 500 x g for 5 minutes at 20 °C. The supernatant was then discarded and 5 µl fluorescently labeled antibody was added to each Eppendorf. Directly conjugated antibodies were as follows: phycoerythrin (PE)-conjugated ecto-5'-nucleotidase (PE-*CD73*; Biolegend), fluorescein isothiocyanate (FITC)-conjugated thymocyte differentiation antigen 1 (FITC-*CD90*; Biolegend) and the glycoprotein *CD44* (FITC-Biolegend), Allophycocyanin (APC)-conjugated for integrin b1 (APC-*CD29*; Biolegend). Incubation was performed for 45 minutes at room temperature in the dark. Cells then were washed twice with filtered PBS to remove the excess of antibody and analyzed using Guava Easycite Millipore flow cytometer with GUAVASOFT 2.2.3.

Molecular analysis

Total RNA was extracted from cells at different passages (P0, P1, P2, P3) to characterize MSCs from the three gestational tissues as presumptive stem cells and at P2 to determine their immunomodulatory and immunosuppressive potential. Total RNA was extracted from cells using TRI Reagent® (Sigma) according to the manufacturer's protocol.

Retrotranscription

The cDNA was synthesized from total RNA (500 ng) using a PrimeScript RT-Reagent Kit Takara, under the following conditions: 37°C for 15 minutes, 85°C for 5 seconds and hold at 4°C.

Gene expression analysis

The gene expression evaluation was performed using human specific sequences. Oligonucleotide primers were designed using open source Primer-BLAST, across an exon-exon junction in order to avoid genomic DNA amplification and make manual corrections to make better amplification. Sequence conditions and the references used are shown in tables 1-2.

Table 1-2. ***The primer sequences, the melting temperature used and the size of the amplification product.***

GENE	Sequences (5'→ 3')	Tm (°C)	Product size (bp)
Mesenchymalmarkers			
CD44 molecule (CD44)	S:GGAGCAGCACTTCAGGAGGTTAC	63	129
	A:GGAATGTGTCTTGGTCTCTGGTAGC	63	
5'-nucleotidase, ect (CD73)	S: GCTCTTCACCAAGGTTCAGC	59	203
	A: GTGGCTCGATCAGTCCTTCC	60	
Thy-1 cell surface antigen (CD90)	S: CTTTGGCACTGTGGGGGTGC	64	211
	A: GATGCCCTCACACTTGACCAG	61	
Endoglin (CD105)	S: CCTGGAGTTCCCAACGGGCC	65	186
	A: GGCTCTTGGAAGGTGACCAGG	62	
Hematopoieticmarkers			
CD34 molecule (CD34)	S: GTGTCTACTGCTGGTCTTGG	57	200
	A: CAGTGATGCCCAAGACAGC	58	
Protein tyrosine phosphatase, receptor type C (CD45)	S: GACAACAGTGGAGAAAGGACG	58	170
	A: GCTGTAGTCAATCCAGTGGGG	60	
Pluripotentmarkers			
POU class 5 homeobox1 (Oct 4)	S: CGATCAAGCAGCGACTATGC	59	200
	A: AGAGTGGTGACGACGGAGACAGG	60	
Nanoghomeobox (Nanog)	S: GCAAGAACTCTCCAACATCC	56	200
	A: GGTCTGGTTGCTCCACAT	56	
Housekeeping			
Glyceraldehyde-3-phosphatedehydrogenase (GAPDH)	S: TCCACTGGCGTCTTCACC	68	78
	A: GGCAGAGATGATGACCCTTT	70	

GENE	Sequences (5'→ 3')	Tm (°C)	Product size (bp)
Pro-inflammatory			
Tumor necrosis factor (TNF-α)	S:TCTGGCCCAGGCAGTCAGATC	64	180
	A: TACAGGCCCTCTGATGGCACC	64	
Interferon γ (INF-γ)	S: ATGCAGAGCCAAATTGTCTCC	58	184
	A: GGACATTCAAGTCAGTTACCG	56	
Interleukin 1 beta (IL-1β)	S: TGCTCTGGGATTCTCTTCAGC	59	164
	A: CTGGAAGGAGCACTTCATCTG	60	
Interleukin 6 (IL-6)	S: AACTCCTTCTCCACAAGCGC	60	188
	A: ATGCCGTCGAGGATGTACCG	62	
Anti-inflammatory			
Cytochrome c oxidase subunit II (COX-2)	S: TGAGTTATGTGTTGACATCCAG	62	190
	A: TCATTTGAATCAGGAAGCTGC	60	
Trasforming growth factor beta (TGF-β)	S:TGGTCATGAGCTTCGTCAAC	58	171
	A: TCTCATTGTCGAAGCGTTCC	58	
Interleukin 10 (IL-10)	S: GAGATGATCCAGTTTTACCTGG	56	142
	A: AGGGAAGAAATCGATGACAGC	58	
Arginase	S: TCTCCTCAGAGAACTACAGG	55	189
	A: TTCTGGATACCAAGTCGATC	54	

S, sense; A, antisense; bp, base pairs

The Polymerase Chain Reaction (PCR) was performed in a 20 µl final volume with JumpStart™ Taq DNA Polymerase (Sigma) under the following conditions: initial denaturation at 95 °C for 2 minutes, 32 cycles at 95 °C for 30 seconds (DENATURATION), 58 °C for 30 seconds (ANNEALING), 72 °C for 30 seconds (ELONGATION) and final elongation at 72 °C for 10 minutes. For conventional PCR, primers were used at 10 µM final concentrations. After the amplification reaction, the resulting products were examined by electrophoresis in a 1,6 % agarose gel impregnated with ethidium bromide and photographed with a UV trans-illuminator.

Quantitative PCRs were performed with SYBR® green method in a StepOne™ Real-Time PCR System, StepOne cycler software v2.3. Triplicate PCR reactions were carried out for each sample analyzed. The reactions were set on a strip in a final volume of 10 µl by mixing, for each sample, 1 µl of cDNA, 5 µl of PowerUp SYBR™ Green Master Mix containing SYBR Green as a fluorescent intercalating agent, 0,4 µl of forward primer, 0,4 µl of reverse primer and 3,5 µl MQ water. The thermal profile for all reactions was 10 minutes at 95 °C and then 40 cycles of 15 seconds at 95 °C, 1 minutes at 60 °C. Fluorescence monitoring occurred at the end of each cycle. Human glyceraldehyde-3-phosphate dehydrogenase (GAPDH) was employed as a reference gene in each sample in order to standardize the results by eliminating variation in cDNA quantity.

Differentiative potential

To evaluate plasticity in MSCs isolated from early and term fetal tissues, cells were differentiated into the adipogenic and osteogenic lineages.

MSCs were seeded at the density of 14 x 10^3 cells/cm^2 in 12-well plates and cultured until they reached about 80-90% confluence. For the induction of osteogenic and adipogenic differentiation, cells were cultured using StemProOsteogenic and Adipogenic Differentation Kit (Gibco) according to the manifacture's instructions for up to 2 weeks. To confirm mineral deposition and cytoplasmic inclusions of lipids, conventional Von Kossa and Oil Red O staining were performed, respectively.

Immuno-suppressive/modulatory potential assessment

THP1 monocytes proliferation test.

The ability of MSCs isolated from early and late gestational tissues to reduce the peripheral blood mononuclear cells (PBMCs, ATCC® TIB-202™) proliferation was proved by co-culturing cells in a 1) cell-to-cell contact setting or 2) in a transwell system, or by using conditioned medium generated from freshly isolated stem cells. For 1) and 2) MSCs and THP1 were plated at 1:10 ratio. THP1 proliferation was induced by stimulating PBMCs with 2% phytoemagglutinin (PHA; Sigma-Aldrich) in HG-DMEM

complete media. THP1 in absence of MSCs were used as controls. Monocytes proliferation was assessed after 2 days in culture.

hCV-MSCs-associated immunosuppressive potential.

In order to investigate the immunosuppressive potential we examined the expression of genes responsible for the production of soluble factors, such as *TNF-α, IL-6, PGE-2, TGF-β* and *IL-10* known to be mediators of the immunosuppressive action of MSCs as reported for cells obtained from other sources. The cytokines profile was tested at the expression level in two different test conditions: 1) treating hCV-MSCs with pro-inflammatory cytokines *TNF-α* and *IFN-γ* (Prepotech) at the concentrations of 20 ng/mL each, for 24h/48h, and 2) co-culturing these cells in a transwell system with monocytes stimulated to follow the inflammatory M1 macrophage pathway. hCV-MSCs and THP1 were plated at 1:10 ratio.

MSCs obtained from chorionic villi were seeded at the density of 38 x 10^3 in the 24-well plate and cultured for 48h at 37°C before stimulation and co-culturing started. After 24h/48h hCV-MSCs were removed from cultures and total RNA was then extracted using TRI REAGENT according to manufacturer's instruction.

The human leukaemia-derived monocytic cell line THP1 (ATCC) was the cell line used for *in vitro* studies investigating the MSC-immunosuppressive properties. Cells were maintained in Roswell Park Memorial Institute medium (RPMI) 1640 supplemented with 10% fetal bovine serum (FBS) (EuroClone), 5% L-glutamine (Sigma) and 1% Antibiotics/Antimitotic (A/A, Corning) at 37° in 5% CO_2. Cells were grown to a density of 3 x 10^5 cells/ml. Monocytes-to-macrophage differentiation of THP1 was induced with phorbol myristate acetate (PMA) at a final concentration of 10 ng/ml in 6-well plates. Incubation with PMA was performed for 24h incubation. After PMA treatment, non-activated cells (in suspension) were discarded and activated macrophages were first washed with phosphate-buffered saline solution (PBS) 1X (Sigma) to remove non-adherent cells residues and then were exposed for 24h and 48h at 37°C to pro-inflammatory stimuli with a combination of tumor necrosis factor alpha (*TNF-α*) + interferon gamma (*IFN-γ*) at the concentrations of 20 ng/ml each. Adding *TNF-α* and

IFN-ɣ, THP1 cells will polarize already differentiated macrophages towards a pro-inflammatory phenotype (M1).

Quantitative reverse transcription polymerase chain reaction (qPCR) analysis was used to evaluate the expression of immunosuppressive-associated markers in hCV-MSCs such as *TNF-α, IL-6, PGE-2, TGF-β* and *IL-10.*

hCV-MSCs-associated immunomodulatory potential.

To assess the functional relationship between the immune cells and hCV-MSCs, the expression of classical M1 markers (*IL-1β, TNF-α, IL-6*) and alternative M2 markers (*IL-10, TGF-β, COX-2* and *ARG*) were detected with co-culturing polarized M1 and with hCV-MSCs in a transwell system. Differentiated macrophages (M∅) and macrophages polarized towards the pro-inflammatory phenotype (M1) were used as negative and positive controls, respectively.

In co-culture, THP1 cells (38 x 10^4) were differentiated to a macrophage phenotype; following differentiation cells were polarized to M1-like phenotype upon stimulation with pro-inflammatory stimuli (*TNF-α + IFN-γ*) and then seeded together with hCV-MSCs (38 x 10^3) by a trans-well membrane (0.4 μm pore size, Corning) at a 1:10 ratio and cultured for 24h and 48h at 37°. After 24h/48h THP1 cells were removed from cultures, were kept at -80°C until RNA extraction was performed.

Statistical analysis

Statistical analysis was performed using GraphPad Instat 3.00 for Windows (GraphPad Software). Three replicates for each experiment (doubling time, colony forming unit, quantitative PCR (PCR), cytometry analysis and PBMC proliferation test) were performed and the results are reported as mean ± standard deviation (SD). One-way analysis of variance for multiple comparisons by the Student-Newman-Keuls multiple comparison test were used to assess differences between gruops. Differences were considered statistically significant for p values < 0.05. For quantiative PCR data, non-parametric tests were used. Saphiro-Wilk normality test proved that the datasets were normaly distributed ($p > 0.05$).

3.2 RESULTS

The three areas of the placental anatomy from which our MSCs were isolated were: the chorionic villus tissue and the amniotic fluid from the first and the second trimester of gestation, respectively. The third tissue harvested was the amniotic membrane from term placenta. From each area equivalent amounts of tissue were collected in order to compare the yields in terms of retrieved cells after trypsinization treatment at P0: 10g for chorionic villus tissue and for amniotic membrane, 10ml for amniotic fluid. In practice, yield was higher for hCV-MSCs assessing around $1.2 \times 10^6 \pm 3 \times 10^5$ cells for 10g of starting material whereas it was lower for hAF-MSCs (7×10^5 cells $\pm$ 6.2×10^4) and for hAM-MSCs (3×10^5 cells $\pm$ 1.2×10^5) (Figure 4).

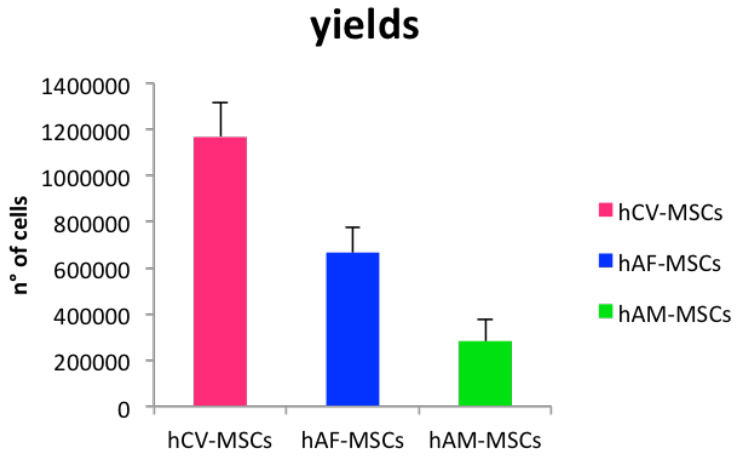

Figure 4. ***Comparison of the yields from equivalent amounts of starting material.***

After isolation, MSC cells were seeded at a density of $20 \times 10^3/cm^2$. Following 48 h of culture, only a few MSCs were attached to the tissue culture plastic, while red blood cells and most other cellular debris did not attached. Under a microscope, after the 48 h media exchange, cells appeared significantly different from more extensively expanded MSCs. Some debris and immune cells were visible as floating or attached clumps but these did not interfere with the growth of the MSCs. The longer fibroblastic cells adhered to the bottom of the flask were likely a mix of cells including MSCs, hematopoietic, trophoblastic or endothelial cells. Again, the non-

MSC cells did not compromise the MSC cultures, as these cells did not generally survive more than 1-2 passages in the MSC culture conditions.
Despite some variation in the initial appearance of cultures, the subsequent expansion results are generally consistent.

Morphology of MSC cultures over time.

About their morphology, it may be important to notice that differences in cell shape/morphology and cell arrangements/organization were observed after direct plating. Three morphological cell types were predominantly evident in our MSCs: I) larger flattened fibroblstic cells (Figure 5A), II) cobblestone-like cells, resembling epithelioid cells (Figure 5C). III) small spindle-shaped cells (Figure 5E). The initial growth of MSCs as primary culture (P0) was highly heterogeneous whereas with passaging, a more homogeneous cell population of mostly spindle-shaped and fibroblast-like cells prevailed.
Initially the cells grew very slowly and cell adhesion occurred in 7-10 days. The MSCs were expanded until passage 5 (P5) and not over as they started becoming “sleeping cells”. In fact at higher passages, a higher senescence rate was found with morphological changes of the cells and stagnated proliferation.

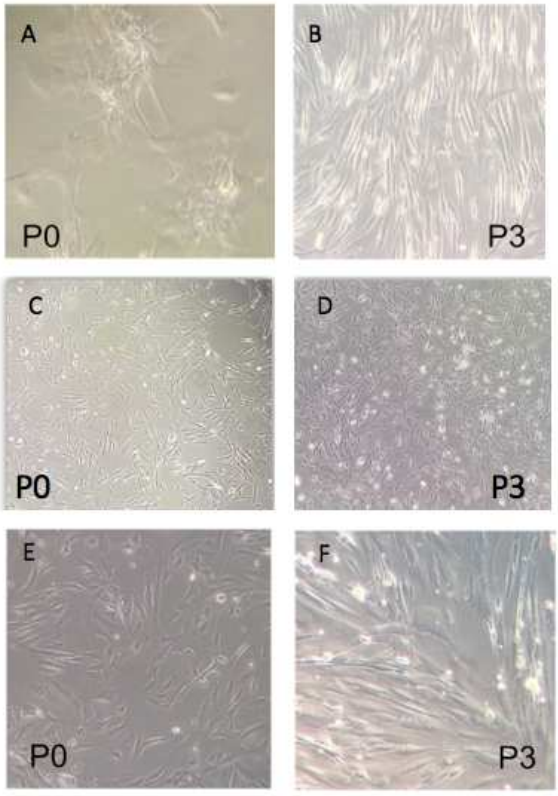

Figure 5. Chorionic villi- (A-B) amniotic fluid- /C-D) and amniotic membrane (E-F) derived mesenchymal stem cells on day 7 (P0) and at passage 3 (P3). 10X magnification.

In this representative example, seven days following isolation, small fibroblastic MSC colonies were visible, although non-MSC cells could also be seen as round or loosely attached cells. The attached cells were what was originally termed a "colony unit forming fibroblast" (CFU-F) and later termed MSC. Fifteen days following isolation, fibroblastic MSC colonies were large. Generally, 20 days were needed for the monolayer could be 80-90% confluent and at this point the cells were passaged. From passage 2 onwards, the MSC monolayer developed the characteristic whirlpool-like morphology at confluence.

Through the imaging technique it was possible to visualize the cells structure. The cytoskeleton was highlighted through the green staining that derives from the high affinity between a green probe, the ActinGreen (Life Technologies) and the F-actin structures. The nucleus was highlighted by Hoechst (Sigma Aldrich).

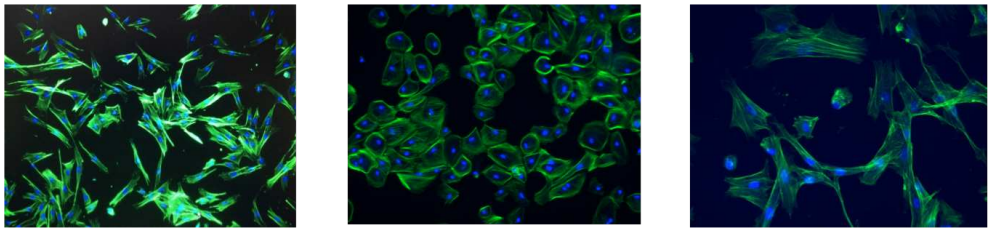

Figure 6. hCV- hAF- hAM-MSCs respectively. Green: F-Actin, Blue: Nuclei. 10X magnification

Each expanded cell population was characterized to ensure that it conforms to standard MSC criteria including (1) plastic adherence (2) the presence of mesenchymal surface markers and the absence of hematopoietic surface markers, and (3) the capacity to undergo mesodermal differentiation.

As shown in Figure 5, the MSCs in culture were plastic adherent and showed a fibroblastic-like morphology; this validates that the cells met the first criteria that define MSC.

Proliferation assay.

Growth curves

To build the growth curves three biological replicates (P1A, P1B and P1C) of MSCs from the three cell types at passage P2 were used. As it can be seen from the chart (Figure 7), the lag phase was similar for the three samples with a 3-days duration. After 3 days in culture, significant differences in proliferation parameters were found ($p < 0.05$) and it was possible to notice that cells derived from different gestational ages had different exponential growth phase. The proliferative capacity of hCV-MSCs *in vitro* was generally greater with a more extensive log phase (3-13 days) than that registered for hAF-MSCs (3-11 days) and hAM-MSCs (2-8 days).

Doubling time (DT) confirmed data set provided above. In fact, it was similar (5.5 ± 0.3 vs 5.2 ± 0.2) in hCV-MSCs and AM-MSCs for the first passages (P2 and P3) compared with hAF-MSCs (8.5 ± 0.5) and it remained constant until P5 in hCV-MSCs, while significantly increasing in hCV-MSCs and AM-MSCs ($p < 0.05$) (Figure 8).

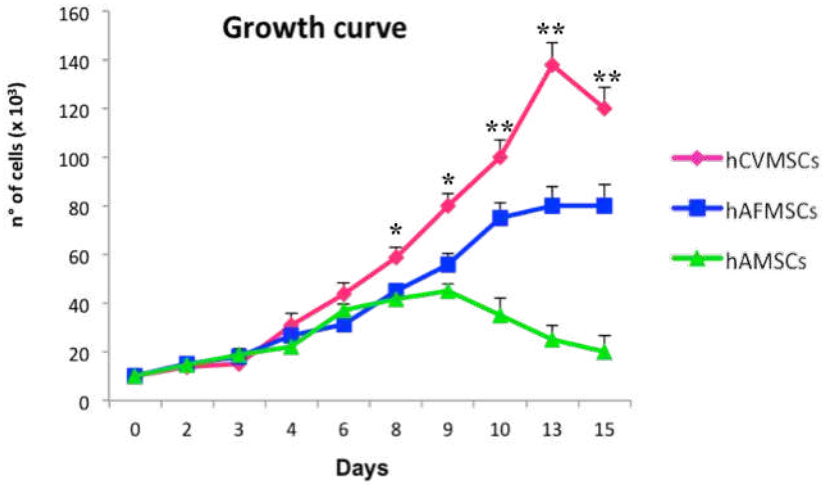

Figure 7. ***Growth curves at P2 for three biological replicates from hCV- hAF- and hAM-MSCs. *p <0.05, and **p <0.01 with respect to hAM-MSCs.***

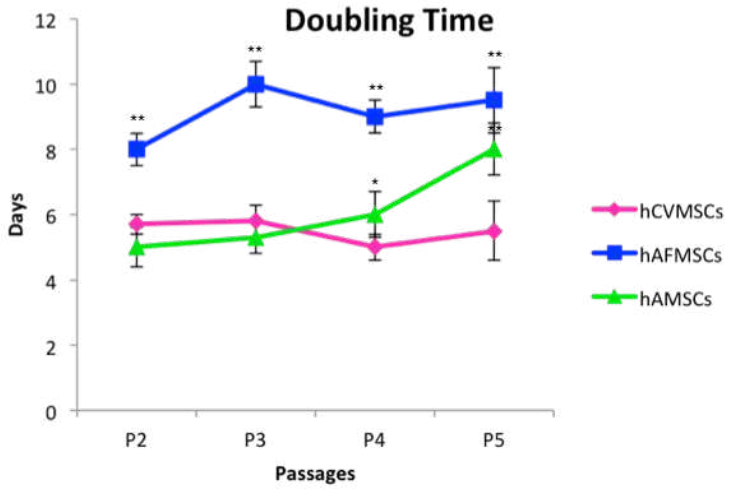

Figure 8. Proliferation studies. Doubling time of hCV-MSCs, hAF-MSCs and hAM-MSCs from passage 2 to passage 5. *p <0.05, and **p <0.01 with respect to P2.

Colony-forming unit (CFU) assay was performed from hCV-MSCs, AF-MSCs and AM-MSCs to analyse their clonogenic potential. The results obtained are shown in Table 1. After 15 days of culture, the number of cell colonies formed at P1 after seeding cells at different densities was counted. The results demonstrated an increase in CFU-F frequency with increasing cell seeding density. For each density of seeding, hCV-MSCs showed a higher CFU in comparison with hAF- and hAM-MSCs.

Table *1. CFU-F assay*

	density cells/cm^2	Total cells	CFU	1 CFU each
hAM-MSCs	350	3325	0	0
	1000	9500	2 ± 0.3	4750
	3500	33250	8 ± 0.6	4156
	density cells/cm^2	Total cells	CFU	1 CFU each
hAF MSCs	1500	14250	2.5 ± 0.7	7125
	3000	28500	4 ± 0.4	5700
	4500	42750	10.5 ± 0.7	4275
	density cells/cm^2	Total cells	CFU	1 CFU each
hCV MSCs	5000	47500	4 ± 1.4	15833
	10000	95000	8 ± 0.7	11875
	15000	142500	14 ± 0.7	10178

Molecular characterization

The second defining MSC characteristic is the presence of mesenchymal surface markers and the absence of hematopoietic surface markers. As there is no single marker capable of definitively identifying an MSC, panels of markers were generally used in conjunction with flow cytometry analysis to identify cells that were mesenchymal but not hematopoietic.

MSCs from the three different tissues at passage P2 were characterized from a molecular point of view and they have revealed to retain pluripotent features and typical mesenchymal phenotype (Figure 9). Indeed they resulted positive for *Nanog* and *Oct-4*, markers of pluripotency, and for *CD73*, *CD90, CD44, CD105* markers of the mesenchymality. Moreover, all categories of MSCs did not express the hematopoietic markers *CD34* and *CD45*, as expected.

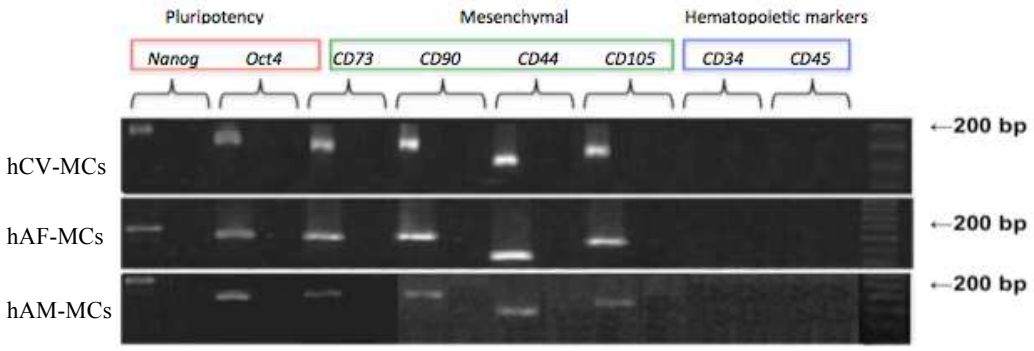

Figure 9. ***Molecular characterization of MSCs from each cell line.***

RT-PCR was also performed to evaluate the expression of puripotency and MSC-associated markers in hCV- and AF-MSCs in comparison with hAM-MSCs. The age of gestation affected cells phenotype: the expression levels of pluripotency (*Nanog* and *Oct4*)- and MSC (*CD44, CD29, CD73, CD105*)-associated markers was significantly lower ($p<0.01$) in cells isolated at late gestation age (hAF- and AM-MSCs) than those recorded in hCV-MSCs isolated from fetuses at earlier stage of gestation (Figure 10).

a

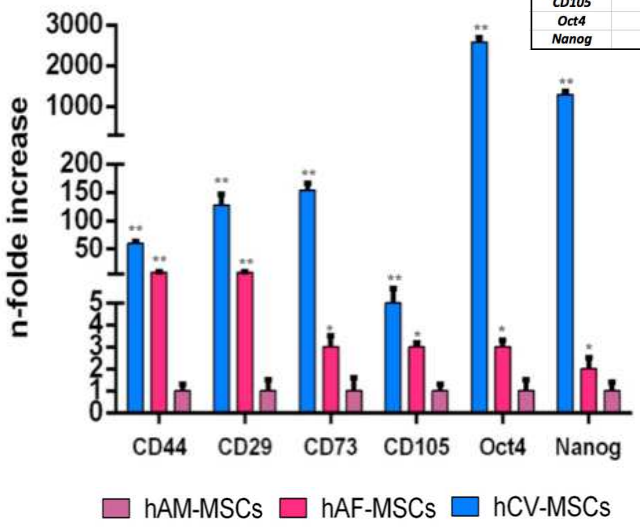

b

	hAM-MSCs	hAF-MSCs	hCV-MSCs
CD44	1	9 ± 1.4	60 ± 4.5
CD29	1	9.4 ± 2.1	127 ± 20.2
CD73	1	3.7 ± 1.8	154 ± 12.6
CD105	1	2.99 ± 1.1	5± 0.2
Oct4	1	3.6 ± 0.4	2586 ± 110.3
Nanog	1	2.8 ± 0.77	1296 ± 71.1

Figure 10. ***Quantitative PCR analysis (a). In the table (b) are shown mRNA levels (RT-PCR) for the expression of pluripotency and MSC-associated markers. Data represent the mean and the SD of at least three independent experiments.***
**** = p<0.05, ** = p<0.01 in comparison with hAM-MSCs.***

Flow Cytometry Analysis

Flow cytometry analysis showed a morphologically homogenenous $CD44^+$, $CD29^+$, $CD73^+$ and $CD90^+$ cell populations emerging from the three different fetal tissues soon after isolation (P1). The MFI values of mesenchymal markers were significantly higher ($p<0.01$) in hCV-MSCs isolated at early stage of gestation. Conversely, they drammatically lowered in hAM-MSCs collected from term placenta (Figures 11-12).

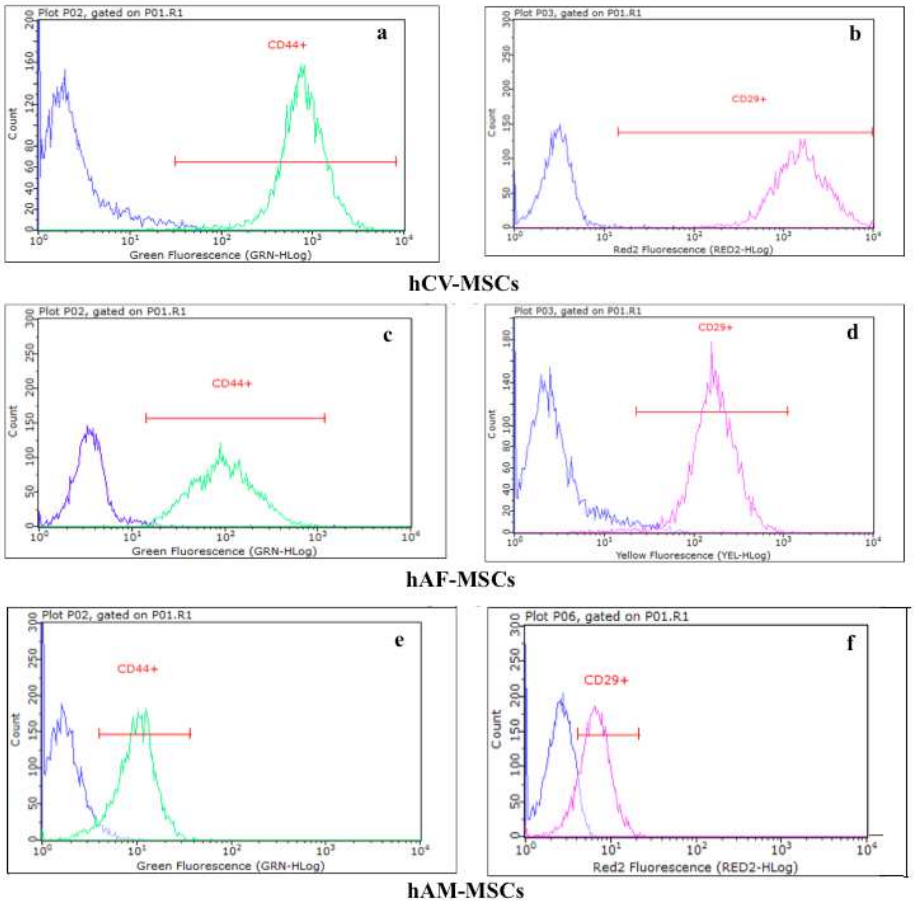

Figure 11. ***Flow cytometric analysis reveals CD44+ and CD29+ cells in hCV-(a-b) AF- (c-d) and AM-MSCs (e-f).***

a

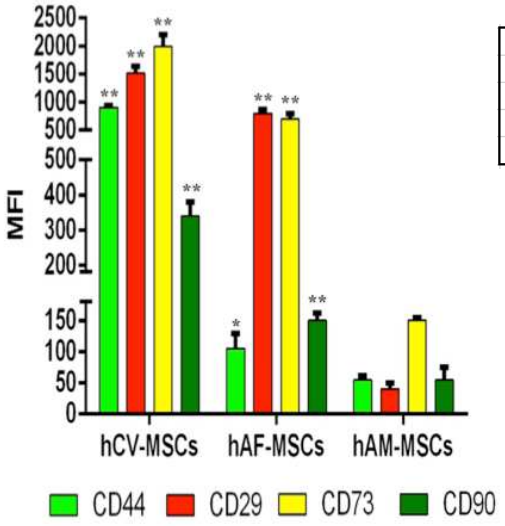

b

	hCV-MSCs	hAF-MSCs	hAM-MSCs
CD44	900 ± 41	105 ± 24	55 ± 6.1
CD29	1522 ± 122	800 ± 73	40 ± 4.5
CD73	2000 ± 205	702 ± 104	150 ± 5.2
CD90	340 ± 41	153 ± 12	55 ± 20

Figure 12. ***MFI values (a) of the antigens for mesenchymal markers CD44, CD29, CD73 and CD90. On the right (b) MFI ratios variation, analyzed by flow cytometry, was calculated in early and late gestational tissues. * = p<0.05, ** = p<0.01 in comparison with hAM-MSCs .***

Multipotent differentiation

The differentiation potential of hCV- AF- and AM-MSCs was evaluated at P3. MSCs from the three gestational stages were able to produce mineralized extracellular matrix and to develop vacuoles containing lipid droplets under osteogenic- and adipogenic-inductive conditions (Figure 13). Osteogenic differentiation was confirmed by Von Kossa staining in all cell lines while the control was negative for the staining. Similarly, our stem cells were able to undergo adipogenic differentiation as demonstrated by the development of positive staining for Oil Red O after culture cells in adipogenic induction medium, while the cells mainteined in regular control medium showed no lipid deposits. Interestingly, calcium deposition and lipid vacuoles started to appear earlier in hCV-MSCs compared to hAF- and AM-MSCs (~ 6 vs 10 and 14 days respectively).

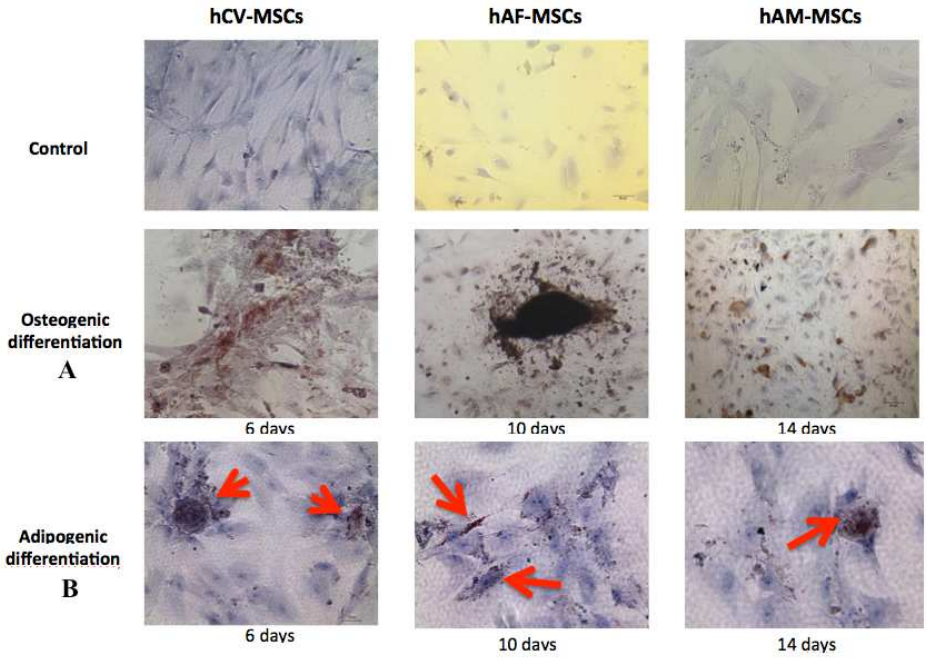

Figure 13. ***Staining of differentiated and undifferentiated (control) hCV- AF- and AM-MSCs. (A) Von Kossa staining after osteogenic induction and (B) Oil red O-stained cytoplasmic neutral lipids after adipogenic induction. 20X magnification.***

Immunosuppressive potential

The immunosuppressive potential was functionally evaluated through THP1 proliferation test. All MSCs obtained from early or late tissues were able to downregulate the proliferation of PHA-stimulated PBMCs under all test conditions (cell-to-cell contact, transwell cultures and using CM) following 2 days of co-culture (Figure 14).

Consistent with the previous findings, the inhibitory effect observed in hCV-MSCs was greater, showing a significant 69.3%, decrease ($p<0.05$) in PBMCs proliferation whereas late MSCs (hAF- and AM-MSC) were less effective, with values assessed around 65% and 52% decrease, respectively.

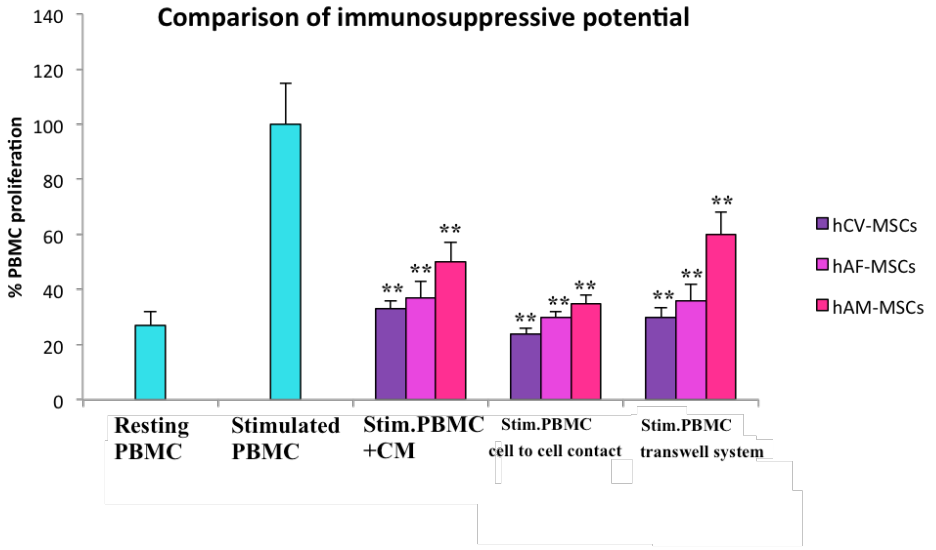

Figure 14. ***Effect of all MSC cell types on the proliferation of stimulated PBMCs following 48h of co-culture. Data represent the mean and SD of three independen experiments. ** = p<0.01 in comparison with stimulated PBMCs.***

To study the immunosuppressive and immunomodulatory features of MSCs we decided to select hCV-MSC cell line for our studies since these cells displayed a higher proliferative activity, a greater expression of pluripotency- and MSC-associated markers, an earlier differentiative potential and, finally, a superior efficiency to inhibit monocytes proliferation than hAF- and AM-MSCs.

In detail, we examined the expression of anti/pro-inflammatory cytokines, *TNF-α*, *IL-6*, *PGE2*, *TGF-β* and *IL-10* as immunosuppression mediators under three test conditions: 1) untreated and 2) stimulated cells with pro-inflammatory cytokines TNF-α and IFN-γ, and 3) transwell system-based cultures between hAF-MSCs and M1-like macrophages at both 24 and 48 hours. As shown in Figure 15, the expression of *TNF-α, IL-6 and PGE-2* cytokines significantly increased ($p<0.01$) of about 65.4 ± 6.2-fold, 1729 ± 17.4-fold and 8.4 ± 1.2-fold, respectively, in hAF-MSCs stimulated with *TNF-α* and *IFN-γ* at 24h with the only exception of *TGF-β* and I*L-10* whose

expression was decreased in comparison with the untreated cells and assessed around 0.55 ± 0.12- and 0.62 ± 0.21-fold, respectively.

The expression of *TNF- α* (2.54 ± 0.7-fold), *IL-6* (2696 ± 98.2-fold), *PGE-2* (3.61 ± 0.82-fold), *TGF-β* (147.23 ± 14.53-fold) also significantly increased ($p<0.01$) in hAF-MSCs stimulated with pro-inflammatory cytokines at 48 hours. Compared with untreated cells used as control *IL-10* mRNA levels were found very low (0.03 ± 0.001-fold) ($p<0.01$).

A considerable statistically significant ($p < 0.01$) increase in the expression of immunosuppressive molecules was determined when cells were co-cultured with M1 polarized macrophages at both time points. Compared with the levels observed in the previous test conditions, hAF-MSCs in transwell system produced much higher levels of cytokines expression. In fact, data showed an outstanding upregulation in the expression of *TNF-α* (212.5 ± 21.7-fold and 31 ± 6.2-fold), *IL-6* (8370.34 ± 65.1-fold and 3382 ± 34.9-fold), *PGE-2* (97 ± 15.8-fold and 5.43 ± 1.2-fold) at both time point of co-culturing. However, very low expression for *TGF*-β and *IL-10* genes was detected (0.6 ± 0.1-fold and 0.5 ± 0.14-fold, respectively) at 24 h in comparison with unstimulated cells.

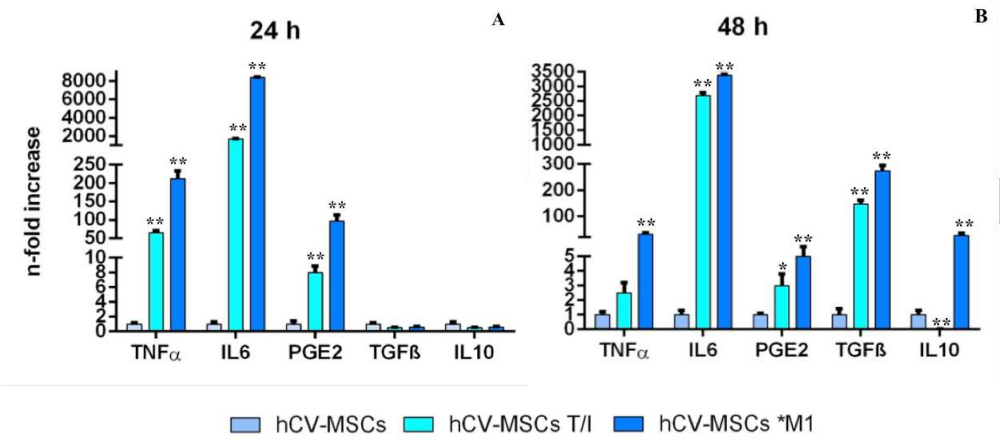

Figure 15. ***Quantitative PCR analysis for the expression of genes associated to immunosuppressive potential at 24- 48h. Asterisks depict significant (*p<0.05) and highly significant (**p<0.01) differences with negative control hCV-MSCs.***

Immunomodulatory potential

The immunomodulatory potential of hCV-MSCs was also evaluated on the activity of the immune cells (THP1 monocytes) after M1 polarization induction and setting up a co-culture system with our stem cells. RT-PCR was performed to evaluate the expression of pro- and anti-inflammatory genes in M1-activated immune cells. As shown in Figure 16, M1 polarized macrophages seeded with hCV-MSCs in a transwell system displayed a 4.3 ± 0.81-fold decrease in the expression of *TNF-α* at 24h and 86.7 ± 7.5-fold decrease at 48h in the comparison of M1 macrophages used as positive control ($p<0.01$). The expression of *IL-6* and *IL-1β* was found 6300 ± 56.4-fold and 3.21 ± 0.6-fold decreased at 24h and 566 ± 23.4–fold and 2075 ± 146.4-fold at 48h, respectively. Interestingly, data showed a significant upregulation in the expression of *TGF-β*, *IL-10*, *COX-2* and *ARG* that assessed around 1306 ± 150.3-fold, 570 ± 60.7-fold, 9825 ± 302-fold and 88805 ± 812-fold at 24h and around 120 ± 9.4-fold, 569 ± 47-fold, 175022 ± 1724-fold respectively ($p<0.01$). By contrast, the level of *COX*-2 was detected significantly lower (0.02 ± 0.0012-fold) at 48h in comparison with data observed at 24h ($p<0.01$).

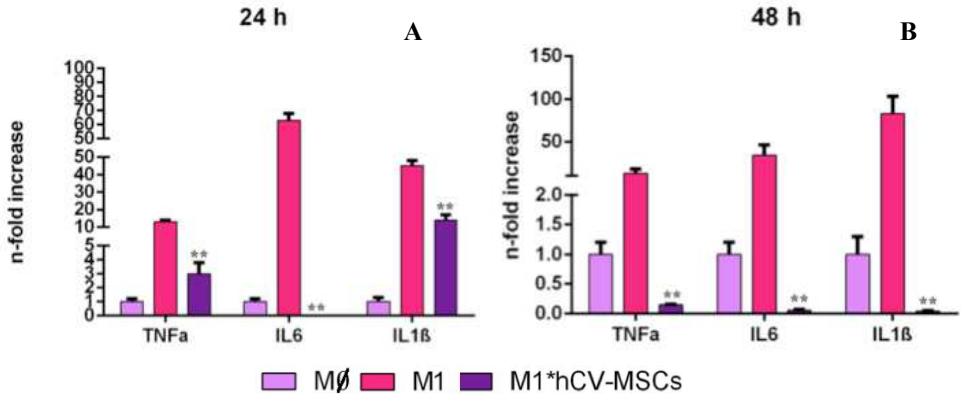

Figure 16. ***Quantitative PCR analysis for the expression of genes associated to immunodulatory potential at 24 (A)- 48h (B). Asterisks depict highly significant (**p<0.01) differences with positive contro MØ.***

3.4 DISCUSSION

Stem cells derived from extra-embryonic compartments have attracted great interest in recent years as a valuable source of stem cells for the needs of regenerative medicine due to their higher proliferation rates, broader differentiation and extensive proliferative potential in comparison with cells obrained from adult tissues. [18, 41, 98, 157, 160, 161]. However, few studies to date have broadly investigated whether their *in vitro* phenotype, stemness properties, plasticity as well as their immunoregulatory properties could be influenced by gestational stage of isolation [65, 162]. Furthermore, strictly paired quantitative analysis between stem cells isolated from extra-embryonic tissues over the entire duration of gestation were missing and non-paired analysis may neglet the substantial inter-individual variances detected in the present study that should be taken into account in future trials focusing on therapeutic applications prior to human clinical use.

Indeed, our study demonstrated that gestational age is a key factor influencing morphological and functional properties of early and late MSCs, thus affecting the outcome of cell based therapies.

We previously isolated our stem cells (hCV- AF- and AM-MSCs) from human fetal tissues (chorionic villus, amniotic fluid and amniotic membrane) confirming that these cells have specific characteristics in common with embryonic and adult stem cells, implying that these cells may represent an “intermediate stage” between pluripotent stem cells and lineage-restricted adult stem cells. In fact, they express representative mesenchymal (*CD44, CD29, CD90, CD73* and *CD105*) and pluripotent genes (*Nanog* and *Oct4*) involved in the undifferentiated state of cells, are highly proliferative and retain high plasticity. These findings suggest that fetal tissues can effectively yield a mesenchymal stem cell population confirming the role that has been attributed to these tissue and expanding the number of sources of MSCs obtained from adult tissues. In addition, the *in vitro* differentiation studies suggest that these cells are prone to differentiate easily under appropriate culture conditions and retain high plasticity, as supported by their capacity to differentiate into adipocytes and osteocytes. Due to their ability to differentiate toward multiple cell types, our MSCs could play a key role in the development of cell-based strategies.

We also provided evidence of the more distinct stemness properties of hCV-MSCs compared to the counterparts hAF-MSCs and hAM-MSCs. Similarly to cells isolated from umbilical cord blood (UBC) collected from premature neonate [163], our data demonstrated that hCV-MSCs obtained at early stage of gestation dispayed a higher proliferative activity, a greater expression of pluripotency- and MSC-associated markers and an earlier differentiative potential. Taken together, these results led us to hypothesize that cells isolated from the first trimester of gestation dispay a more undifferentiated state and these primitive properties could be related to the higher concentration of stem/progenitor cells within the chorionic villus tissue, as well as, to a more rapid progression in cell cycle required in preterm fetuses in order to drive an intense organogenesis, as previously discussed for umbilical cord blood-derived cells from premature neonate [163]. The hypothesis of a large amount of stem/progenitor cells from MSCs isolated at early stage of gestation could be supported by the higher expression of pluripotency- and MSC-associated markers and by the shorter period of time required for differentiation toward osteogenic and adipogenic lineages. By definition, MSC must possess in vitro mesodermal differentiation capacity. Mesodermal differentiation potential is commonly assessed through either tri- or bi-lineage differentiation assays. Bi-lineage assays generally assess osteogenic and adipogenic differentiation capacity, while tri-lineage assays additionally assess chondrogenic differentiation capacity. In the representative results presented here, we showed that the expanded MSC populations formed both calcium deposits, indicative of osteogenic differentiation, and lipid vacuoles, indicative of adipogenesis. We did not carry out chondrogenic differentiation for several reasons. Firstly, while mesodermal differentiation capacity is a defining characteristic of MSC, it is likely of secondary importance [164-166], especially where the therapeutic benefit is likely to be derived from the MSC paracrine secretions [167]. Secondly, although Dominici et al. proposed minimal criteria for the clinical production of human adult bone marrow-derived MSC [44], more recent studies indicate MSC from different niches have different inherent properties and differentiation capabilities [168-173]. In fact, Parolini et al. proposed that placenta-derived MSC

should differentiate into "one or more mesodermal" lineages rather than all three lineages [41]. Finally, many MSC studies exclude chondrogenic differentiation as it occurs through a similar intracellular signaling pathway as osteogenesis (*TGF-β* family pathway) [174-176].

A great immuno-suppressive potential in reducing PBMCs proliferation was indeed associated to each of the gestational stages studied, with hCV-MSCs being more effective in comparison with MSCs derived from more advanced gestational stages. Differences among the experimental conditions applied were found, within the same cell line. In the three experimental groups, the greatest capability to decrease the number of proliferating immune cells was found in cell-to-cell contact setting suggesting that the inhibitory ability involves more than one mechanism of action, although it is largely mediated by the direct interaction between cells via adhesion molecules, as reported by previous studies. In fact, cell–cell adhesion mediated by ICAM-1 and VCAM-1 is critical for mesenchymal stem cell (MSC)-mediated immunosuppression [111, 123, 177-179]. More recently, several findings indicated a species variation in the mechanisms of MSC-mediated immunosuppression. Interestingly, in the human MSC system, it has been found that cell–cell contact is important for immunosuppression, indicating that adhesion molecules might also play a role in the human MSC-mediated immunosuppressive effect [152].

These preliminary results led us to select hCV-MSCs, the cells with highest stem cell characteristics, to be used for further immunosuppresive and immunomodulatory studies.

In the present study we provided evidence of the expression of immunosuppression-related genes in hCV-MSCs, demonstrating that the levels of *TNF-α, IL-6, PGE-2, TGF-β* and *IL-10* by hCV-MSCs, stimulated with pro-inflammatory cytokines and co-cultured with M1 polarized macrophages, increased at 24h, with their consequent amplification at 48h. Interestingly, very low levels of *TGF-β* and *IL-10* expression were found in both stimulated and co-cultured hCV-MSCs with immune cells at 24h confirming the hypothesis that the messenger RNA expression of these cytokines is induced later on, soon after the expression of primary cytokines such as *TNF-α* and *IL-6 [126]* .

Our data also demonstrated that the immunosuppressive effect of the hCV-MSCs is related to the presence of external stimuli such as pro-inflammatory cytokines or the presence of M1-activated cells, proving that MSCs are not spontaneously immunosuppressive but the priming by inflammatory cytokines and by immune cell interaction is essential for MSCs-mediated immunosuppression. This result is consistent with several studies indicating that MSCs need to be 'licensed' to become immunosuppressive [123, 178-180]

Among the paracrine actions underlying the anti-inflammatory effect of chorioni villi-derived cells are their interactions with immune cells of innate and adaptive immunity. Many studies have reported the ability of placenta-derived cells to induce M2 macrophage differentiation [148] and to abolish the production of pro-inflammatory cytokine by immune cells, likely through the action of soluble inhibitory factor [124, 148, 150].

Consistent with previous results, when M1 polarized macrophages were seeded together with hCV-MSCs in a transwell system, the expression of anti-inflammatory cytokines (*IL-10, TGF-β, COX2* and *ARG*) by immune cells considerably increased, displaying an M2-like phenotype. In contrast, a reduction of the expression of the pro-inflammatory cytokines (*TNF-α, IL-6* and *IL-1β*) at both time points, 24h and 48h, has occurred in comparison with the positive control (M1-like phenotype), confirming the immunomodulation properties.

The results of these studies demonstrated that our MSCs mainly interact with immune cells by secreting cytokines such as *TNF-α, IL-6, PGE-2, TGF-β* and *IL-10*. In an inflammatory environment, they act as immune suppressors by interacting with monocytes and are capable of supporting the switch of macrophages from the pro-inflammatory M1-phenotype to the anti-inflammatory M2-phenotype. The so called polarization of macrophages towards the M2-phenotye may reduce tissue inflammation and accelerate healing process in injured tissue.

In conclusion, this study reinforce our hypothesis that stem cells derived from preterm fetal tissues hold the ability to react to pro-inflammatory stimuli provided by microenvironment, to interact with immune cells modulating their function and to play a key role in inhibiting immune

responses. Furthermore, hCV-MSCs have expressed the highest stem cell characteristics and have demonstrated to display anti-inflammatory properties that make them good candidates for clinical applications, such as for the treatment of various diseases [88, 181, 182]. However, further research on human chorionic villi-derived mesenchymal stem cells seems mandatory to confirm these findings and to establish hCV-MSCs as a potential cell source for regenerative medicine applications.

CONCLUSIONS

In the early twentieth century, numerous studies have shown that placenta and fetal attachments are a precious source of MSCs with significant clinical relevance, both for wound repair and surgical applications. Nowadays we try to understand more and more about the mechanisms of these placental tissues that have a beneficial effects. This work seems to open an applicative scenario, proposing stem cells derived from preterm fetal tissues, in particulary hCV-MSCs, as promising candidates for the transplantation of different rates of stem/progenitor cells in cell-based regenerative protocols.

4. REFERENCES

1. Taylor, S.G.a.P.R., *Monocyte and Macrophage heterogenity.* Nature Reviews, 2005. 5: p. 953-964.
2. Polak, D.J., *Regenerative medicine. Opportunities and challenges: a brief overview.* J R Soc Interface, 2010. 7 Suppl 6: p. S777-81.
3. Chien, K.R., *Regenerative medicine and human models of human disease.* Nature, 2008. 453(7193): p. 302-5.
4. Graf, T. and T. Enver, *Forcing cells to change lineages.* Nature, 2009. 462(7273): p. 587-94.
5. Lengner, C.J., *iPS cell technology in regenerative medicine.* Ann N Y Acad Sci, 2010. 1192: p. 38-44.
6. Ben-David, U. and N. Benvenisty, *The tumorigenicity of human embryonic and induced pluripotent stem cells.* Nat Rev Cancer, 2011. 11(4): p. 268-77.
7. Mimeault, M. and S.K. Batra, *Concise review: recent advances on the significance of stem cells in tissue regeneration and cancer therapies.* Stem Cells, 2006. 24(11): p. 2319-45.
8. Hipp, J. and A. Atala, *Sources of stem cells for regenerative medicine.* Stem Cell Rev, 2008. 4(1): p. 3-11.
9. Chen, F., et al., *Mucormycosis spondylodiscitis after lumbar disc puncture.* Eur Spine J, 2006. 15(3): p. 370-6.
10. D'Ippolito, G., et al., *Age-related osteogenic potential of mesenchymal stromal stem cells from human vertebral bone marrow.* J Bone Miner Res, 1999. 14(7): p. 1115-22.
11. Mareschi, K., et al., *Expansion of mesenchymal stem cells isolated from pediatric and adult donor bone marrow.* J Cell Biochem, 2006. 97(4): p. 744-54.
12. Ohi, Y., et al., *Incomplete DNA methylation underlies a transcriptional memory of somatic cells in human iPS cells.* Nat Cell Biol, 2011. 13(5): p. 541-9.
13. Blasco, M.A., M. Serrano, and O. Fernandez-Capetillo, *Genomic instability in iPS: time for a break.* EMBO J, 2011. 30(6): p. 991-3.
14. Robinton, D.A. and G.Q. Daley, *The promise of induced pluripotent stem cells in research and therapy.* Nature, 2012. 481(7381): p. 295-305.
15. Favaron, P.O., et al., *The Amniotic Membrane: Development and Potential Applications - A Review.* Reprod Domest Anim, 2015. 50(6): p. 881-92.
16. Berika, M., M.E. Elgayyar, and A.H. El-Hashash, *Asymmetric cell division of stem cells in the lung and other systems.* Front Cell Dev Biol, 2014. 2: p. 33.
17. Yoo, Y.D. and Y.T. Kwon, *Molecular mechanisms controlling asymmetric and symmetric self-renewal of cancer stem cells.* J Anal Sci Technol, 2015. 6(1): p. 28.
18. Igura, K., et al., *Isolation and characterization of mesenchymal progenitor cells from chorionic villi of human placenta.* Cytotherapy, 2004. 6(6): p. 543-53.
19. Zhang, X., et al., *Successful immortalization of mesenchymal progenitor cells derived from human placenta and the differentiation*

abilities of immortalized cells. Biochem Biophys Res Commun, 2006. 351(4): p. 853-9.
20. Evans, M.J. and M.H. Kaufman, *Establishment in culture of pluripotential cells from mouse embryos.* Nature, 1981. 292(5819): p. 154-6.
21. Ilancheran, S., et al., *Stem cells derived from human fetal membranes display multilineage differentiation potential.* Biol Reprod, 2007. 77(3): p. 577-88.
22. Sarugaser, R., et al., *Human mesenchymal stem cells self-renew and differentiate according to a deterministic hierarchy.* PLoS One, 2009. 4(8): p. e6498.
23. Sarugaser, R., et al., *Human umbilical cord perivascular (HUCPV) cells: a source of mesenchymal progenitors.* Stem Cells, 2005. 23(2): p. 220-9.
24. Sarugaser, R., et al., *Isolation, propagation, and characterization of human umbilical cord perivascular cells (HUCPVCs).* Methods Mol Biol, 2009. 482: p. 269-79.
25. Pittenger, M.F., et al., *Multilineage potential of adult human mesenchymal stem cells.* Science, 1999. 284(5411): p. 143-7.
26. Zuk, P.A., et al., *Multilineage cells from human adipose tissue: implications for cell-based therapies.* Tissue Eng, 2001. 7(2): p. 211-28.
27. Hanada, K., et al., *BMP-2 induction and TGF-beta 1 modulation of rat periosteal cell chondrogenesis.* J Cell Biochem, 2001. 81(2): p. 284-94.
28. Mackay, A.M., et al., *Chondrogenic differentiation of cultured human mesenchymal stem cells from marrow.* Tissue Eng, 1998. 4(4): p. 415-28.
29. Kooreman, N.G. and J.C. Wu, *Tumorigenicity of pluripotent stem cells: biological insights from molecular imaging.* J R Soc Interface, 2010. 7 Suppl 6: p. S753-63.
30. Peault, B., *[Mesenchymal stem cell: in quest of an identity?].* Med Sci (Paris), 2011. 27(3): p. 227-8.
31. Chen, C.W., et al., *Perivascular multi-lineage progenitor cells in human organs: regenerative units, cytokine sources or both?* Cytokine Growth Factor Rev, 2009. 20(5-6): p. 429-34.
32. Crisan, M., et al., *A perivascular origin for mesenchymal stem cells in multiple human organs.* Cell Stem Cell, 2008. 3(3): p. 301-13.
33. Mathur, A. and J.F. Martin, *Stem cells and repair of the heart.* Lancet, 2004. 364(9429): p. 183-92.
34. Herzog, E.L., L. Chai, and D.S. Krause, *Plasticity of marrow-derived stem cells.* Blood, 2003. 102(10): p. 3483-93.
35. Corradetti, B., et al., *Osteoprogenitor cells from bone marrow and cortical bone: understanding how the environment affects their fate.* Stem Cells Dev, 2015. 24(9): p. 1112-23.
36. Cuti, T., et al., *Capacity of muscle derived stem cells and pericytes to promote tendon graft integration and ligamentization following anterior cruciate ligament reconstruction.* Int Orthop, 2017. 41(6): p. 1189-1198.

37. Vishnubalaji, R., et al., *Skin-derived multipotent stromal cells--an archrival for mesenchymal stem cells.* Cell Tissue Res, 2012. 350(1): p. 1-12.
38. Lee, S., et al., *Mesenchymal Stem Cells Derived from Human Exocrine Pancreas Spontaneously Express Pancreas Progenitor-Cell Markers in a Cell-Passage-Dependent Manner.* Stem Cells Int, 2016. 2016: p. 2142646.
39. Gronthos, S., et al., *Surface protein characterization of human adipose tissue-derived stromal cells.* J Cell Physiol, 2001. 189(1): p. 54-63.
40. Suchanek, J., et al., *Human dental pulp stem cells--isolation and long term cultivation.* Acta Medica (Hradec Kralove), 2007. 50(3): p. 195-201.
41. Parolini, O., et al., *Concise review: isolation and characterization of cells from human term placenta: outcome of the first international Workshop on Placenta Derived Stem Cells.* Stem Cells, 2008. 26(2): p. 300-11.
42. Haynesworth, S.E., et al., *Characterization of cells with osteogenic potential from human marrow.* Bone, 1992. 13(1): p. 81-8.
43. Friedenstein, A.J., R.K. Chailakhjan, and K.S. Lalykina, *The development of fibroblast colonies in monolayer cultures of guinea-pig bone marrow and spleen cells.* Cell Tissue Kinet, 1970. 3(4): p. 393-403.
44. Dominici, M., et al., *Minimal criteria for defining multipotent mesenchymal stromal cells. The International Society for Cellular Therapy position statement.* Cytotherapy, 2006. 8(4): p. 315-7.
45. Peault, B., *Are mural cells guardians of stemness?: From pluri- to multipotency via vascular pericytes.* Circulation, 2012. 125(1): p. 12-3.
46. Zheng, B., et al., *Prospective identification of myogenic endothelial cells in human skeletal muscle.* Nat Biotechnol, 2007. 25(9): p. 1025-34.
47. Bonab, M.M., et al., *Aging of mesenchymal stem cell in vitro.* BMC Cell Biol, 2006. 7: p. 14.
48. Jin, H.J., et al., *Comparative analysis of human mesenchymal stem cells from bone marrow, adipose tissue, and umbilical cord blood as sources of cell therapy.* Int J Mol Sci, 2013. 14(9): p. 17986-8001.
49. Vidal, M.A., et al., *Cell growth characteristics and differentiation frequency of adherent equine bone marrow-derived mesenchymal stromal cells: adipogenic and osteogenic capacity.* Vet Surg, 2006. 35(7): p. 601-10.
50. Vidal, M.A., et al., *Comparison of chondrogenic potential in equine mesenchymal stromal cells derived from adipose tissue and bone marrow.* Vet Surg, 2008. 37(8): p. 713-24.
51. Martin, G.R., *Isolation of a pluripotent cell line from early mouse embryos cultured in medium conditioned by teratocarcinoma stem cells.* Proc Natl Acad Sci U S A, 1981. 78(12): p. 7634-8.
52. Ringe, J., et al., *Porcine mesenchymal stem cells. Induction of distinct mesenchymal cell lineages.* Cell Tissue Res, 2002. 307(3): p. 321-7.

53. Guillot, P.V., et al., *Stem cell differentiation and expansion for clinical applications of tissue engineering.* J Cell Mol Med, 2007. 11(5): p. 935-44.
54. Evangelista, M., M. Soncini, and O. Parolini, *Placenta-derived stem cells: new hope for cell therapy?* Cytotechnology, 2008. 58(1): p. 33-42.
55. Parolini et al., *Placental Stem/Progenitor Cells: Isolation and Characterization.* Perinatal Stem Cells, 2014.
56. Karahuseyinoglu, S., et al., *Biology of stem cells in human umbilical cord stroma: in situ and in vitro surveys.* Stem Cells, 2007. 25(2): p. 319-31.
57. Bieback, K., et al., *Critical parameters for the isolation of mesenchymal stem cells from umbilical cord blood.* Stem Cells, 2004. 22(4): p. 625-34.
58. Laughlin, M.J.e.a., *Hematopoietic engraftment and survival in adult recipients of umbilical-cord blood from unrelated donors.* N Engl J Med 344, 2001: p. 1815-1822.
59. Carlin, R., et al., *Expression of early transcription factors Oct-4, Sox-2 and Nanog by porcine umbilical cord (PUC) matrix cells.* Reprod Biol Endocrinol, 2006. 4: p. 8.
60. Karahuseyinoglu, S., et al., *Functional structure of adipocytes differentiated from human umbilical cord stroma-derived stem cells.* Stem Cells, 2008. 26(3): p. 682-91.
61. Hall, J.G., et al., *Unrelated umbilical cord blood transplantation for an infant with beta-thalassemia major.* J Pediatr Hematol Oncol, 2004. 26(6): p. 382-5.
62. Kurtzberg, J., A.D. Lyerly, and J. Sugarman, *Untying the Gordian knot: policies, practices, and ethical issues related to banking of umbilical cord blood.* J Clin Invest, 2005. 115(10): p. 2592-7.
63. Marongiu, F., et al., *Isolation of amniotic mesenchymal stem cells.* Curr Protoc Stem Cell Biol, 2010. Chapter 1: p. Unit 1E 5.
64. Miki, T. and S.C. Strom, *Amnion-derived pluripotent/multipotent stem cells.* Stem Cell Rev, 2006. 2(2): p. 133-42.
65. Izumi, M., et al., *Quantitative comparison of stem cell marker-positive cells in fetal and term human amnion.* J Reprod Immunol, 2009. 81(1): p. 39-43.
66. Bailo, M., et al., *Engraftment potential of human amnion and chorion cells derived from term placenta.* Transplantation, 2004. 78(10): p. 1439-48.
67. Li, H., et al., *Immunosuppressive factors secreted by human amniotic epithelial cells.* Invest Ophthalmol Vis Sci, 2005. 46(3): p. 900-7.
68. Avila, M., et al., *Reconstruction of ocular surface with heterologous limbal epithelium and amniotic membrane in a rabbit model.* Cornea, 2001. 20(4): p. 414-20.
69. Kubo, M., et al., *Immunogenicity of human amniotic membrane in experimental xenotransplantation.* Invest Ophthalmol Vis Sci, 2001. 42(7): p. 1539-46.
70. Yuge, I., et al., *Transplanted human amniotic epithelial cells express connexin 26 and Na-K-adenosine triphosphatase in the inner ear.* Transplantation, 2004. 77(9): p. 1452-4.

71. Sankar, V. and R. Muthusamy, *Role of human amniotic epithelial cell transplantation in spinal cord injury repair research.* Neuroscience, 2003. 118(1): p. 11-7.
72. Magatti, M., et al., *Human amnion mesenchyme harbors cells with allogeneic T-cell suppression and stimulation capabilities.* Stem Cells, 2008. 26(1): p. 182-92.
73. Waked, N. and V. El-Kazzi, *[Amniotic membrane utilization in ophthalmological surgical procedures].* J Med Liban, 2005. 53(1): p. 39-44.
74. Ollivier, F.J., et al., *Amniotic membrane transplantation for corneal surface reconstruction after excision of corneolimbal squamous cell carcinomas in nine horses.* Vet Ophthalmol, 2006. 9(6): p. 404-13.
75. Lassaline, M.E., et al., *Equine amniotic membrane transplantation for corneal ulceration and keratomalacia in three horses.* Vet Ophthalmol, 2005. 8(5): p. 311-7.
76. Plummer, C.E., et al., *The use of amniotic membrane transplantation for ocular surface reconstruction: a review and series of 58 equine clinical cases (2002-2008).* Vet Ophthalmol, 2009. 12 Suppl 1: p. 17-24.
77. Arcelli, R., et al., *Equine amniotic membrane transplantation in some ocular surface diseases in the dog and cat: a preliminary study.* Vet Res Commun, 2009. 33 Suppl 1: p. 169-71.
78. Solomon, A., et al., *Suppression of inflammatory and fibrotic responses in allergic inflammation by the amniotic membrane stromal matrix.* Clin Exp Allergy, 2005. 35(7): p. 941-8.
79. Dua, H.S., et al., *The amniotic membrane in ophthalmology.* Surv Ophthalmol, 2004. 49(1): p. 51-77.
80. Koizumi, N.J., et al., *Growth factor mRNA and protein in preserved human amniotic membrane.* Curr Eye Res, 2000. 20(3): p. 173-7.
81. Page, D.R.A.a.K.R., *Pathways of water transfer between liquor amnii and the fetoplacental unit at term.* European Journal of Obstetrics and Gynecology and Reproductive Biology, 1973. 3: p. 155–158.
82. Lotgering, F.K. and H.C. Wallenburg, *Mechanisms of production and clearance of amniotic fluid.* Semin Perinatol, 1986. 10(2): p. 94-102.
83. Underwood, M.A., W.M. Gilbert, and M.P. Sherman, *Amniotic fluid: not just fetal urine anymore.* J Perinatol, 2005. 25(5): p. 341-8.
84. Torricelli, F., et al., *Identification of hematopoietic progenitor cells in human amniotic fluid before the 12th week of gestation.* Ital J Anat Embryol, 1993. 98(2): p. 119-26.
85. S. Da Sacco, S.S., F. Boldrin et al, *Human amniotic fluid as a potential new source of organ specific precursor cells for future regenerative medicine applications* Journal of Urology, 2010. 183(3): p. 193–1200.
86. Wapner, R.J., D.A. Driscoll, and J.L. Simpson, *Integration of microarray technology into prenatal diagnosis: counselling issues generated during the NICHD clinical trial.* Prenat Diagn, 2012. 32(4): p. 396-400.

87. Torricelli et al, *Identification of hematopoietic progenitor cells in human amniotic fluid before the 12th week of gestation.* Ital J Anat Embryol 98, 1993: p. 119-126.
88. De Coppi, P., et al., *Isolation of amniotic stem cell lines with potential for therapy.* Nat Biotechnol, 2007. 25(1): p. 100-6.
89. Sessarego, N., et al., *Multipotent mesenchymal stromal cells from amniotic fluid: solid perspectives for clinical application.* Haematologica, 2008. 93(3): p. 339-46.
90. Castellucci, M., et al., *The development of the human placental villous tree.* Anat Embryol (Berl), 1990. 181(2): p. 117-28.
91. Fauza, D., *Amniotic fluid and placental stem cells.* Best Pract Res Clin Obstet Gynaecol, 2004. 18(6): p. 877-91.
92. Kaufmann, P., *Development and differentiation of the human placental villous tree.* Bibl Anat, 1982(22): p. 29-39.
93. Castellucci, M. and P. Kaufmann, *A three-dimensional study of the normal human placental villous core: II. Stromal architecture.* Placenta, 1982. 3(3): p. 269-85.
94. Schweikhart, G. and P. Kaufmann, *[Problems of distinction of normal, arteficial and pathological structures in mature human placental villi. I. Ultrastructure of the syncytiotrophoblast (author's transl)].* Arch Gynakol, 1977. 222(3): p. 213-30.
95. Kaufmann, P., et al., *Cross-sectional features and three-dimensional structure of human placental villi.* Placenta, 1987. 8(3): p. 235-47.
96. Brambati, B. and G. Simoni, *Diagnosis of fetal trisomy 21 in first trimester.* Lancet, 1983. 1(8324): p. 586.
97. Castrechini, N.M., et al., *Mesenchymal stem cells in human placental chorionic villi reside in a vascular Niche.* Placenta, 2010. 31(3): p. 203-12.
98. Fukuchi, Y., et al., *Human placenta-derived cells have mesenchymal stem/progenitor cell potential.* Stem Cells, 2004. 22(5): p. 649-58.
99. Miao, Z., et al., *Isolation of mesenchymal stem cells from human placenta: comparison with human bone marrow mesenchymal stem cells.* Cell Biol Int, 2006. 30(9): p. 681-7.
100. Wulf, G.G., et al., *Mesengenic progenitor cells derived from human placenta.* Tissue Eng, 2004. 10(7-8): p. 1136-47.
101. Li, C.D., et al., *WITHDRAWN: Isolation and Identification of a Multilineage Potential Mesenchymal Cell from Human Placenta.* Placenta, 2005.
102. Poloni, A., et al., *Human mesenchymal stem cells from chorionic villi and amniotic fluid are not susceptible to transformation after extensive in vitro expansion.* Cell Transplant, 2011. 20(5): p. 643-54.
103. Wang, Y., et al., *Safety of mesenchymal stem cells for clinical application.* Stem Cells Int, 2012. 2012: p. 652034.
104. Rosland, G.V., et al., *Long-term cultures of bone marrow-derived human mesenchymal stem cells frequently undergo spontaneous malignant transformation.* Cancer Res, 2009. 69(13): p. 5331-9.
105. Rubio, D., et al., *Spontaneous human adult stem cell transformation.* Cancer Res, 2005. 65(8): p. 3035-9.
106. Bernardo, M.E., et al., *Human bone marrow derived mesenchymal stem cells do not undergo transformation after long-term in vitro*

culture and do not exhibit telomere maintenance mechanisms. Cancer Res, 2007. 67(19): p. 9142-9.
107. Aggarwal, S. and M.F. Pittenger, *Human mesenchymal stem cells modulate allogeneic immune cell responses.* Blood, 2005. 105(4): p. 1815-22.
108. Kunisaki, S.M., R.W. Jennings, and D.O. Fauza, *Fetal cartilage engineering from amniotic mesenchymal progenitor cells.* Stem Cells Dev, 2006. 15(2): p. 245-53.
109. al, S.e., Heart Valve Dis., 2008. 14 (4): p. 446-55.
110. Parolini et al., *Placental Stem/Progenitor Cells: Isolation and Characterization.* Perinatal Stem Cells, 2007: p. 1118-13.
111. Insausti, C.L., et al., *Amniotic membrane-derived stem cells: immunomodulatory properties and potential clinical application.* Stem Cells Cloning, 2014. 7: p. 53-63.
112. In 't Anker, P.S., et al., *Isolation of mesenchymal stem cells of fetal or maternal origin from human placenta.* Stem Cells, 2004. 22(7): p. 1338-45.
113. Marcus, A.J., et al., *Isolation, characterization, and differentiation of stem cells derived from the rat amniotic membrane.* Differentiation, 2008. 76(2): p. 130-44.
114. Lange-Consiglio, A., et al., *Characterization and potential applications of progenitor-like cells isolated from horse amniotic membrane.* J Tissue Eng Regen Med, 2012. 6(8): p. 622-35.
115. Corradetti, B., et al., *Mesenchymal stem cells from amnion and amniotic fluid in the bovine.* Reproduction, 2013. 145(4): p. 391-400.
116. Chen, J., et al., *Isolation and characterization of porcine amniotic fluid-derived multipotent stem cells.* PLoS One, 2011. 6(5): p. e19964.
117. Mauro, A., et al., *Isolation, characterization, and in vitro differentiation of ovine amniotic stem cells.* Vet Res Commun, 2010. 34 Suppl 1: p. S25-8.
118. Park, S.B., et al., *Isolation and characterization of canine amniotic membrane-derived multipotent stem cells.* PLoS One, 2012. 7(9): p. e44693.
119. Vidane, A.S., et al., *Cat amniotic membrane multipotent cells are nontumorigenic and are safe for use in cell transplantation.* Stem Cells Cloning, 2014. 7: p. 71-8.
120. Gao, Y., et al., *Isolation and biological characterization of chicken amnion epithelial cells.* Eur J Histochem, 2012. 56(3): p. e33.
121. Wojakowski, W. and M. Tendera, *Mobilization of bone marrow-derived progenitor cells in acute coronary syndromes.* Folia Histochem Cytobiol, 2005. 43(4): p. 229-32.
122. Kawada, H., et al., *Nonhematopoietic mesenchymal stem cells can be mobilized and differentiate into cardiomyocytes after myocardial infarction.* Blood, 2004. 104(12): p. 3581-7.
123. Ren, G., et al., *Mesenchymal stem cell-mediated immunosuppression occurs via concerted action of chemokines and nitric oxide.* Cell Stem Cell, 2008. 2(2): p. 141-50.

124. Rossi, D., et al., *Characterization of the conditioned medium from amniotic membrane cells: prostaglandins as key effectors of its immunomodulatory activity.* PLoS One, 2012. 7(10): p. e46956.
125. Cortinovis, M., et al., *Mesenchymal stromal cells to control donor-specific memory T cells in solid organ transplantation.* Curr Opin Organ Transplant, 2015. 20(1): p. 79-85.
126. Singer, N.G. and A.I. Caplan, *Mesenchymal stem cells: mechanisms of inflammation.* Annu Rev Pathol, 2011. 6: p. 457-78.
127. Groh, M.E., et al., *Human mesenchymal stem cells require monocyte-mediated activation to suppress alloreactive T cells.* Exp Hematol, 2005. 33(8): p. 928-34.
128. Sato, K., et al., *Nitric oxide plays a critical role in suppression of T-cell proliferation by mesenchymal stem cells.* Blood, 2007. 109(1): p. 228-34.
129. Meisel, R., et al., *Human bone marrow stromal cells inhibit allogeneic T-cell responses by indoleamine 2,3-dioxygenase-mediated tryptophan degradation.* Blood, 2004. 103(12): p. 4619-21.
130. Corradetti, B., et al., *Amniotic membrane-derived mesenchymal cells and their conditioned media: potential candidates for uterine regenerative therapy in the horse.* PLoS One, 2014. 9(10): p. e111324.
131. Stamler, J.S., et al., *S-nitrosylation of proteins with nitric oxide: synthesis and characterization of biologically active compounds.* Proc Natl Acad Sci U S A, 1992. 89(1): p. 444-8.
132. Niedbala, W., B. Cai, and F.Y. Liew, *Role of nitric oxide in the regulation of T cell functions.* Ann Rheum Dis, 2006. 65 Suppl 3: p. iii37-40.
133. Corradetti B. (eds), *The Immune Response to Implanted Materials and Devices: The Impact of the immune System on the Success of an implant.* Springer, 2017. 1: p. XVIII, 241\254.
134. Janeway, C.A., Jr., *How the immune system protects the host from infection.* Microbes Infect, 2001. 3(13): p. 1167-71.
135. Murray, P.J., et al., *Macrophage activation and polarization: nomenclature and experimental guidelines.* Immunity, 2014. 41(1): p. 14-20.
136. Mantovani, A., et al., *The chemokine system in diverse forms of macrophage activation and polarization.* Trends Immunol, 2004. 25(12): p. 677-86.
137. Martinez, F.O. and S. Gordon, *The M1 and M2 paradigm of macrophage activation: time for reassessment.* F1000Prime Rep, 2014. 6: p. 13.
138. Davis, M.J., et al., *Macrophage M1/M2 polarization dynamically adapts to changes in cytokine microenvironments in Cryptococcus neoformans infection.* MBio, 2013. 4(3): p. e00264-13.
139. Owen, M., *Marrow stromal stem cells.* J Cell Sci Suppl, 1988. 10: p. 63-76.
140. Caplan, A.I., *Mesenchymal stem cells.* J Orthop Res, 1991. 9(5): p. 641-50.
141. Owen, M. and A.J. Friedenstein, *Stromal stem cells: marrow-derived osteogenic precursors.* Ciba Found Symp, 1988. 136: p. 42-60.

142. al., A.e., *Mixed enzymatic-explant protocol for isolation of mesenchymal stem cells from Wharton's jelly and encapsulation in 3D culture system.* Biomedical Science and Engineering, 2012. 5: p. 580-86.
143. Shaer, A., et al., *Isolation and characterization of Human Mesenchymal Stromal Cells Derived from Placental Decidua Basalis; Umbilical cord Wharton's Jelly and Amniotic Membrane.* Pak J Med Sci, 2014. 30(5): p. 1022-6.
144. Terada, N., et al., *Bone marrow cells adopt the phenotype of other cells by spontaneous cell fusion.* Nature, 2002. 416(6880): p. 542-5.
145. Nygren, J.M., et al., *Bone marrow-derived hematopoietic cells generate cardiomyocytes at a low frequency through cell fusion, but not transdifferentiation.* Nat Med, 2004. 10(5): p. 494-501.
146. Magatti, M., et al., *Human amnion favours tissue repair by inducing the M1-to-M2 switch and enhancing M2 macrophage features.* J Tissue Eng Regen Med, 2016.
147. Abumaree, M.H., et al., *Human placental mesenchymal stem cells (pMSCs) play a role as immune suppressive cells by shifting macrophage differentiation from inflammatory M1 to anti-inflammatory M2 macrophages.* Stem Cell Rev, 2013. 9(5): p. 620-41.
148. Silini, A.R., et al., *The Long Path of Human Placenta, and Its Derivatives, in Regenerative Medicine.* Front Bioeng Biotechnol, 2015. 3: p. 162.
149. Cho, D.I., et al., *Mesenchymal stem cells reciprocally regulate the M1/M2 balance in mouse bone marrow-derived macrophages.* Exp Mol Med, 2014. 46: p. e70.
150. Magatti, M., et al., *Amniotic mesenchymal tissue cells inhibit dendritic cell differentiation of peripheral blood and amnion resident monocytes.* Cell Transplant, 2009. 18(8): p. 899-914.
151. Kang, J.W., et al., *Immunomodulatory effects of human amniotic membrane-derived mesenchymal stem cells.* J Vet Sci, 2012. 13(1): p. 23-31.
152. Ren, G., et al., *Species variation in the mechanisms of mesenchymal stem cell-mediated immunosuppression.* Stem Cells, 2009. 27(8): p. 1954-62.
153. Chung, Y., et al., *Embryonic and extraembryonic stem cell lines derived from single mouse blastomeres.* Nature, 2006. 439(7073): p. 216-9.
154. Thomson, J.A., et al., *Embryonic stem cell lines derived from human blastocysts.* Science, 1998. 282(5391): p. 1145-7.
155. Nakagawa, M., et al., *Generation of induced pluripotent stem cells without Myc from mouse and human fibroblasts.* Nat Biotechnol, 2008. 26(1): p. 101-6.
156. Takahashi, K., et al., *Induction of pluripotent stem cells from adult human fibroblasts by defined factors.* Cell, 2007. 131(5): p. 861-72.
157. Bajek, A., et al., *Human amniotic-fluid-derived stem cells: a unique source for regenerative medicine.* Expert Opin Biol Ther, 2014. 14(6): p. 831-9.
158. Hemberger, M., et al., *Stem cells from fetal membranes - a workshop report.* Placenta, 2008. 29 Suppl A: p. S17-9.

159. Barboni, B., et al., *Gestational stage affects amniotic epithelial cells phenotype, methylation status, immunomodulatory and stemness properties.* Stem Cell Rev, 2014. 10(5): p. 725-41.
160. Lim, R., *Concise Review: Fetal Membranes in Regenerative Medicine: New Tricks from an Old Dog?* Stem Cells Transl Med, 2017. 6(9): p. 1767-1776.
161. Parolini, O., et al., *Amniotic membrane and amniotic fluid-derived cells: potential tools for regenerative medicine?* Regen Med, 2009. 4(2): p. 275-91.
162. Lim, R., et al., *Preterm human amnion epithelial cells have limited reparative potential.* Placenta, 2013. 34(6): p. 486-92.
163. Luzo, A.C., et al., *Early proliferation of umbilical cord blood cells from premature neonates.* Vox Sang, 2007. 93(2): p. 145-53.
164. da Silva Meirelles, L., A.I. Caplan, and N.B. Nardi, *In search of the in vivo identity of mesenchymal stem cells.* Stem Cells, 2008. 26(9): p. 2287-99.
165. Bianco, P., et al., *The meaning, the sense and the significance: translating the science of mesenchymal stem cells into medicine.* Nat Med, 2013. 19(1): p. 35-42.
166. Bianco, P., P.G. Robey, and P.J. Simmons, *Mesenchymal stem cells: revisiting history, concepts, and assays.* Cell Stem Cell, 2008. 2(4): p. 313-9.
167. Caplan, A.I. and D. Correa, *The MSC: an injury drugstore.* Cell Stem Cell, 2011. 9(1): p. 11-5.
168. Barlow, S., et al., *Comparison of human placenta- and bone marrow-derived multipotent mesenchymal stem cells.* Stem Cells Dev, 2008. 17(6): p. 1095-107.
169. Pelekanos, R.A., et al., *Comprehensive transcriptome and immunophenotype analysis of renal and cardiac MSC-like populations supports strong congruence with bone marrow MSC despite maintenance of distinct identities.* Stem Cell Res, 2012. 8(1): p. 58-73.
170. Guillot, P.V., et al., *Human first-trimester fetal MSC express pluripotency markers and grow faster and have longer telomeres than adult MSC.* Stem Cells, 2007. 25(3): p. 646-54.
171. da Silva Meirelles, L., P.C. Chagastelles, and N.B. Nardi, *Mesenchymal stem cells reside in virtually all post-natal organs and tissues.* J Cell Sci, 2006. 119(Pt 11): p. 2204-13.
172. Wegmeyer, H., et al., *Mesenchymal stromal cell characteristics vary depending on their origin.* Stem Cells Dev, 2013. 22(19): p. 2606-18.
173. Chen, Y.S., et al., *Small molecule mesengenic induction of human induced pluripotent stem cells to generate mesenchymal stem/stromal cells.* Stem Cells Transl Med, 2012. 1(2): p. 83-95.
174. Xu, C., et al., *Cross-Talking Between PPAR and WNT Signaling and its Regulation in Mesenchymal Stem Cell Differentiation.* Curr Stem Cell Res Ther, 2016. 11(3): p. 247-54.
175. Zhuang, H., et al., *Molecular Mechanisms of PPAR-gamma Governing MSC Osteogenic and Adipogenic Differentiation.* Curr Stem Cell Res Ther, 2016. 11(3): p. 255-64.

176. James, A.W., *Review of Signaling Pathways Governing MSC Osteogenic and Adipogenic Differentiation.* Scientifica (Cairo), 2013. 2013: p. 684736.
177. Tipnis, S., C. Viswanathan, and A.S. Majumdar, *Immunosuppressive properties of human umbilical cord-derived mesenchymal stem cells: role of B7-H1 and IDO.* Immunol Cell Biol, 2010. 88(8): p. 795-806.
178. Shi, Y., et al., *How mesenchymal stem cells interact with tissue immune responses.* Trends Immunol, 2012. 33(3): p. 136-43.
179. Ren, G., et al., *Inflammatory cytokine-induced intercellular adhesion molecule-1 and vascular cell adhesion molecule-1 in mesenchymal stem cells are critical for immunosuppression.* J Immunol, 2010. 184(5): p. 2321-8.
180. Chamberlain, G., et al., *Concise review: mesenchymal stem cells: their phenotype, differentiation capacity, immunological features, and potential for homing.* Stem Cells, 2007. 25(11): p. 2739-49.
181. Murphy, S., et al., *Human amnion epithelial cells prevent bleomycin-induced lung injury and preserve lung function.* Cell Transplant, 2011. 20(6): p. 909-23.
182. Furth, M.E. and A. Atala, *Stem cell sources to treat diabetes.* J Cell Biochem, 2009. 106(4): p. 507-11.

5. PUBLICATION

Heparan sulfate: a potential candidate for the development of biomimetic immunomodulatory membranes

Bruna Corradetti[1,2], Francesca Taraballi[3,5*], Ilaria Giretti[2], Guillermo Bauza[3,4], Rossella S. Pistillo[2], Federica Banche Niclot[3], Laura Pandolfi[3], Ennio Tasciotti[3,4,5]

Department of Nanomedicine, Houston Methodist Research Institute, Houston, TX 77030, USA; [2] Department of Life and Environmental Sciences, Università Politecnica delle Marche, 60131, Ancona, Italy; [3] Center for Biomimetic Medicine, Houston Methodist Research Institute, Houston, TX, 77030, USA; [4]Center for NanoHealth, Swansea University Medical School, Swansea University Bay, Singleton Park, SA2 8PP, Wales, UK.; [5]Department of Orthopaedic & Sports Medicine, The Houston Methodist Hospital, Houston, TX 77030, USA.

Correspondence:
Corresponding author: ftaraballi2@houstonmethodist.org

Key words: mesenchymal stem cells, microenvironment, immune response, regeneration, tissue engineering, biomolecules, heparan sulfate, collagen

ABSTRACT

Clinical trials have demonstrated that heparan sulfate (HS) could be used as a therapeutic agent for the treatment of inflammatory diseases. Its anti-inflammatory effect makes it suitable for the development of biomimetic innovative strategies aiming at modulating stem cells behavior toward a pro-regenerative phenotype in case of injury or inflammation. Here we propose collagen type I meshes fabricated by solvent casting and further cross-linked with HS (Col-HS) to create a biomimetic environment resembling the extracellular matrix of soft tissue. Col-HS meshes were tested for their capability to provide physical support to stem cells growth, maintain their phenotypes and immunosuppressive potential following inflammation. HS-Col effect on stem cells was investigated in standard conditions as well as in an inflammatory environment recapitulated *in vitro* through a mix of pro-inflammatory cytokines (TNFα and IFNγ; 20ng/ml). A significant increase in the production of molecules associated with immunosuppression was demonstrated in response to the material and when cells were grown in presence of pro-inflammatory stimuli, compared to bare collagen membranes (Col), leading to a greater inhibitory potential when MSC were exposed to stimulated peripheral blood mononuclear cells. Our data suggest that the presence of HS is able to activate the molecular machinery responsible for the release of anti-inflammatory cytokines, potentially leading to a faster resolution of inflammation.

INTRODUCTION

Tissues consist of cellular and non-cellular components [1,2]. The extracellular matrix (ECM) represents an intricate network of macromolecules, such as water, proteins and polysaccharides that are produced by the cells and are assembled into an organized network in close association with the cell surface [3]. The ECM structure is often remodeled and its molecular components are subjected to post-translational modifications [4]. The production and deposition of these components outside the cell surface provide structural ad functional integrity to connective tissue and organs and acts as physical scaffold for the cellular constituents. The role of ECM is also crucial in the response to growth factors, cytokines and mechanical signals mediated by cell surface receptor, and in the provision of biochemical and biomechanical cues that are required for tissue morphogenesis, differentiation and homeostasis [5]. Given the ability of ECM to provide biochemical and mechanical properties to any specific tissue (e.g. tensile and compressive strength and elasticity), its physical, topological and biochemical composition is tissue-specific, but largely heterogeneous, and depends on the biochemical and biophysical interaction of various cellular components (e.g. epithelial, fibroblast, adipocyte, endothelial elements) and the cellular microenviroment [6]. The relative amounts of the different types of matrix macromolecules and their organization in the ECM reflect the needs of the specific host tissue. Among all components of the ECM, glycosaminoglycans (GAGs) play a series of activities as they influence cell proliferation, differentiation and

gene expression [7,8], modulate protein gradient formation and signal transduction [9]. They are able to connect ECM structure, retain growth factors, maintain chemokines extracellular rate and prevent growth factors degradation. In particular, heparan sulfate (HS) acts as cofactor in many biological processes, interacting with diverse protein ligands (such as growth factor, viral proteins, enzymes, protease inhibitors, ECM molecules) [10,11]. Furthermore, its activity changes if it is linked to the core protein or if it is free. It has been demonstrated that HS binds a wide variety of proteins (including chemokines, growth factors, morphogens, enzymes and extracellular matrix component) that contain basic aminoacids with a specific and direct interaction [12]. HS activity influences cytokines processing and consequently their activity [12], while others ligands require some additional sequences to explicate their role, such as the interaction between HS and FGF receptor[13].

HS applied on Mesenchymal Stem Cells (MSC) biology shows its ability to maintain cell growth, proliferation, viability and stemness, decreasing the presence of apoptotic cells. Helledie et al. have recently evaluated the effect of HS on MSC immunophenotype, showing an increase in the expression of integrins (CD105 and CD73 molecules), a greater differentiative potential, and a more active secretion of molecules that support bone repair in an *in vivo* bone defect [14].

HS has been also demonstrated to play an important role in inflammation, due to its promising anti-inflammatory properties and the consequent potential to be used as therapeutic agent in some type of inflammatory

diseases [15]. Such diseases include for example rheumatoid arthritis and diabetic nephropathy, where it helps prevent leukocyte adhesion and consequently the propagation of inflammation [16]. Inflammation involves a series of events following a tissue injury caused by the presence of harmful stimuli, such as infection or physical damage. The first step of this reaction is the movement of T lymphocytes, monocytes and neutrophils from the vascular system to damage site, with a cascade of biochemical reactions, which is activated to create the appropriate inflammatory response. These biochemical reactions increase the levels of chemoattractans, including complex components and cytokines, like tumor necrosis factor-α (TNF-α) and interleukin-1β leading to an increased expression of the adhesion molecules (e.g. ICAM and VCAM) and selectins [16].

Therapeutically active MSC have been demonstrated to take part in the inflammatory cascade and contribute to tissue homeostasis by releasing trophic factors that act as anti-inflammatory immune modulators [1,17-19]. Their beneficial potential can be altered or improved through the exposure to bioactive molecules and the development of a naturally inspired bioactive material able to support and retain such capability in the context of injury or damage is still much needed[20].

In the present study, we describe a collagen-based mesh functionalized with HS with the aim of modulating inflammation by supporting MSC therapeutic potential. Although different studies describe a similar strategy [21,22], the translational point of view was never investigated, and the evaluation of the immunosuppressive potential of MSC on a bioactive material has never been provided. **Figure 1** summarizes the approach we propose. In addition to describe the proposed material in terms of topography and stability of its functionalization, we evaluated the effect of such meshes to

support the capability of MSC to adhere, proliferate, and maintain their conventional features, as well as to actively respond to an inflammatory environment, as we previously demonstrated in the context of cartilage-resembling materials [18,23]. Using rat bone marrow-derived MSC as surrogate local progenitor cells, we investigated the influence of our biomimetic natural material in retaining the immunosuppressive potential of MSC either in standard conditions or in response to the combination of pro-inflammatory cytokines [tumor necrosis factor-a (TNF-α) and interferon-gamma (IFN-γ)]. The capability of the proposed platform to support MSC anti-inflammatory role was finally proved in lymphocyte reaction assay.

MATERIALS AND METHODS

Meshes preparation and characterization

Type I collagen mesh (Col) from bovine tendon (5% collagen gel in acetic acid) were produced by a solvent-casting method as previously described [24,25]. Briefly, 1 g of type I collagen (Nitta Casings Inc.) was dissolved in an acetate buffer (pH 3.5) at the final concentration of 20 mg/mL. The collagen suspension was precipitated by the addition of sodium hydroxide (0.1 M) solution at pH 5.5. The resulting collagen slurry was mild cross-linked with 1.5 mM solution of 1,4-butanediol diglycidyl ether (BDDGE) (Sigma-Aldrich) for 48 hrs. The cross-linked collagen was washed 3 times in water and then the slurry was molden in metal racks, at a thickness of 2 mm and air dried under a fume hood for 3 days (final thickness: 0.1 mm). Covalent functionalization of heparin sulfate (HS) to collagen meshes was performed using the coupling reaction with 1-ethyl-3-(3-dimethyl aminopropyl)carbodiimide (EDC) and N-hydroxysuccinimide (NHS). After

weight the collagen matrices, each sample were incubated in a solution of 50 mM 2-morpholinoethane sulfonic acid (MES) (pH 5.5) in ethanol. After 1h the samples were place in a solution of 5 mM EDC and 5mM NHS and 0.2% (w/v) heparin sulfate (HS). After reaction for 24 hrs, the matrices were washed 3 times in PBS. For the stability study collagen meshes have been incubated with the same concentration of HS in the absence of crosslinker.

SEM imaging. HS-Col morphology was evaluated by scanning electron microscopy (SEM) (Quanta 600 FEG, FEI Company, Hillsboro, OR). Dried samples were sputter coated with 10 nm of Pt/Pd and imaged at a voltage of 10 mA.

Fourier Transform Infrared (FT-IR). FTIR spectra were measured in attenuated total reflection (ATR) using a Nicolet 6700 FT-IR Spectrometer (ThermoFisherScientific). Col and HS-Col meshes were without any sample manipulation. Spectra were analyzed by the software EZ OMNIC (Nicolet) after baseline correction between 1800 and 750 cm^{-1}. The presence of HS was also confirmed by histochemical staining. The meshes were stained by Alcian blue, which labels the proteoglycans.

ELLA Assays (Enzyme Linked Lectin Assay). HS crosslinked and absorbed on collagen meshed has been incubate in PBS for 14 day at 37°C to evaluate the stability of binding between HS and collagen mesh. At each time point the samples were treated with a solution of 2% BSA in PBS (100 µL) and shaken (14 hrs, 5°C). The patches after the blocking step have been incubated at room temperature with a solution of WGA peroxidase labeled

(Sigma-Aldrich) (0.01 mg/mL, 200 µL) in PBS for 2 hrs with shaking. After 3 washes in PBS we treated the samples with the peroxidase substrate OPD for 1 h. The absorbance was measured at 450 nm in triplicate.

Cell cultures

Rat compact bone mesenchymal stem cells (MSC) were isolated as previously reported[26] and maintained in standard culture media represented by Dulbecco's Modified Eagle's Medium (Sigma) supplemented with 10% fetal bovine serum (Euroclone), 1% L-Glutammine (Gibco) and 1% antibiotic/antimycotic solution (containing penicillin, streptomycin, and amphotericin B, Gibco) at 37°C in a humidified atmosphere with 5% CO_2. For maintenance of cultures, cells were plated at a cell density of 5 x 10^3 cells per cm^2. Medium was changed twice per week thereafter or according to the experiment requirements. Adherent cells were detached and subcultured using TrypLE Express (Invitrogen, ThermoFisher Scientific) before reaching confluence (80%) and subsequently replated at the same density for culture maintenance[18]. When seeded onto meshes, MSC were harvested, resuspended in standard cell culture medium, and seeded at the density of 1 x 10^4 cells/well in 12 well-plates (Corning). Inserts (Corning) were used to hang membranes (Col and HS-Col) and allow for cell adherence onto the collagen without reaching well surface. Standard culture medium was then added to each well. All procedures performed in studies involving animals were in accordance with the ethical standards of the institution where the studies were conducted.

MSC characterization before culture onto meshes

Upon reaching confluence, cells were collected and characterized for the expression of MSC-associated markers (CD105, CD90, and CD105) with a FortessaTM cell analyzer (Beckton Dickinson), under the assistance of the HMRI Flow Cytometry Core. Antibodies used (APC/Cy7-CD73, PE/Cy7-CD105, and AlexaFluor 700-CD90) were purchased from BioLegend. Briefly, MSC were recovered by trypsin method and by spinning down at 500 g for 5 min. They were then washed with FACS buffer labeled with directly conjugated antibodies according to manufacturer's indications.

At passage 3 cells were also assessed for their capability to undergo osteogenic and chondrogenic differentiation following a previously reported procedure [26]. Briefly, to induce osteogenesis MSC were seeded at the density of 5,000 cells/cm^2 in 12-well plates. Osteogenic induction was performed over 14-day period using a StemPro Osteogenesis Differentiation Kit (Gibco). To confirm differentiation, conventional von Kossa was performed. For chondrogenesis, cells were seeded at the density of 5,000 cells/cm2. Induction was performed using the StemPro Chondrogenesis Differentiation Kit (Gibco) for a 14-day period. Extracellular matrix constituted by proteoglycans was visualized by conventional Alcian Blue staining.

Effect of fibroblast-growth factor (FGF) and HS on cell proliferation

To test the effect of HS in retaining fibroblast-growth factor (FGF) and improve cell proliferation, MSC were exposed to different conditions and

the growth rate recorded over a 7-day period was compared. Conditioned included: 1) MSC grown in 2D culture systems (CTRL) and treated with FGF (10 ng/ml, w/FGF; PeproTech), soluble HS (25 ng/ml, w/ sHS; Carbosinth), and a combination of both (w/ sHS and FGF), 2) MSC grown onto Col in presence of soluble HS (Col w/ sHS), FGF (Col w/ FGF), and a combination of the two (Col w/ sHS and FGF), and 3) MSC grown onto HS-Col in presence in presence (HS-Col w/ FGF) and absence (HS-Col) of FGF. Experiment was set in triplicate. MTT assay (Life Technologies) was performed according to manufacturer's procedures. The concentration of FGF to be used was previously defined in a range of 1-100 ng/ml (data not shown).

Assessment of MSC morphology, metabolic activity, and immunofluorescence

MSC were seeded at the density of 100,000 cells/cm^2 onto HS-Col, Col meshes and cultured for 24 hrs to assess their immediate response to the material in terms of proliferation, morphology, adherence, and MSC-associated genes expression. Cell proliferation onto membranes was evaluated by Alamar Blue (ThermoFisher Scientific) according to manufacturer's instructions during a 3-day period as previously reported[18]. Optical density was measured at wavelengths of 570 and 600 nm. Data are shown as mean of 3 independent biological replicates. Values have been reported as %AB over time, which is associated with the presence of metabolically active cells. For comparison, data obtained from MSC grown

in two-dimensional conditions (CTRL) were also acquired.

Seven days after being seeded onto meshes or in 2D conditions cells were washed and fixed in 4% PFA for 20 min. Cell membranes were then permeabilized with 0.1% Triton X-100 for 10 minutes and then blocked by 10% goat serum in PBS for 1 hour at RT. Cells were stained with phalloidin (Alexa Fluor – 555, Invitrogen by Life Technologies) and anti-Vinculin (FITC conjugated, Sigma Aldrich) and DAPI to identify actin cytoskeleton and focal adhesion (Actin Cytoskeleton and Focal Adhesion Staining Kit, Millipore) at a dilution of 1/100 in blocking solution at RT in darkness, and subsequently the nuclei stained with DAPI (ThermoFisher Scientific Inc.) according to manufacturer instructions. Samples were imaged with a confocal laser microscope (A1 Nikon Confocal Microscope), and the images were analyzed through the NIS-Elements software (Nikon). Col and HS-Col sample were imaged by confocal laser microscopy and Z-stacks were acquired.

Evaluation of the immunosuppressive potential of MSC grown onto meshes

To evaluate the efficacy of HS in supporting MSC retain their immunosuppressive potential, cells were seeded at the density of 100,000 cells/cm^2 onto HS-Col, Col meshes and cultured for 24 hrs at 37°C before stimulation with pro-inflammatory cytokines occurred. Stimulation was performed as previously reported[18,27]. Briefly, a combination of rat recombinant IFN-γ and TNF-α (20 ng/ml; PeproTech) was used and

exposure lasted for 48 and 72 hrs. Cells cultured in 2D conditions (CTRL), whether stimulated (Positive CTRL) or not, were used as negative and positive controls respectively. The expression of immunosuppressive markers was determined in also on MSC grown onto meshes in absence of stimulation. At each time point the levels of expression of genes associated to MSC immunosuppressive potential were analyzed as follows.

Peripheral Blood Mononuclear Cells proliferation test

Peripheral blood mononuclear cells (PBMC) were obtained from heparinized whole blood samples using density gradient centrifugation (Lymphoprep; Axis-Shield, Oslo, Norway) following the manufacturer's instructions. PBMC proliferation was induced as previously reported [18]. The effect of human MSC grown onto meshes (either Col or HS-Col) on T lymphocyte proliferation was determined after 48 hours in a cell–cell contact setting with MSC and PBMC plated at a 1:10 ratio by using CellTrace CFSE Cell Proliferation Kit (Life technologies). Briefly, twenty-four hours after seeding the MSC onto meshes, PBMC were stained with CFSE following the manufacturer's indications and co-cultured. The percentage of proliferating PBMC in each experimental condition was analyzed by flow cytometry (Millipore).

Gene expression analysis

Total RNA was extracted from cells using TRI Reagent® (Sigma) and complementary DNA (cDNA) was synthetized from RNA using iScript™

cDNA Synthesis Kit (BioRad) according to the manufacturer's protocol. Gene expression analysis was performed using specific oligonucleotide primers, designed based on rat (*Rattus norvegicus*) specific sequences and reported in Table. Pro-inflammatory markers include interleukin-6 (*Il-6*), tumor necrosis factor-alpha (*Tnf-α*), and inducible nitric oxide synthase (*iNos*). Immunosuppression-associated markers include prostaglandin E2 synthase (*Pges2*), transforming growth factor beta (*Tgf-β)*, and cyclooxygenase (*Ptgs2)*. Mesenchymal-associated markers include: *Cd90*, *Cd29*, and *Cd73*. Quantitative (Real time) PCR was executed using StepOne™ Real-Time PCR System with SYBR® green method. The presence of pro-inflammation markers was tested on each sample, while immunosuppression-associated markers analysis was performed only on non-inflamed samples, at different growth conditions. Glyceraldehyde 3-phosphate dehydrogenase (*Gapdh*) was used as reference gene. Each sample was analyzed in triplicate.

Differentiation assays were used to establish the plastic potential of the cells used in the study as well as to understand whether the structural and chemical stimuli provided by the meshes could induce cell reprogramming towards two lineages of the mesodermic layer. MSC grown in 2D and/or in 3D (Col or HS-Col) conditions were harvested following 14 days from induction or culture in standard media. RNA was extracted using RNeasy mini kit (Qiagen). cDNA was reverse transcribed from 150 ng of total RNA with iScript retrotranscription kit (Bio-Rad Laboratories, Hercules, CA). Amplifications were carried on using TaqMan® Fast Advanced Master Mix

on a StepOne Plus real-time PCR system (Applied Biosystems, Foster City, CA). The following target probes (Applied Biosystems) were applied to evaluate the expression of: osteocalcin (*Bglap*), and alkaline phosphatase (*Alp*) for osteogenic differentiation. Transcription factor Sox-9 (*Sox9*) and Aggrecan (*Acan*) were evaluated for chondrogenic differentiation. The expression of each gene was first normalized to the level of housekeeping gene Beta Actin *(Actb)*. Relative fold changes were normalized to the respective control. Technical triplicates for each biologic sample were evaluated, and results were reported as mean ± standard deviation.

Statistical Analysis

Statistical analysis was performed by using GraphPad Instat 3.00 for Windows (GraphPad Software, La Jolla, CA, http://www. graphpad.com/). Three replicates to evaluate the metabolic state of the cells and gene expression were performed. The results are reported as mean±SD, with $p<0.05$ used as a threshold for significance. One-way analysis of variance for multiple comparisons by the Student-Newman-Keuls multiple comparison test was used.

RESULTS

Material Characterization

Collagen type I from bovine tendon was used for the preparation of meshes by the solvent casting method. Since collagen contains several free amines groups (32/1000 amino acid residues) we decided to use that as graph point for the dock of heparin sulfate (HS) that is characterized by the free carboxyl groups in order to obtain Collagen type meshes functionalized with HS (HS-Col) (**Figure 2A**). The topography of the surfaces has been analyzed by SEM. **Figure 2B** shows the topography of the HS-Col demonstrating that the crosslink do not affect the collagen nanostructure. The presence of HS is confirmed by FTIR (**Figure 2C** shows the averaged (n = 3) of FTIR spectra of Col and HS-Col. Amide I (1,700–1,600 cm-1), and Amide II (1,600–1,500 cm-1) are related to the stretching vibration of C=O bonds, and C–N stretching and N–H bending vibration respectively and are present in both samples, as well as the Amide III region (≈1200–1300 cm-1). In HS-Col we found at ≈1080 cm-1 (C–O stretching of carbohydrate residues in collagen and proteoglycans), ≈845 cm-1 and ≈1120 cm-1 (C–O-S stretching) and ≈1397 cm-1 (COO- stretching of amino side chains) vibrational modes of glycosaminoglycans [28] . We also performed a simple Alcian blue stainining in order to confirm the presence of HS on the collagen surface (**Figure 2D**). After mounting the membrane on the insets (**Figure 2E**) we performed the ELLA assays. Although the presence of HS at the first time point was not significant different, the stability of the HS

adsorbed is significantly lower, in fact after 14 days we lost the half concentration of HS onto the surface (**Figure 2F**).

Effect of fibroblastic-growth factor (FGF) and HS on cell proliferation

After ensuring the cell population was homogeneously positive for MSC-associated markers (**Supplementary Figure 1A**) and confirming its differentiative potential towards osteogenic and chondrogenic lineages (**Supplementary Figure 1B**), the efficacy of the proposed HS-Col meshes in acting as synthetic extracellular matrix and its capability to localize growth factors and improve MSC proliferation were assessed in the context of FGF over a 7-day period. MTT assay revealed that the presence of crosslinked HS allows for the fine control of FGF provided to cells (**Figure 3**). An overall decrease in cell proliferation was observed when cells were grown onto 3D structures, both Col and HS-Col compared to controls (CTRL), although the group HS-Col w/FGF showed a statistically significant ($P<0.01$) increase compared to Col w/sHS and FGF at day 3 and 7. A block in cell growth was observed in the experimental group Col w/sHS and FGF, and no differences were shown between MSC grown in standard conditions supplemented with FGF (CTRL w/FGF) and a combination of FGF and sHS (CTRL w/ sHS and FGF).

Cell viability, morphology, and spreading

Alamar blue assay demonstrated that both HS-Col and Col supported metabolically active cells growth during a period of 3 days (**Figure 4A**). As revealed by optical microscopy after 7 days of culture (**Figure 4B**),

MSC spread across the meshes and reached confluence, as compared to 2D control (CTRL). Cells grown in presence of Col and HS-Col displayed a more spindle-shaped morphology compared to CTRL. To compare the cell structures formed by MSC adhering to meshes (both, Col and HS-Col), antibodies to actin and vinculin were used (**Figure 4C**). Diffused cytoplasmic labeling was demonstrated when cells were seeded onto Col meshes, together with an intense staining confirming focal adhesions linking the ECM with intracellular cytoskeleton. MSC grown onto HS-Col displayed a more elongated shape than their Col counterparts and maintained physical contact among them through extensions, with marked focal adhesions but without completely spreading.

MSC-associated markers expression and the differentiative potential

Flow cytometry demonstrated a slight reduction in the percentage of MSC-associated markers at 3 days compared to controls (CTRL) following MSC culture onto HS-Col and Col (**Figure 4D**). To understand the effect of HS-Col on MSC at a genetic level, real-time PCR was used to evaluate the expression of mesenchymal-associated markers, including *Cd29*, *Cd73* and *Cd90* (**Figure 4E**). Molecular analysis showed that at 72 hours the expression of integrin *Cd29* was significantly ($p<0.01$) higher in cells seeded onto Col than HS-Col and 2D controls (CTRL). A statistically significant increase compared to control (CTRL) in the expression levels of the same gene was found in Col-HS. The expression of *Cd73* and *Cd90* in cells treated with HS-Col was found lower than 2D control (0.475-fold and 0.155-fold, respectively). No significant differences were identified for the expression of these latter genes in Col.

Being cultured for 14 days onto meshes did not induce any increase in the expression of the osteogenesis-associated genes tested (**Supplementary**

Figure 2A), although the presence of collagen induced a statistically significant increase ($p<0.01$) in the expression levels of the chondrogenic marker *Acan* compared to the 2D control. For this gene values were assessed around 6.97±1.71 and 10.43±4.23 for Col and HS-Col respectively. The presence of our meshes was associated to a great activation of both, osteogenic and chondrogenic genes, following 14 days of induction towards the two lineages (**Supplementary Figure 2B**).

Immunosuppressive potential

To understand whether the exposure of MSC to HS-Col and Col could represent a source of stress for the cells, their response to the material was tested in absence of any other pro-inflammatory molecule. At 48 and 72 hrs, the levels of expression of genes encoding for immunosuppressive factors (*Tnf-α*, *iNos*, and *Il-6*) were evaluated in comparison with untreated cells (CTRL) or inflamed cells used as positive controls. **Figure 5A** shows a great increase in the expression of *Tnf-α* and *iNos* in cells grown onto HS-Col for 48 hrs compared to CTRL (13.32±0.23 and 19.02±0.15, respectively). No significant differences in the expression levels of *Il-6* were found in Col and HS-Col at the same time point or at 72 hrs. Interestingly, the expression of *Tnf-α* diminished overtime in presence of HS, showing lower values than Col (2.11±0.11 vs 12.24±1.3). The *iNos* expression was found even increased at 72 hrs in both, Col and HS-Col. Concomitantly, a significant increase in the expression of markers mediating the reduction of inflammation (*Tgf-β*, *Pges2*, and *Ptgs2*) was observed at 48 hrs in comparison with the CTRL and Col, with values assessed around 3.83±0.50 for *Tgf-β*, 4.78±0.50 for *Ptgs2*, and 57.41±8.60 for *Pges2* (**Figure 5B**). Values were found even increased at 72 hrs in the case of *Ptgs2 and Tgf-b* (6.35±0.29, and 9.46±0.38), the same trend being observed also for cells

exposed to Col. The expression levels of *Pge-2* were found reduced overtime when cells were grown onto HS-Col.

To test the efficacy of the proposed material to support MSC immunosuppressive potential, cells grown onto Col and HS-Col meshes were stimulated with the pro-inflammatory cytokines TNF-α and IFN-γ (at the concentration of 20 ng/ml) for 48 and 72 hrs. qPCR was used to evaluate the relative amount of genes responsible for the production of pro-inflammatory molecules, which are responsible for the activation of such process, including *Tnf-α*, *iNos*, and *Il-6*. Data were normalized to the respective untreated control (CTRL, value=1). Consistent with the previous findings, in response to stimulation cells grown onto Col produced nearly identical amounts of immunosuppressive genes (*iNos* and *Tnf-α*) compared with those cultured in 2D and standard conditions, whereas cells grown onto HS-Col scaffolds produced significantly higher amounts. **Figure 6A** shows a significant increase in the expression of *Tnf-α, iNos,* and *Il-6* in MSC grown onto inflamed HS-Col compared to those seeded onto inflamed Col at 48 hrs. Values were assessed around 4.82±1.23, 6.03±1.46, and 4.24±0.41 for *Tnf-a*, *iNos*, and *Il-6*, respectively. At 72 hrs a marked decrease in the expression of *iNos* was found in inflamed HS-Col compared to 48 hrs (6.03±1.46 vs 1.88±0.22), which was found even lower than the expression levels found in Col at the same time point (2.63±0.52). Finally, when the immunosuppressive potential of MSC grown onto HS-Col was evaluated in a lymphocyte reaction assay, a marked reduction in the proliferation of PHA-stimulated PBMC was noticed after 2 days of coculture compared to their Col counterparts, with percentage of proliferative cells assessed around 44% and 72% respectively (**Figure 6B**).

DISCUSSION

Stem cells are widely used in regenerative medicine applications because of their properties, particularly their ability to secrete bioactive molecules that are known to have an immunosuppressive potential and to participate in the recreation of the correct pro-regenerative microenvironment following an injury[29]. They are closely associated with surrounding environment, which is responsible for influencing the way they respond to stimuli. The ability of biomaterials mimicking the ECM to promote constructive tissue remodeling can be attributed to both their structure and composition. Several tissue-engineering based approaches have been developed so far in the attempt to recapitulate the composition of the ECM (e.g collagen, glycosaminoglycans, etc.) and provide endogenous cells with the physical, chemical, and mechanical stimuli needed to support their biological activities during development, homeostasis, and response to injury [30]. We recently developed collagen-based scaffolds functionalized with chondroitin sulfate and demonstrated their capability to induce a cartilage resembling environment able to support stem cell differentiation and immunosuppression, thus holding the promise for the treatment of orthopedic chronic diseases [1,18,23,26,31-34]. Among GAGs, also HS has been proposed to take part in ECM composition, to retain growth factors and chemokines and prevent growth factors degradation [11]. In the process of developing our biomimetic materials for tissue engineering applications, we first tried to understand how HS bioactivity could change when provided as soluble molecule, or absorbed/crosslinked onto collagen based

membranes. We confirmed that HS influences the activity of FGF and actively participates in the presentation of the ligand on the receptor improving its activation and consequently cell proliferation [11-13]. We also provided evidences about the fact that HS supports such activity when crosslinked onto collagen-based scaffolds and it is significantly reduced when it is in its soluble form or absorbed.

We then proposed collagen-based membranes crosslinked with heparan sulfate, which mimics the extracellular matrix of connective tissues to study their effect on MSC proliferation, adhesion, gene expression, as well as on their potential to release immunosuppressive molecules suggested to lead to the resolution of inflammation following an injury or an implant.

Biomimetic meshes could be very usefully for the repair of different tissues. We recently demonstrated that could be a valid alternative to the clinical polymeric materials used in soft tissue repair [25] as well as in cell delivery for more regenerative medicine approaches [35].

In agreement with the existing literature and with our previous observations [23,32,33,36], data presented herein show that in presence of a 3D culture system cells proliferation appears to be slower compared to cells cultured in two-dimensional standard conditions, because of the different growth surface and the need of differently reorganizing. This statement supports the apparent discrepancies between the metabolic state of the cells and their proliferative potential. Our findings are confirmed by the ICC analysis revealing that cells grown onto membranes tend to form focal adhesion and to create a bond between the synthetic ECM and their cytoskeleton [37]. To compare the cell adhesion structures formed by MSC adhering to the two matrices tested (Col and HS-Col), the presence of focal

adhesions, which are presumably activated through the interaction between integrin receptors on cells, was further confirmed by the high expression of *CD29* (or integrin-β1) at a molecular level, 72 hrs after seeding. Our data suggest that MSC are able to create a strong connection with the collagen substrate, being the most represented protein in ECM [38]. These observations were further confirmed by the levels of *Cd73* and *Cd90* expression, as demonstrated by real-time PCR. Their expression levels in cells grown within HS-Col were found lower than control. Especially, *Cd90* appears to be significantly down-regulated respect of control. According to these results, Ode et al. have proved that a down-regulation of *Cd73* expression is observed during differentiation, particularly during chondrogenesis, and when cells are exposed to mechanical stimulation [39]. In other studies it has also been demonstrated that a decreasing ability of cells to migrate is associated to a lower expression of *Cd73* and *Cd29*, and the reduction of mRNA level of *Cd90* after mechanical stimulation, as well as during the differentiation [40,41]. Based on this, we can speculate that membranes cause a sort of stress in cells thus inducing a down regulation of the typical mesenchymal-associated markers. If this is the case, MSC grown onto HS-Col membranes lose their undifferentiated state and the stress they undergo could eventually lead their specification towards a more committed lineages [14], as suggested by the matrix deposition revealed in Figure 4B. We next assessed the immunosuppressive potential of these membranes and, at the same time, their ability to support the immune-regulatory capability attributed to MSC[42] in response to pro-

inflammatory stimuli for their potential use in regenerative medicine applications. The first step was to evaluate the expression of pro-inflammatory molecules (*Tnf-α*, *iNos*, and *Il-6*) at mRNA level, following 48 and 72 hrs culture onto Col or HS-Col, in the attempt to understand whether or not the contact with collagen or HS-Col and their topographical properties could affect stem cell immunosuppressive behavior. Our data demonstrated that high levels of the inducible nitric oxide synthase were produced by cells exposed to HS-Col compared to cells grown onto Col or in 2D conditions, with values that were found reduced compared to other experimental groups at 72 hrs. To date, these molecules are released by MSC to contrast or modulate the activities of several immune cell types, included but not limited to T and NK cells proliferation, B cell maturation, macrophages polarization, and dendritic cell maturation activation. This suggests that the 3D environment provided by Col-HS resulted in a greater stress for cells, probably due to the different mechanical stimuli that the material induces in the cells. Interestingly, however, such activity was further stimulated when cells were inflamed with TNF-α (20 ng/ml) and IFN-γ (20 ng/ml), leading to a marked accumulation ($p<0.01$) of pro-inflammatory molecules, as observed in HS-Col compared to Col. These data were corroborated by the significant increase in the expression of genes encoding for other immunosuppressive molecules, which are normally associated to the resolution of inflammation, such as *Pges2*, *Ptgs2*, and *Tgf-β* [43,44]. To further validate the potential of HS-Col meshes to support MSC immunosuppression and understand whether the bioactivity of the immune modulating molecules produced by MSC following stimulation could lead to a reduced T cell proliferation [43,44], the effect of HS-Col was tested in a

functional assay. A greater capability to inhibit T cell growth was detected when MSC were grown onto meshes (both Col and HS-Col) although the presence of HS crosslinked onto the collagen membranes was associated to a greater MSC immunogenic capability [18].

CONCLUSIONS

Here we proposed HS-functionalized biomimetic meshes resembling the composition of extracellular matrix of soft tissue. We demonstrated that the surface modifications applied on the collagen-based material affect MSC behavior and improve their immunosuppressive competence. The proposed material represents a proof of concept for further developing immunomodulatory materials with the capability of supporting and enhancing MSC potential, and ultimately reducing inflammation at the site of implant.

Conflict of interest

The authors have no competing interests.

Authors and contributors

BC and FT conceived the idea for this project. BC and FT designed and conducted the experiments. BC and FT wrote the manuscript. FT prepared meshes and performed their chemical characterization, cells characterization and staining assisted by GB, FBN and LP. BC conducted the cellular and molecular work assisted by IG and GB. ET provided mentoring and contributed the funding support.

Acknowledgements

The authors gratefully acknowledge funding supports from the following sources: the Hearst Foundation (Project ID, 18130017) and the Cullen Trust for Health Care Foundation (Project ID, 18130014).

REFERENCES

1 Perrini, C. *et al.* Microvesicles secreted from equine amniotic-derived cells and their potential role in reducing inflammation in endometrial cells in an in-vitro model. *Stem Cell Res Ther* **7**, 169, doi:10.1186/s13287-016-0429-6 (2016).

2 Wagers, A. J. The stem cell niche in regenerative medicine. *Cell Stem Cell* **10**, 362-369, doi:10.1016/j.stem.2012.02.018 (2012).

3 Frantz, C., Stewart, K. M. & Weaver, V. M. The extracellular matrix at a glance. *J Cell Sci* **123**, 4195-4200, doi:10.1242/jcs.023820 (2010).

4 Burghardt, R. C. *et al.* Integrins and extracellular matrix proteins at the maternal-fetal interface in domestic animals. *Cells Tissues Organs* **172**, 202-217, doi:66969 (2002).

5 Schultz, G. S. & Wysocki, A. Interactions between extracellular matrix and growth factors in wound healing. *Wound Repair Regen* **17**, 153-162, doi:10.1111/j.1524-475X.2009.00466.x (2009).

6 Brizzi, M. F., Tarone, G. & Defilippi, P. Extracellular matrix, integrins, and growth factors as tailors of the stem cell niche. *Curr Opin Cell Biol* **24**, 645-651, doi:10.1016/j.ceb.2012.07.001 (2012).

7 Lamoureux, F., Baud'huin, M., Duplomb, L., Heymann, D. & Redini, F. Proteoglycans: key partners in bone cell biology. *Bioessays* **29**, 758-771, doi:10.1002/bies.20612 (2007).

8 Oohira, A. *et al.* Effects of lipid-derivatized glycosaminoglycans (GAGs), a novel probe for functional analyses of GAGs, on cell-to-substratum adhesion and neurite elongation in primary cultures of fetal rat hippocampal neurons. *Arch Biochem Biophys* **378**, 78-83, doi:10.1006/abbi.2000.1775 (2000).

9 Hacker, U., Nybakken, K. & Perrimon, N. Heparan sulphate proteoglycans: the sweet side of development. *Nat Rev Mol Cell Biol* **6**, 530-541, doi:10.1038/nrm1681 (2005).

10 Perrimon, N. & Bernfield, M. Specificities of heparan sulphate proteoglycans in developmental processes. *Nature* **404**, 725-728, doi:10.1038/35008000 (2000).

11 Dreyfuss, J. L. *et al.* Heparan sulfate proteoglycans: structure, protein interactions and cell signaling. *An Acad Bras Cienc* **81**, 409-429 (2009).

12 Lortat-Jacob, H., Turnbull, J. E. & Grimaud, J. A. Molecular organization of the interferon gamma-binding domain in heparan sulphate. *Biochem J* **310 (Pt 2)**, 497-505 (1995).

13 Sasisekharan, R., Ernst, S. & Venkataraman, G. On the regulation of fibroblast growth factor activity by heparin-like glycosaminoglycans. *Angiogenesis* **1**, 45-54, doi:10.1023/A:1018318914258 (1997).

14 Helledie, T. *et al.* Heparan sulfate enhances the self-renewal and therapeutic potential of mesenchymal stem cells from human adult bone marrow. *Stem Cells Dev* **21**, 1897-1910, doi:10.1089/scd.2011.0367 (2012).

15 Li, J. P. & Vlodavsky, I. Heparin, heparan sulfate and heparanase in inflammatory reactions. *Thromb Haemost* **102**, 823-828, doi:10.1160/TH09-02-0091 (2009).

16 Rops, A. L. *et al.* Heparan sulfate proteoglycans in glomerular inflammation. *Kidney Int* **65**, 768-785, doi:10.1111/j.1523-1755.2004.00451.x (2004).

17 Corradetti, B. *et al.* Amniotic membrane-derived mesenchymal cells and their conditioned media: potential candidates for uterine regenerative therapy in the horse. *PLoS One* **9**, e111324, doi:10.1371/journal.pone.0111324 (2014).

18 Corradetti, B. *et al.* Chondroitin Sulfate Immobilized on a Biomimetic Scaffold Modulates Inflammation While Driving Chondrogenesis. *Stem Cells Transl Med* **5**, 670-682, doi:10.5966/sctm.2015-0233 (2016).

19 Lange-Consiglio, A. *et al.* Equine Amniotic Microvesicles and Their Anti-Inflammatory Potential in a Tenocyte Model In Vitro. *Stem Cells Dev* **25**, 610-621, doi:10.1089/scd.2015.0348 (2016).

20 Willerth, S. M. & Sakiyama-Elbert, S. E. in *StemBook* (2008).

21 Meade, K. A. *et al.* Immobilization of heparan sulfate on electrospun meshes to support embryonic stem cell culture and differentiation. *Journal of Biological Chemistry* **288**, 5530-5538 (2013).

22 Mothéré, M., Singabraya, D., Driguez, P. A., Siñeriz, F. & Papy-Garcia, D. Poly (ethylene glycol acrylate)-functionalized hydrogels for heparan sulfate oligosaccharide recognition. *Journal of Molecular Recognition* (2016).

23 Taraballi, F. *et al.* Biomimetic collagenous scaffold to tune inflammation by targeting macrophages. *J Tissue Eng* **7**, 2041731415624667, doi:10.1177/2041731415624667 (2016).

24 Taraballi, F. *et al.* Amino and carboxyl plasma functionalization of collagen films for tissue engineering applications. *Journal of colloid and interface science* **394**, 590-597 (2013).

25 Minardi, S. *et al.* Biomimetic collagen/elastin meshes for ventral hernia repair in a rat model. *Acta Biomaterialia* (2016).

26 Corradetti, B. *et al.* Osteoprogenitor cells from bone marrow and cortical bone: understanding how the environment affects their fate. *Stem Cells Dev* **24**, 1112-1123, doi:10.1089/scd.2014.0351 (2015).

27 Hegyi, B., Kudlik, G., Monostori, E. & Uher, F. Activated T-cells and pro-inflammatory cytokines differentially regulate prostaglandin E2 secretion by mesenchymal stem cells. *Biochem Biophys Res Commun* **419**, 215-220, doi:10.1016/j.bbrc.2012.01.150 (2012).

28 Corradetti, B. *et al.* Chondroitin sulfate immobilized on a biomimetic scaffold modulates inflammation while driving chondrogenesis. *Stem cells translational medicine* **5**, 670-682 (2016).

29 Caplan, A. I. Adult mesenchymal stem cells for tissue engineering versus regenerative medicine. *J Cell Physiol* **213**, 341-347, doi:10.1002/jcp.21200 (2007).

30 Corradetti, B. *The innate immune and inflammatory response to implanted materials and devices*. (Springer Science+Business Media, 2016).

31 Fernandez-Moure, J. S. *et al.* Enhanced osteogenic potential of mesenchymal stem cells from cortical bone: a comparative analysis. *Stem Cell Res Ther* **6**, 203, doi:10.1186/s13287-015-0193-z (2015).

32 Minardi, S. *et al.* IL-4 Release from a Biomimetic Scaffold for the Temporally Controlled Modulation of Macrophage Response. *Ann Biomed Eng* **44**, 2008-2019, doi:10.1007/s10439-016-1580-z (2016).

33 Minardi, S. *et al.* Biomimetic Concealing of PLGA Microspheres in a 3D Scaffold to Prevent Macrophage Uptake. *Small* **12**, 1479-1488, doi:10.1002/smll.201503484 (2016).

34 Minardi, S. *et al.* Evaluation of the osteoinductive potential of a bio-inspired scaffold mimicking the osteogenic niche for bone augmentation. *Biomaterials* **62**, 128-137, doi:10.1016/j.biomaterials.2015.05.011 (2015).

35 Pandolfi, L. *et al.* A nanofibrous electrospun patch to maintain human mesenchymal cell stemness. *Journal of Materials Science: Materials in Medicine* **28**, 44 (2017).

36 Taraballi, F. *et al.* Potential avoidance of adverse analgesic effects using a biologically "smart" hydrogel capable of controlled bupivacaine release. *J Pharm Sci* **103**, 3724-3732, doi:10.1002/jps.24190 (2014).

37 Wozniak, M. A., Modzelewska, K., Kwong, L. & Keely, P. J. Focal adhesion regulation of cell behavior. *Biochim Biophys Acta* **1692**, 103-119, doi:10.1016/j.bbamcr.2004.04.007 (2004).

38 Hynes, R. O. & Naba, A. Overview of the matrisome—an inventory of extracellular matrix constituents and functions. *Cold Spring Harbor perspectives in biology* **4**, a004903 (2012).

39 Ode, A. *et al.* CD73/5'-ecto-nucleotidase acts as a regulatory factor in osteo-/chondrogenic differentiation of mechanically stimulated mesenchymal stromal cells. *Eur Cell Mater* **25**, 37-47 (2013).

40 Ode, A. *et al.* CD73 and CD29 concurrently mediate the mechanically induced decrease of migratory capacity of mesenchymal stromal cells. *Eur Cell Mater* **22**, 26-42 (2011).

41 Wiesmann, A., Buhring, H. J., Mentrup, C. & Wiesmann, H. P. Decreased CD90 expression in human mesenchymal stem cells by applying mechanical stimulation. *Head Face Med* **2**, 8, doi:10.1186/1746-160X-2-8 (2006).

42 Caplan, A. I. & Sorrell, J. M. The MSC curtain that stops the immune system. *Immunol Lett* **168**, 136-139, doi:10.1016/j.imlet.2015.06.005 (2015).

43 Zinocker, S. & Vaage, J. T. Rat mesenchymal stromal cells inhibit T cell proliferation but not cytokine production through inducible nitric oxide synthase. *Front Immunol* **3**, 62, doi:10.3389/fimmu.2012.00062 (2012).

44 Zinocker, S., Wang, M. Y., Rolstad, B. & Vaage, J. T. Mesenchymal stromal cells fail to alleviate experimental graft-versus-host disease in rats transplanted with major histocompatibility complex-mismatched bone marrow. *Scand J Immunol* **76**, 464-470, doi:10.1111/j.1365-3083.2012.02758.x (2012).

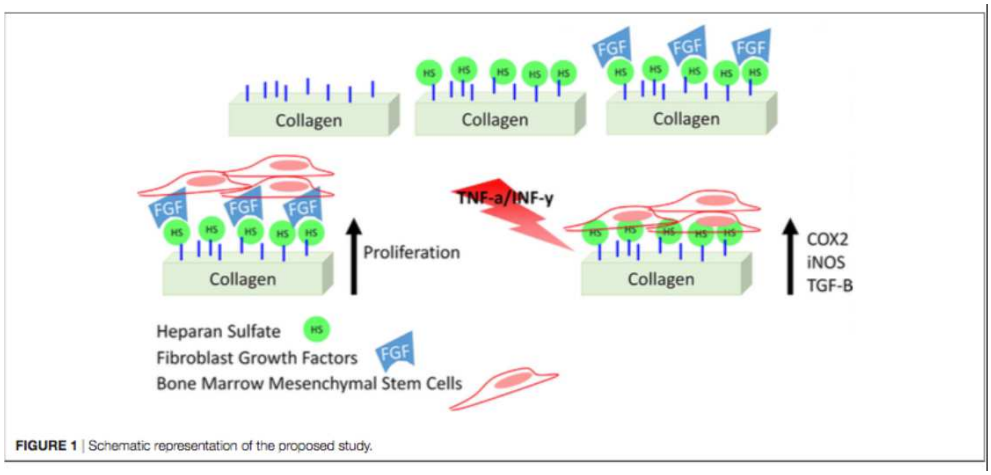

FIGURE 1 | Schematic representation of the proposed study.

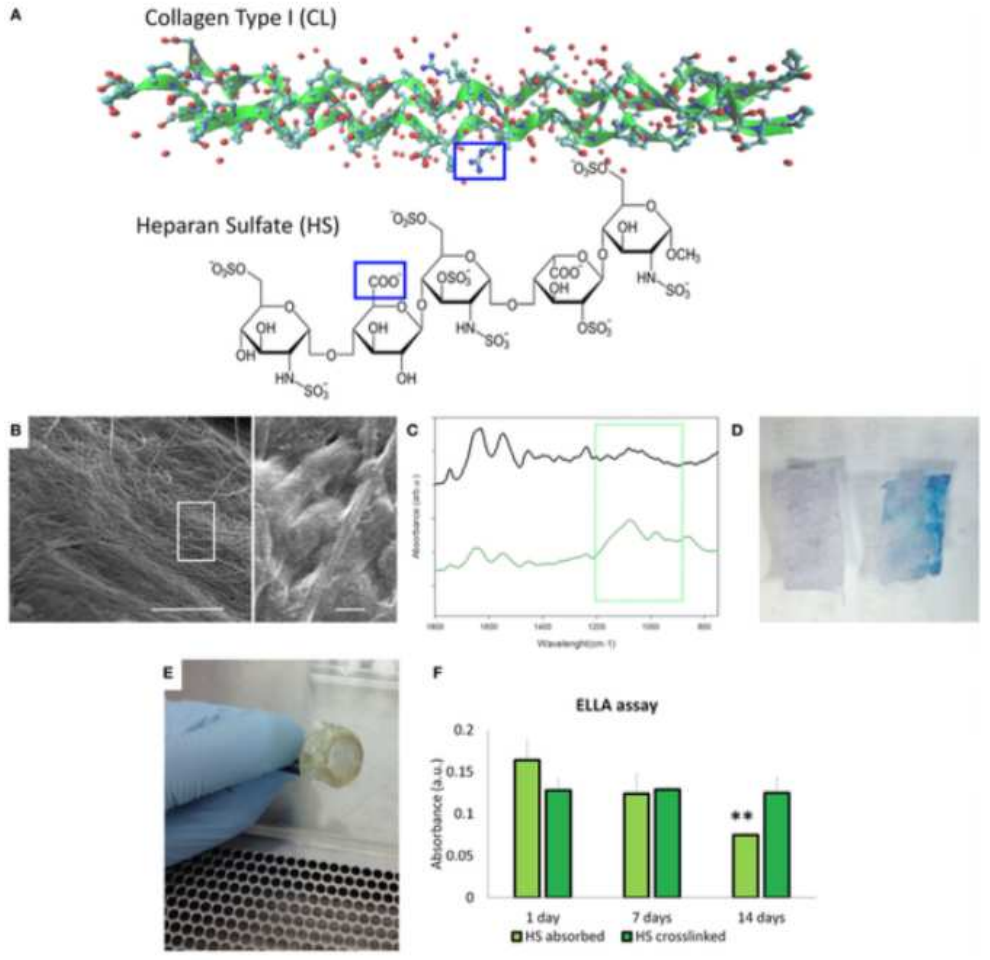

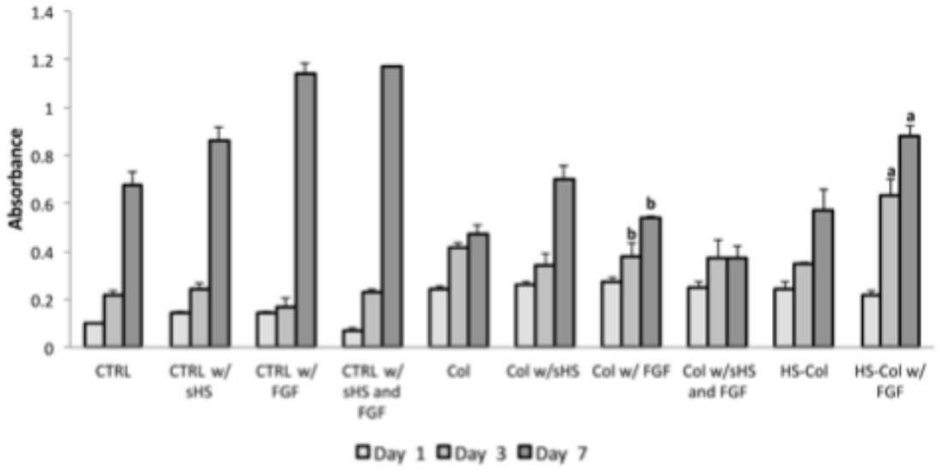
Absorbance
1.4
1.2
1
0.8
0.6
0.4
0.2
0
CTRL
CTRL w/ sHS
CTRL w/ FGF
CTRL w/ sHS and FGF
Col
Col w/sHS
Col w/ FGF
Col w/sHS and FGF
HS-Col
HS-Col w/ FGF
a
b
Day 1
Day 3
Day 7

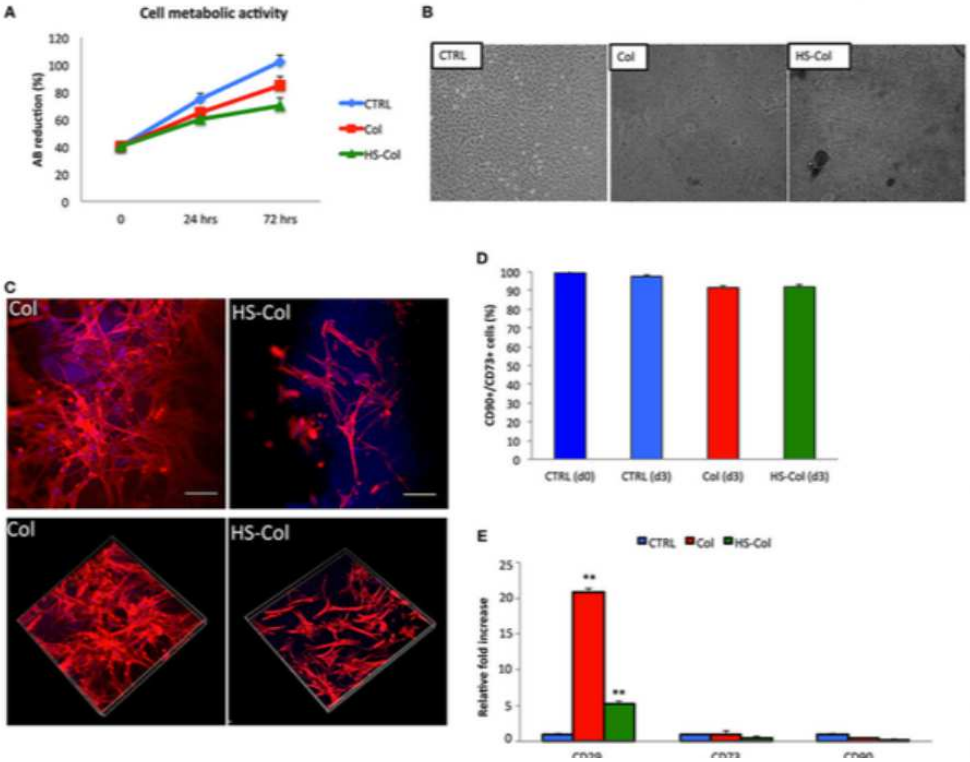
A
Cell metabolic activity
A8 reduction (%)
120
100
80
60
40
20
0
0
24 hrs
72 hrs
CTRL
Col
HS-Col
B
CTRL
Col
HS-Col
C
Col
HS-Col
Col
HS-Col
D
CD90+/CD73+ cells (%)
100
90
80
70
60
50
40
30
20
10
0
CTRL (d0)
CTRL (d3)
Col (d3)
HS-Col (d3)
E
CTRL
Col
HS-Col
Relative fold increase
25
20
15
10
5
0
**
**

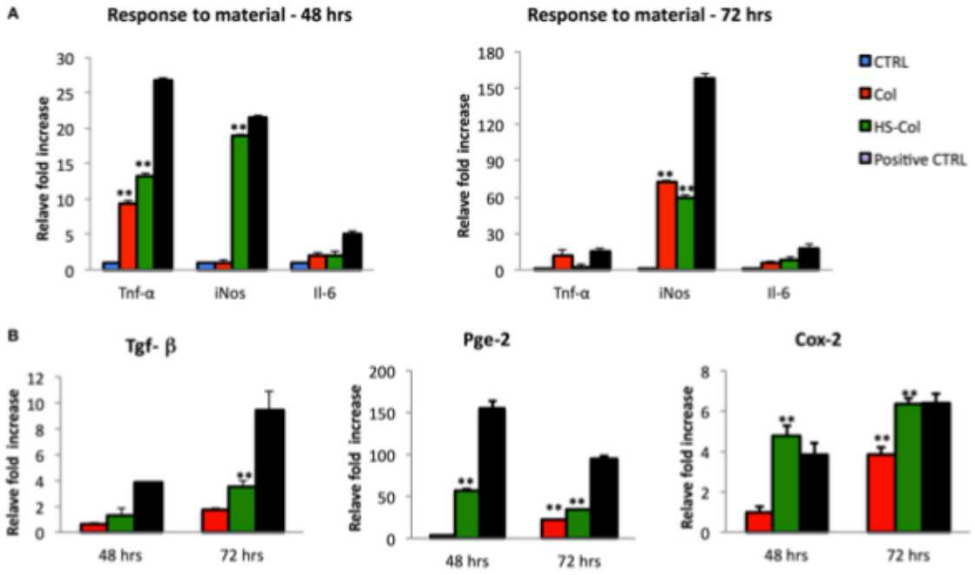
A
Response to material - 48 hrs
Relave fold increase
Tnf-α
iNos
Il-6
Response to material - 72 hrs
CTRL
Col
HS-Col
Positive CTRL
B
Tgf- β
Relave fold increase
48 hrs
72 hrs
Pge-2
Cox-2

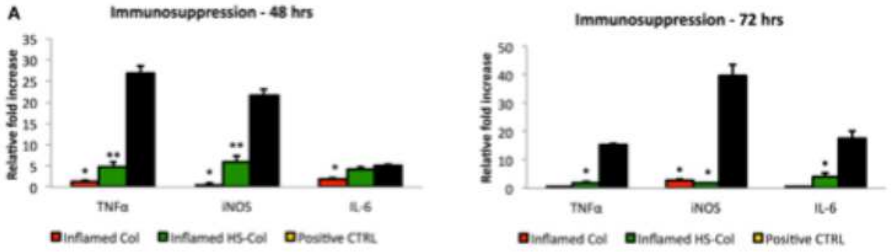
A
Immunosuppression - 48 hrs
Relative fold increase
TNFα
iNOS
IL-6
Inflamed Col
Inflamed HS-Col
Positive CTRL
Immunosuppression - 72 hrs

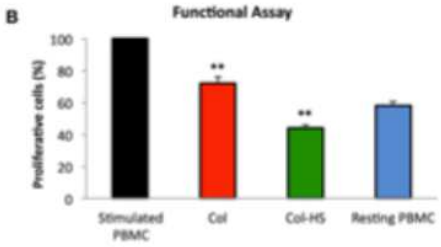
B
Functional Assay
Proliferative cells (%)
Stimulated PBMC
Col
Col-HS
Resting PBMC